Forecasting Extreme Water Levels in Estuaries for Flood Warning.

Stage 2: Review of External Forecasts and Numerical Modelling Techniques

R&D Project Record W5/010/2

I D Cluckie*, R J Griffith*, R Harpin, J Qin*, J M Wicks

Research Contractor:

Halcrow Water
&
University of Bristol*

Publishing Organisation:
Environment Agency
Rio House
Waterside Drive
Aztec West
Almondsbury
Bristol BS32 4UD

Tel: 01454 624400 Fax: 01454 624409

Dissemination status
Internal: Released to Regions
External: Restricted

Statement of use
This report describes the second stage of a study aiming to improve the Agency's flood warning systems in estuaries, and complements the work previously described in Project Record W5/010/1. It consists of an overview of the currently available models that can be used for the prediction and forecasting of extreme water levels. It also covers an assessment of the accuracy of existing methods applied at sites in two Agency Regions. The report is supplied for information only, prior to the project entering its final stages in which it is intended that improved methodology will be recommended for use by the Agency. The report will be of interest mainly to those flood defence staff specifically involved in providing flood warnings in estuaries.

Research contractor
This document was produced under R&D Project W5-010 by:

Halcrow Water
Burderop Park
Swindon
Wiltshire
SN4 0QD

Tel: 01929 462314
Fax: 01929 462180

in association with

Water Management Research Centre
Dept. of Civil Engineering
University of Bristol
Lunsford House
Cantocks Close
Bristol
BS8 1UP

Tel: 0117 9289769
Fax: 0117 9289770

Environment Agency Project Leader
The Environment Agency's Project Leader for R&D Project W5-010 was:
Betty Ng (to September 1999) and Henry Brown (from October 1999) Environment Agency, Wales

Further copies of this report are available from:
Environment Agency R&D Dissemination Centre, c/o
WRc, Frankland Road, Swindon, Wilts SN5 8YF
tel: 01793-865000 fax: 01793-514562 e-mail: publications@wrcplc.co.uk

R&D Project Record W5/010/2

CONTENTS

List of Tables

List of Figures

EXECUTIVE SUMMARY

The first Interim Report covering Stage 1 of the Study consisted of a review of current practice and recommendations for work to be carried out in subsequent stages. In particular the Stage 1 Report contained a detailed review of current practice for tidal flood forecasting in England and Wales.

The primary aim of this second Interim Report focuses on a review of "external forecasts" which, in the context of flood forecasting in estuaries for flood warning purposes in England and Wales, relate to storm tide forecasting. An overview of existing operational procedures was included in the Stage 1 review (Section 2.3 of the Stage 1 Interim Report). Section 2 of this report covers operational storm tide forecasting in the UK plus a review of other operational systems in Europe. It benefits from a direct input from the Proudman Oceanographic Laboratory (POL). More detailed information on UK storm surge predictions has been commissioned from POL and will be incorporated as it becomes available.

The report also covers an assessment of the accuracy of existing methods as applied operationally at sites identified in the North West and South West Regions of the Environment Agency for England and Wales. The detailed analysis undertaken is contained in Technical Appendices (Appendices 1 and 2) with the main body of the Report focussing on a review of the current practice form Storm Tide Forecasting and the available literature in the area of forecasting extreme water levels in estuaries for flood warning. The review is a preliminary effort that will be refined after further guidance has been provided by POL and other information has been collected during the remaining duration of the Project.

This Report provides a more general review of numerical methods, especially as employed in estuaries, and exposes some of their fundamental limitations. This section focuses primarily on the problems of numerical modelling and is based mainly on the work of Scott (1996) who formally worked as a member of the Research Group prior to it relocating to the University of Bristol from the University of Salford.

A preliminary review of the available literature on the numerical modelling of estuaries is also included. A limited body of literature concerning the development and application of numerical methods for modelling water movement exists. As new areas are developed in which numerical modelling may be beneficial, and as computing power increases to allow ever more detailed and complex simulations, further research will doubtless occur. It is not the purpose of this review to provide a comprehensive catalogue of numerical modelling techniques for shallow water flow. Rather it is intended to give an overview of modelling and to detail the research which has been done in the relatively less well-developed field of estuary flooding. Unfortunately, the literature available on operational applications is rather sparse with the United Kingdom and The Netherlands being the primary areas of activity.

KEY WORDS

Numerical methods; characteristics; finite difference; finite element; grid generation; tidal propagation; shallow water equations; curvilinear; tidal surge; fluvial flood forecasting.

1. INTRODUCTION

1.1 Objectives and Layout

The overall objective of the study is to develop rigorous but practicable methods for the real-time forecasting of extreme water levels in estuaries, suitable for incorporation into existing Environment Agency flood warning systems.

"Estuary" is defined in the Oxford English Dictionary as "the tidal mouth of a large river". For the purposes of this research we propose that the definition include all rivers for which the Agency has a possible flood warning role. This report will consider the boundaries of a particular estuary to be from a point where the tidal effect starts to have a significant effect on water levels at the upstream end, to a point where the fluvial flow or the estuary shape has an insignificant effect on water levels at the downstream end.

The primary aim of this Report focuses on a review of "external forecasts" which, in the context of flood forecasting in estuaries for flood warning purposes, relate to storm tide forecasting. Section 2 of the report covers operational storm tide forecasting in the UK plus a review of other operational systems in Europe. Section 3 is a review of numerical modelling, especially as applied to estuaries. Concluding remarks are made in Section 4. The report also covers an assessment of the accuracy of existing methods as applied operationally at sites identified in the North West and South West Regions of the Environment Agency for England and Wales. The detailed analysis undertaken is contained in Technical Appendices (Appendices 1 and 2).

1.2 Background

The Environment Agency (Agency) has direct responsibility for flood defence and flood warning in England and Wales. This responsibility includes the provision and maintenance of suitable flood defences and the production of flood warnings for the estuaries of England and Wales.

The forecasting of water levels in estuaries is a complicated process due to the interaction of local tides with river flows, winds and waves. Currently there is a lack of an appropriate methodology (or methodologies) and inadequate data for the confident forecasting of extreme water levels in estuaries. This project was born out of the need to address these problems to ensure the Agency can comprehensively satisfy its flood warning duties.

The project is a three year National R&D study, scheduled for completion by 31 March 2001, that will examine the methods currently used for the forecasting of estuary water levels and develop improved techniques. This is the second report for this project. The first report (R&D Project Report W5/010/1) contained the findings of the initial phase of the project aimed at reviewing the methods currently adopted and the data available to Agency flood warning staff.

2. OPERATIONAL TIDAL SURGE MODELLING

2.1 Introduction

With the likelihood of significant climate change impacts on the generation of future storm surges it seems sensible to review the current state of modelling of tidal surges across Europe. Changes in the sea level are primarily due to variations in the gravitational attraction of the sun and moon. Additionally, the effect of global temperature rise will have a direct impact on the thermal expansion of the water body whilst increased storminess will introduce increased wind stress and barometric pressure effects. Bode and Hardy (1997) recently reviewed developments in storm surge modelling and the PROMISE project (see URL: http://www.pol.ac.uk/promise/) which is targeted at rationalising existing operational models, also provides an overview of current operational practice in Europe.

2.2 Tide, Surge and Wave Dynamics

Tides and storm surges are described by the so-called "long wave equations" (see e.g. Bode and Hardy, 1997). A fundamental assumption is that wavelengths are large compared with the water depth. Tides are generated by gravitational forces acting over the whole water column in the deep ocean. They propagate as waves and are dissipated by bottom friction in shallow water on continental shelves. Local enhancements can occur due to shape effects producing very large tides.

Storm surge generation is represented by two terms in these equations; wind stress/water depth, and the horizontal gradient of atmospheric pressure at the sea surface. The wind effect depends on water depth and increases as the depth decreases whereas the pressure effect is independent of depth. The most important mechanism for surge generation is wind stress acting over shallow water. In deep water, surge elevations are approximately hydrostatic; a 1 HPa decrease in atmospheric pressure gives about 1 cm increase in surge elevation from p = ñgh.

Surges are superimposed on the normal astronomical tides. Where the tidal range is large, the relative timing of a surge peak and tidal high water is critical. The nature of the flooding problem in estuaries due to the combined effects of storm surge + astronomical tide + fluvial flood + local effects is complex. Severe flooding usually only results from the coincidence of two or three of these causal factors (outlined in Figure 2.1). A moderate storm surge, which in itself is not a problem, when combined with a spring tide peak may be devastating. Likewise coincidence with a rare fluvial flood or a particularly severe combination of local effects (e.g. local wind stress/depth, shape or bathymetric impact) may cause a catastrophe. In addition the occurrence of a strong storm surge is likely to coincide with strong wave impact where overtopping of local coastal flood defences may occur. The forecasting of what is a combination of extremes is fundamentally difficult and by definition rare. This is the primary reason for the current lack of data on past performance of operational models within the EA at the present time.

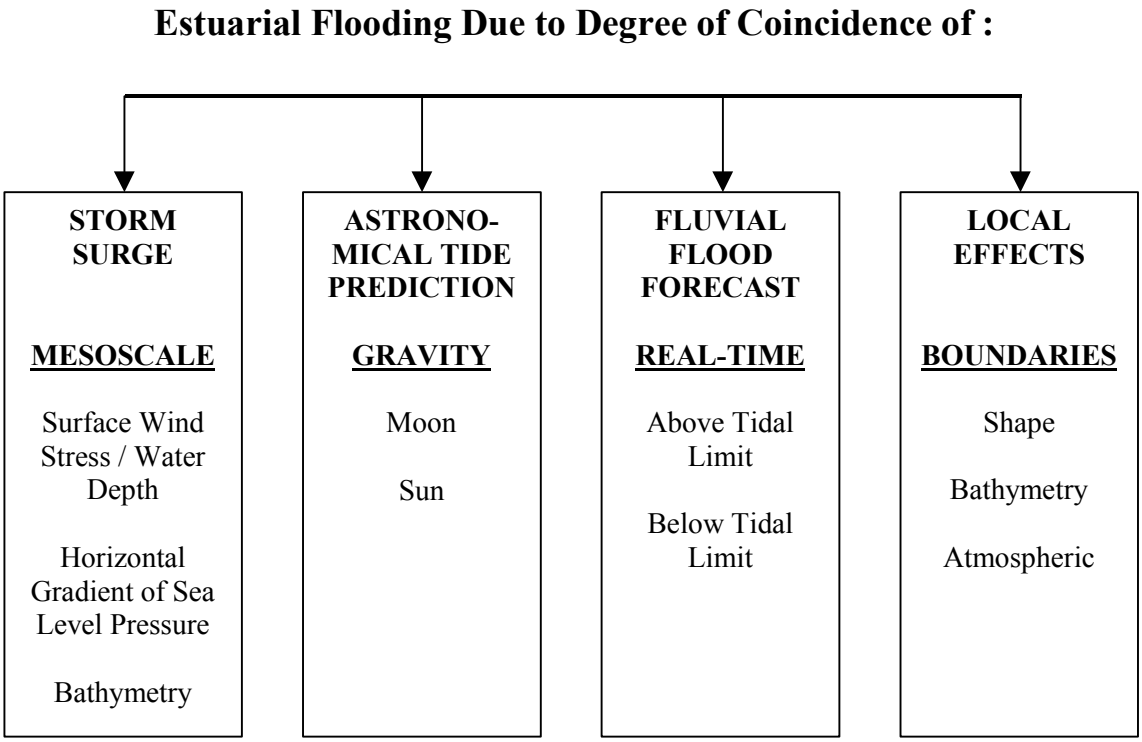

Figure 2.1 Factors Affecting Estuarial Flooding

North West Europe contains a wide range of oceanographic regimes. Resonance produces large tides in the Bristol Channel, the Gulf of St. Malo and the eastern Irish Sea, which dominate their dynamics, whereas tides in the Baltic and Mediterranean are small. The North Sea is large enough to support propagating (as long waves) tides and storm surges. Surges generated north and west of Scotland can travel into the North Sea, south along the east coast of England returning along the Dutch, German and Danish coasts. These are known as externally generated or "external" surges. Extensive areas of very shallow water susceptible to large locally generated ("internal") storm surges occur in the German Bight. In contrast the Iberian peninsular has narrow shelves bounded by deep ocean so surges contain a significant hydrostatic pressure generated component modified by the local effects of coastal winds.

2.3 Overview of UK Tide and Surge Forecasting System

The Met Office has run 2D tide-surge models developed by the Proudman Oceanographic Laboratory routinely since 1978 (Flather, 1979, Flather *et al.* 1991). The present model, CS3, introduced in 1991, covers the NW European shelf (12ºW to 13ºE, and 48º to 63ºN) with resolution 1/6º in longitude by 1/9º in latitude, ~12km. It has open boundary input of 15 tidal harmonics and an external surge component, assumed hydrostatic. Tide generating forces and the drying and flooding of inter-tidal areas are accounted for. The model is driven by wind and surface atmospheric pressure data from the Met Office's limited area atmospheric model (LAM), with resolution about 50km

and 1 hour. Two runs are carried out each day, comprising a hindcast from T-12 to T+00, and a forecast covering T+00 to T+36 hours. The hindcast runs are forced by met data from the atmospheric model assimilation cycle, incorporating met observations. [In mid-July 1999, the LAM forcing was replaced by data from a new meso-scale atmospheric model on a rotated latitude-longitude grid of 0.111º (~12 km). Four surge model runs per day are carried out, each comprising a 6 hour hindcast + 36 hour forecast.] The model is used to predict the storm surge component, accounting for interaction with the tides, by subtracting the model predicted tide from the tide with surge solution. This is added to the harmonically predicted tide based on tide-gauge observations to estimate total water level.

Results are used by the UK Storm Tide Forecasting Service and the Environment Agency (EA) as the basis for flood warnings on the coasts of England and Wales. The UK National Tide Gauge Network consists of gauges at about 35 sites, from which data are retrieved in near real-time to check forecast accuracy and for assimilation. The model forecast accuracy achieved varies for different parts of the coast - typically ~10 cm (RMS).

Additional models have also been introduced to address specific problems. Shelf-scale models did not provide useful surge forecasts for the Bristol Channel, with its large tidal range and strong interactions. This led to the development of a system of 1-way nested local models with 4km and 1.3 km grids linked to a 1D model of the River Severn. These models use boundary tidal input of 26 harmonics and surge components interpolated from the shelf model. Because the tide-surge interactions are so strong, separation of the surge component is difficult. The resulting surge in the upper Channel also exhibits rapid changes around the time of tidal high water, causing problems with interpretation of the results for flood warning. Tuning of the models (Amin and Flather, 1996) provided accuracy for tidal prediction comparable with that of the harmonic method and allowed the models to be used to predict directly total water levels.

To provide surge forecasts necessary for operation of the Thames Barrier, a 2D model of the southern North Sea and eastern English Channel, linked to a 1D model of the River Thames was set up by POL in 1989 and is run by the EA at the Barrier site. Open boundaries are at 55ºN, 5ºE, and at 2ºW. A simple non-optimal assimilation scheme – the "boundary correction method" (Flather, 1984) – uses data from the tide gauges at North Shields and Newhaven to correct errors in open boundary surge input taken from operational shelf model runs carried out at the Met Office. This gives a useful improvement in surge forecast accuracy during the ~9 hour propagation time from the boundary to the Barrier; the lead-time required for decisions on closure. (N.B. The 1D POL model is currently being replaced by a 1D ISIS model of the tidal Thames.)

A larger English Channel – North Sea model (ECNS) uses a similar approach to assimilate data from the tide gauges at Aberdeen and Newlyn. This model has been run at the Met Office for the last 3 years.

The UK has a long coastline with varied tide and surge conditions. Further local models for complex sections have been developed but not yet implemented operationally. Major surge events are generally well handled and moderate surges on large spring tides cause more forecast and warning errors. Some cases, with external surges travelling south along the east coast of England during periods of south-west winds, have been

problematic. Figure 2.2 shows predictions of a typical external surge in November 1998 from the UK operational model archive. Flather and Smith (1993) investigated the causes of a significant under-prediction of surges on the east coast and in the Thames Estuary in January 1993. They showed that a small perturbation near the Wash in the south-west winds was not forecast by the atmospheric model. As a result, model offshore winds were too strong and the predicted surge was too small. In this case the error was generated within the forecast, not from initial conditions, and reached coastal points within a short time. Such errors are difficult to correct. Even the most sophisticated assimilation schemes may be ineffective in such situations.

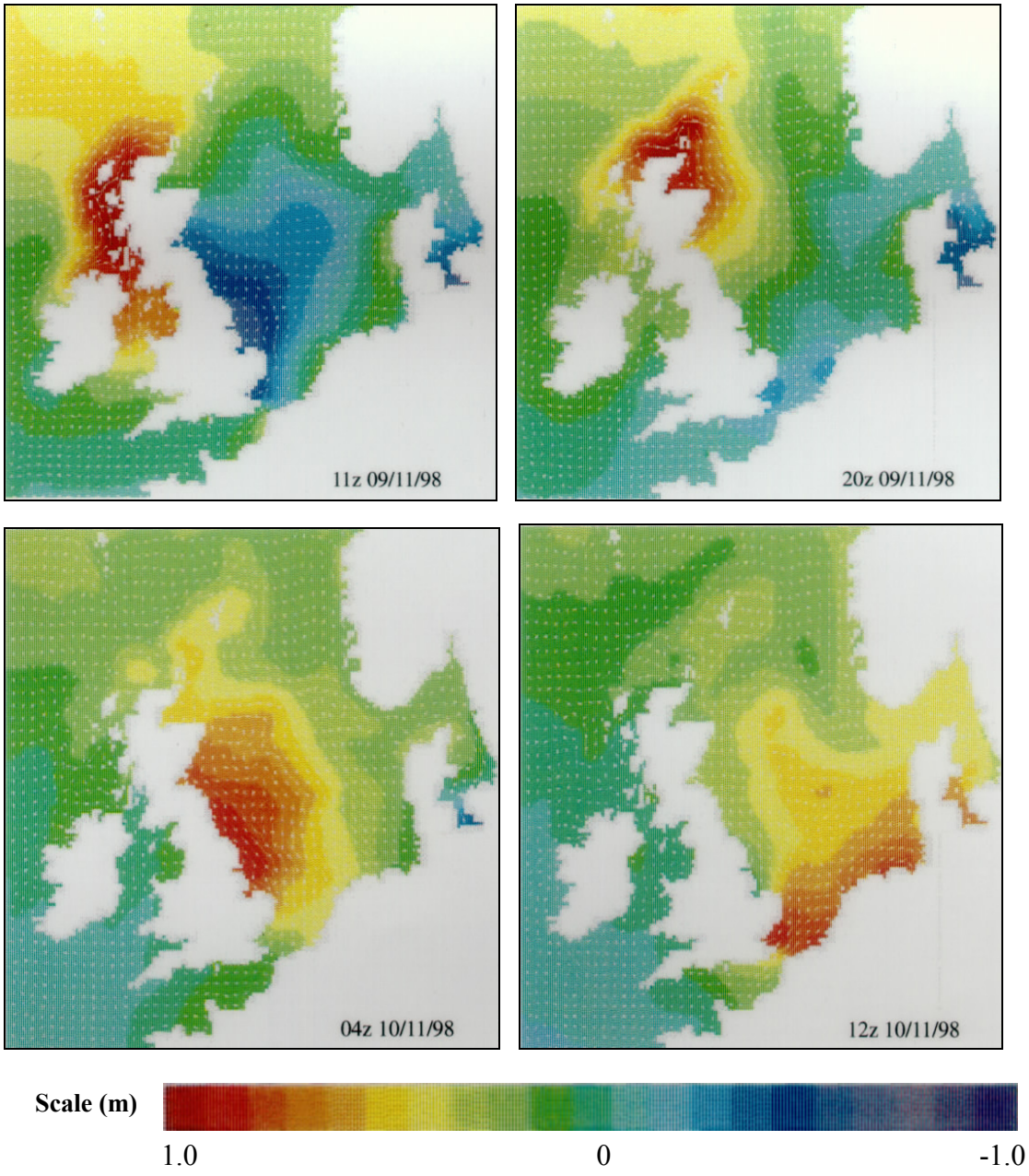

Figure 2.2A Typical External Surge Event from the UK Operational Storm Surge Model Archive, Showing Surge Generation West of Scotland, Followed by Propagation Around the North of Scotland and Southwards Along the East Coast of England into the Southern Bight of the North Sea (source: Flather (2000))

2.4 Overview of Other Operational Systems

2.4.1 Norway - Tides and Storm Surges

At the Norwegian Meteorological Institute (DNMI), the three-dimensional ocean model ECOM (Estuarine, Coastal and Ocean Model), a version of the Princeton Ocean Model, is used to forecast storm surges and currents (Engedahl, 1995). The model is run on a 20km Cartesian grid on a polar stereographic projection covering most of the NW European continental shelf, the eastern Norwegian Sea, & the Barents Sea. For storm surge prediction, ECOM is run in 3D barotropic mode (with 12 "sigma" levels in the vertical); a 3D baroclinic run with 17 sigma levels provides currents (mainly for input to an oil drift model), together with sea surface elevation, temperature and salinity. Runs are carried out twice a day, at 00 and 12 UTC, to produce forecasts to T+48 hours. The forcing consists of fields of 10 m wind and atmospheric pressure at MSL provided six hourly at 50 km resolution by the operational HIRLAM weather prediction model at DNMI. Each forecast is preceded by an 18 hour hindcast forced by six hourly analysed fields from HIRLAM, giving a total simulation time of 66 hours per run.

On lateral open boundaries, both model runs are forced by multi-year monthly mean climatological fields of sea level and currents. At present, the tides are not included. The 3D baroclinic run is also forced by climatological salinity and temperature at the boundaries, and includes monthly mean fresh water inputs from the Baltic and the major European rivers. To prevent the model results from becoming unrealistic, the prognostic fields of salinity and temperature are relaxed towards the climatological mean in the deeper parts (below approximately 500 m). At the surface the fluxes of salinity and temperature are controlled by relaxation (nudging) using climatological mean surface values. All operational forecasts are run on sequential or parallel (CRAY J90 / CRAY T3E) computers in Trondheim.

2.4.2 Denmark - Tides and Storm Surges

Since 1990, the Danish Meteorological Institute (DMI) has run a nested system of 2D models based on "System21", developed at the Danish Hydraulics Institute. This covers the North Sea, Skagerrak, Danish Belts and the Baltic with grid resolutions of about 18km, 6km and 2km (Figure 2.3). Forecasts covering the period T+00 to T+36 hours are run twice each day to predict sea levels for coastal flood warning along the Danish coast (in particular the Danish Wadden Sea). Forecasts start at T = 00 UTC and 12 UTC and are preceded by a 24 hr or 36 hr hindcast starting at 00 UTC on the previous day. Extended water level and current prediction runs for T+00 to T+120 hours were carried out during construction of the Great Belt Link. The 36 hour forecasts are driven by 10 m winds and MSL atmospheric pressure from the DMI version of HIRLAM, with 0.15° and 1 hour resolution, but for the extended 5-day forecasts UK Met Office LAM data at 1.25° and 6-hour resolution are used.

On open boundaries (Scotland to Norway and in the Dover Strait) 10 tidal constituents (no surge) are introduced. Twenty-two Danish tide gauges provide data for validation. In addition, data from 4 British and 6 Swedish stations are used for monitoring and calibration. Vested *et al.* (1995) describe the system and accuracy achieved. Average RMS errors over all stations and for operational forecasts 6 – 18 hours ahead are about

15 cm. Experiments with data assimilation using the Kalman filter approach developed by Heemink (1988) have also been carried out. Assimilation can improve the first few hours of the forecast (Vested *et al.*, 1995).

The network of tide gauges in Denmark is operated collaboratively by DMI, the Royal Danish Administration of Navigation and Hydrography (RDANH), and the Danish Coastal Authority. RDANH is responsible for navigational safely and maintains 13 water level stations, established between 1991 and 1994, and oceanographic stations, established 1994-96, with ADCP and temperature – conductivity chains providing information in the Belt seas (Buch, 1997).

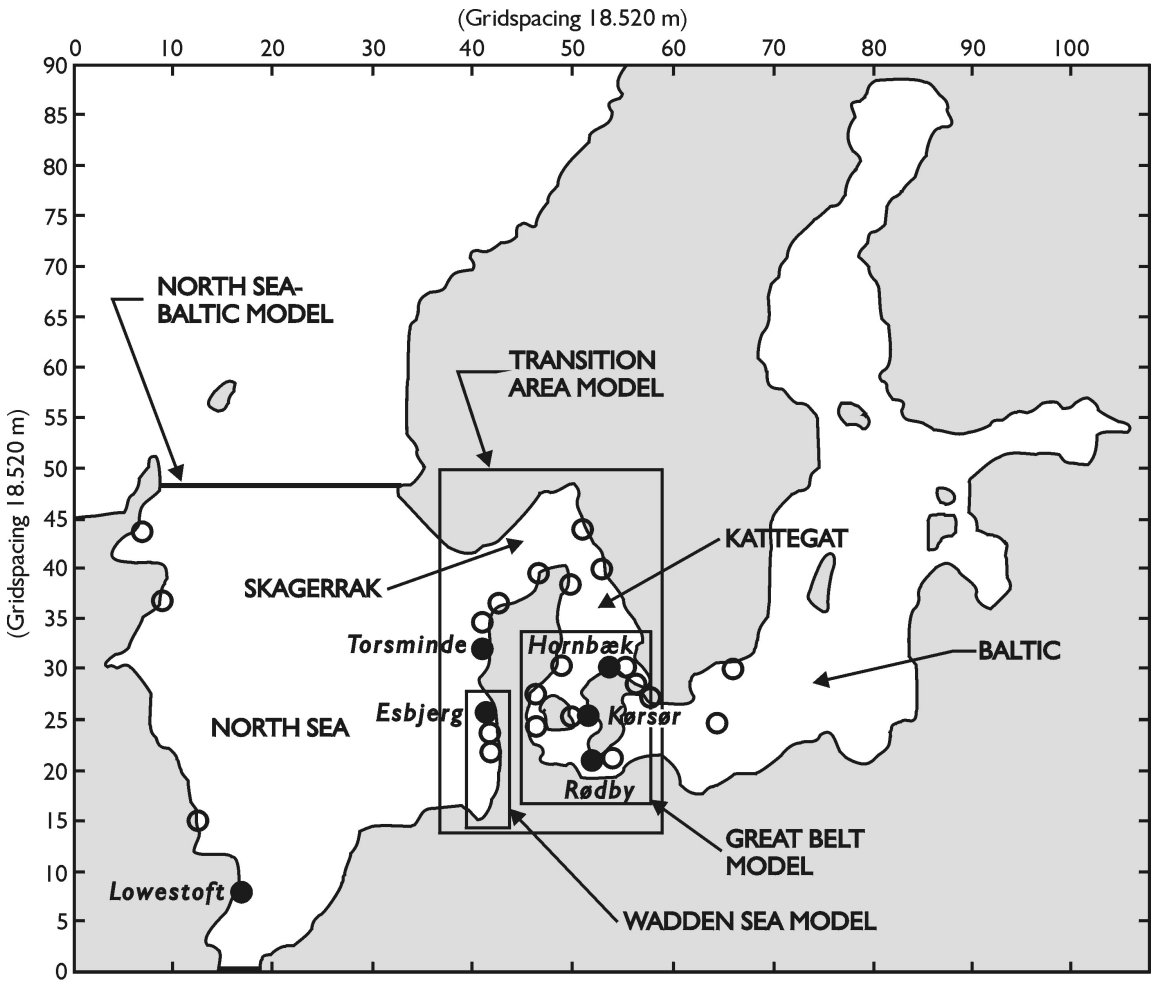

Figure 2.3Overview of the DMI Operational Model (source: Flather (2000))

The "Maritim" service, operated by DMI, RDANH and the Danish Coastal Authority, provides tide predictions, forecast results and measurements in digital and graphical form, updated every few minutes, in real time on the Internet (http://www.dmi.dk/).

At present, real-time wave predictions are not run in Denmark, but a system using cycle 4 of the WAM spectral wave model is being developed and expected to be operational from the end of 1999.

2.4.3 Germany - Tides and Storm Surges

Since 1983 the Bundesamt für Seeschiffahrt und Hydrographie, BSH, have developed and run a system of 3D baroclinic models covering the North Sea, Baltic and English Channel (Kleine, 1994; Dick, 1997) and a new version was introduced at the start of 1999. Nested grids are used with resolution of ~10 km in the whole region, and 1.8 km in the German Bight, Kattegat and western Baltic. The models are forced by meteorological forecast data from global and local area models of the Deutscher Wetterdienst (DWD) (resolution: 30 km/15 km), transmitted to BSH each day. Boundary inputs include tides (14 harmonics), external surges calculated by a 2D north east Atlantic model, and river runoff. For the advection of temperature and salinity an algorithm has been developed which gives low numerical diffusion (Kleine, 1993). Heat fluxes between atmosphere and sea surface are calculated to simulate realistic water temperatures in the surface layer. Since the density distribution and currents are also influenced by the ice distribution, an ice model computing ice thickness and compactness has been included, accounting for ice dynamics and thermodynamics as well as wind and current induced ice drift. Data from a DWD wave forecast model are used to account for the influence of waves on water levels and currents in shallow water; in particular effects of radiation stress producing wave induced currents and wave set-up and set-down. Forecasts covering T+12 to T+60 hours are run once each day (during the night), with initial data from the model fields at T+12 hours of the previous forecast. Water level, currents, salinity, temperature, density and the ice distribution are predicted, with output fields stored every 15 minutes.

Results can then be used in dispersion and transport models (e.g. for pollutants, oil spills and tracking drifting objects). The water level forecasts, together with real-time data from the German, Dutch and UK tide gauges networks, and other tools are used by the water level prediction and storm surge warning service. The accuracy of HW level prediction by the baroclinic circulation model for different German stations is between 10 and 20 cm (RMS); standard deviation is between 15 and 25 cm.

Especially for the water level prediction service of BSH, a 2D tide-surge model has recently been implemented for surge prediction. This model covers only the North Sea with 10 km resolution and is forced by tides and DWD meteorological forecasts. Two runs are carried out, the first with tide and met. forcing; the second run with tide only. By subtracting “tide” from “tide + surge” solutions surge values for German stations are determined. The 'surge model' runs much faster than the 3D-baroclinic model, so that two forecast runs covering T+00 to T+84 hours can be computed each day. The accuracy of the 'surge model' is also higher than that of the 3D-baroclinic model because errors in the models tide predictions are, to a large extent, eliminated. In operational use, the mean absolute deviation between measured and modelled HW and LW surges is between 10 and 15 cm, the standard deviation is about 15 cm. Figure 2.4 shows a frequency distribution of differences between measured and modelled surge values for all high waters in 1998 at Cuxhaven. Generally good agreement is obtained with occasional large errors, up to –80 cm, which can cause problems for flood warning. This is typical of most operational surge models.

For water level predictions in the river Elbe two regional models are run at BSH; a 2D model developed by HYDROMOD (see below), and an inverse 1D model including data assimilation of water levels.

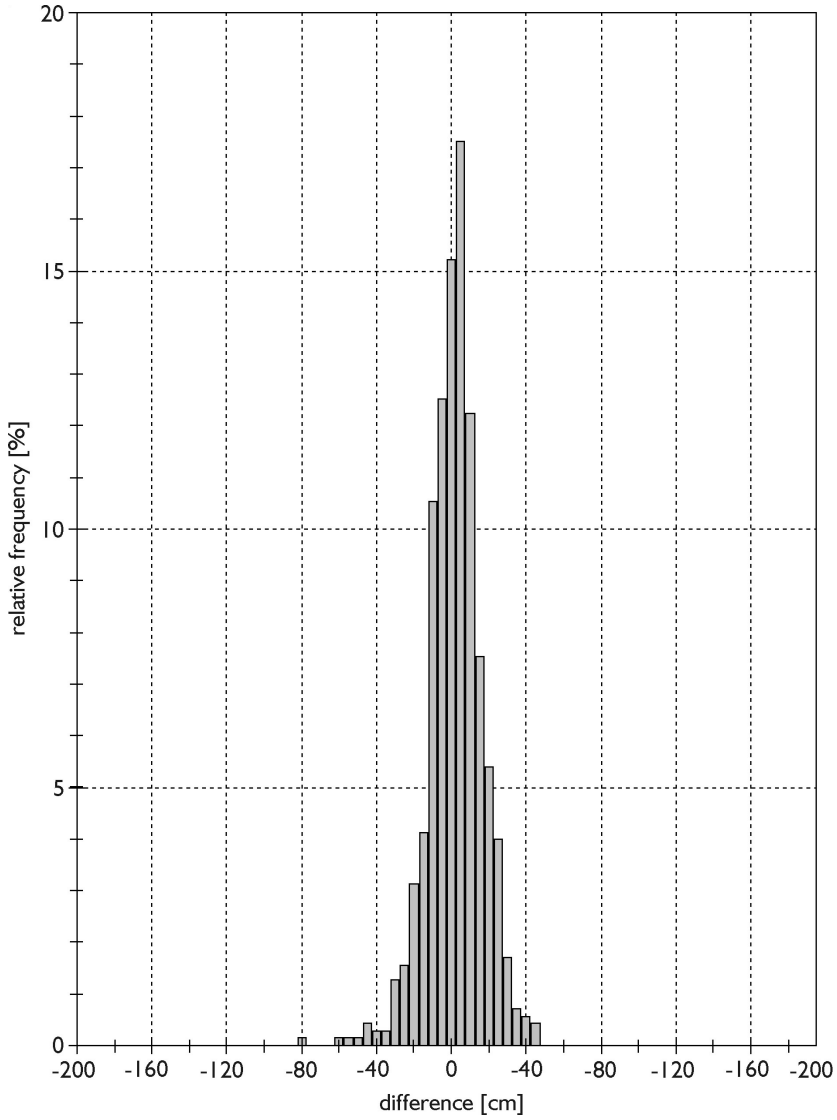

Figure 2.4 Frequency Distribution of Errors (Model - Observed) in Surge Elevation at High Water During 1998 at Cuxhaven (source: Flather (2000))

An operational 3D model for the Elbe estuary, originally developed in the EUREKA-EUROMAR project "OPMOD" (OPerational MODelling of Regional Seas and Coastal Waters), has been run routinely by HYDROMOD in Wedel since autumn 1994 (Nöhren *et al.*, 1995). The model area extends from the tidal weir at Geesthacht (east of Hamburg) to the outer estuary west of Cuxhaven and includes a large area of ecologically important tidal flats, which are part of Wadden Sea national parks. Driven by meteorological and hydrographic data from larger-scale forecast models and field stations, the operational system produces three-dimensional hydrodynamic fields (currents, water level, salinity, water temperature) on a 250 m horizontal grid with a mean vertical resolution of 2 m every three minutes. Output fields and meso-scale model input have been stored since 1995 for statistical analysis and environmental monitoring.

The system is used both for short-term forecasts and medium-term monitoring purposes in the Elbe estuary. For the latter applications water temperature and salinity especially are of great importance. Information about salinity, water temperature, and water level

at the model open boundaries in the German Bight, discharge and temperature information for tributaries and the upper Elbe at Geesthacht as well as global radiation, wind speed and direction over the whole area is essential for accurate forecasts. For model validation and additional environmental assessment purposes, useful hydrographic and meteorological data from field measurement stations along the river are available.

2.4.4 Sweden, Finland, Poland, Germany and Denmark - Baltic Collaboration

Within the framework of EUROGOOS, a development plan for operational modelling of the Baltic Sea has been established (Woods *et al.*, 1996, p112; Woods et al., 1997, p.13; Dahlin, 1997). The partners are the Swedish Meteorological and Hydrological Institute (SMHI), the Finnish Institute of Marine Research (FIMR), the Polish Maritime Institute in Gdansk, BSH in Germany, and RDANH Denmark. The main aim is to establish a common operational system for all states surrounding the Baltic Sea.

Central to this is a high-resolution baroclinic ocean model of the Baltic (HIROMB) developed by BSH and SMHI and based on the 3D model of BSH (see above). This is a 3D primitive equation model with 24 "layers" increasing in thickness from 4m for the surface mixed layer to 60m for the deeper layers. It includes one equation boundary layer dynamics and a viscous-plastic ice model. A system of nested grids, designed to meet the requirements of all partners, is used with resolution ranging from 12 nautical miles (~22 km) for the North Sea reducing to 3 nautical miles (~5.5 km) east of 6°E and covering the eastern North Sea, the Skagerrak, Kattegat and Baltic Sea. Interaction between the two grids occurs at 6°E where flux, temperature, salinity and ice properties are interpolated and exchanged. As in the BSH scheme, a coarse grid storm surge model for the NE Atlantic supplies the water level at the coarse grid open boundary between the Atlantic and the North Sea. Forcing consists of atmospheric pressure, wind speed and direction, humidity, temperature and cloud coverage from HIRLAM and fresh water inflow is given at 80 major river outlets. Wind waves enhance mixing and mass transport (Stokes' drift) in the surface layer and this is accounted for using outputs from the HYPAS wind wave model.

HIROMB was originally set up at SMHI in the summer of 1994 and has run in pre-operational mode since the summer of 1995, making daily 48-hour forecasts of sea level, current, temperature, salinity, and ice conditions.

Wave conditions in the northern Baltic are characterised by complicated fetch geometry and bathymetric effects (focussing etc.). The importance of wave forecasts in the area was highlighted by the "Estonia" disaster in 1994. The HYPAS wind wave model is run at SMHI for the North Sea (including part of the Norwegian Sea) and Baltic, providing wave forecasts and inputs to HIROMB. Daily forecasts from HIROMB are transmitted to all partners and are available, along with wave forecasts from HYPAS on the Internet (password protected pages at http://www.smhi.se/). HIROMB is currently being moved to a fully operational environment.

The Baltic countries also operate observational networks. For example, the Sea Level and Wave Information Service of FIMR operates a network of tide gauges, 12 of which provide real-time data used to provide hindcasts and forecasts (Grönvall, 1997).

2.4.5 The Netherlands - Tides and Storm Surges

Since 1990, KNMI have run the Dutch Continental Shelf Model (DCSM), a 2D tide-surge model based on the "WAQUA" system developed by Delft Hydraulics and Rijkswaterstaat (RIKZ), (Gerritsen *et al.*, 1995; Phillipart and Gebraad, 1997). The present operational model covers the NW European Shelf with resolution 1/4º in longitude by 1/6º in latitude, ~16 km. Ten tidal harmonics and surge elevation, assumed hydrostatic, are introduced on the model open boundaries. Since 1993, the DCSM has been driven by 10 m wind and surface pressure from the KNMI HIRLAM atmospheric model. Forecasts extending to T+48 hours are run every 6 hours, 4 times per day. The model is used to compute the storm surge component of sea level by subtracting model generated tide predictions, derived from "off-line" simulations, from the tide + surge real-time runs. Best estimates of total sea level are then obtained for tide gauge sites by adding the model surge to the more accurate local tide predictions produced by Rijkswaterstaat using the standard harmonic method.

A special feature of DCSM is the use of "state-of-the-art" optimal methods, specifically an adjoint model for calibration (e.g. Phillippart *et al.*, 1998) and since 1992 assimilation of real-time measurements from tide gauges using a steady-state Kalman filter (Heemink, 1988). Assimilation can improve forecasts on the Dutch coast during the first 10-11 hours, compared with equivalent deterministic forecasts, see Figure 2.5 (Hans de Vries, 1998, personal communication). This timescale is, presumably, determined by the surge propagation from NE Scotland to the Dutch coast. Thereafter, results may be less accurate than deterministic equivalents. Also, the success of the assimilation procedure depends on high quality data being used. For these reasons, model results with and without assimilation are produced and disseminated.

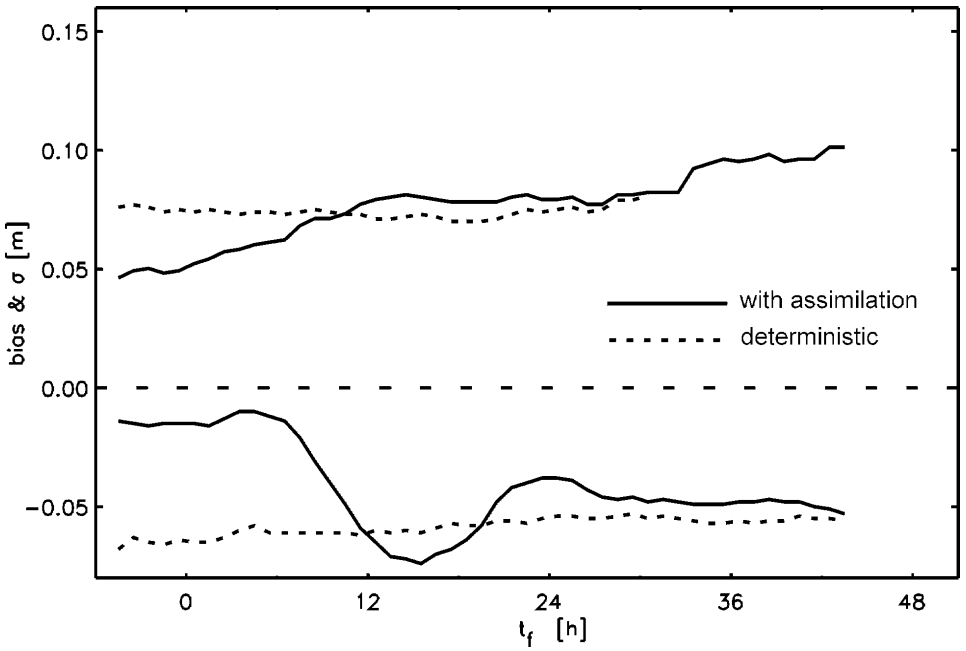

Figure 2.5Mean Error Statistics (Bias and Standard Deviation in Metres) for High Water as a Function of Warning Interval (t_f in Hours) at Hoek van Holland During March-May 1998, from the Dutch CSM Run at KNMI. Dashed Lines are Deterministic Forecasts and Continuous Lines Equivalents Using Assimilation of Tide Gauge Data (source: Flather (2000))

Outputs are supplied to the Hydro Meteo Centres in Hoek van Holland and Middelburg for use in flood warning. Information about the Dutch Storm Surge Warning Service (SVSD), status of coastal sectors and flood barriers can be found on the Internet (http://www.waterland.net/).

2.4.6 Belgium - Tides and Storm Surges

Since the late 1970s, MUMM (Management Unit of the North Sea Mathematical Model) has run a 2D vertically integrated hydrodynamic model, covering the North Sea (Adam, 1979). The horizontal resolution was 20' in latitude and longitude in the northern part of the domain and ~7 km in the southern North Sea. In 1998, a new 2D model covering the whole NW European continental shelf was introduced for operational use at MUMM and at AWK (Afdeling Waterwegen Kust; Ministry of the Flemish Government) (Ozer *et al.*, 1997; Van den Eynde *et al.*, 1998). The new model uses a uniform horizontal resolution (2.5' in latitude and 5' in longitude).

Surface wind and pressure forcing is provided by the UK Met. Office for both models. Tidal forcing, with 8 tidal harmonics, and surge elevation (assumed hydrostatic) are introduced along the model open boundaries. The models are run, automatically, twice each day as soon as the meteorological data are available. Forecasts cover a period of 4 days. Typical accuracy of sea surface elevation (level including model tide) is about 15 cm (RMS). Variability between successive forecasts can be, in some circumstances, relatively high due to changes in meteorological data.

Results of the North Sea model at Ostend are available on the Internet in tabular form at (http://www.mumm.ac.be/docs_en/forecasts/mops/ostend.html). The user interface for the continental shelf model is implemented in HTML providing an easy access to the model forecasts. A similar user interface for the North Sea storm model is also being implemented.

2.4.7 France - Tides and Storm Surges

Météo France has developed a 2D storm surge model configured as a "stand-alone" system to predict surges generated by tropical cyclones. Forcing is provided as a small number of cyclone parameters (position, intensity and size) using an empirical-analytical model. Systems are operational in the French Antilles, New Caledonia, French Polynesia and in La Reunion (Daniel, 1997). At present, surge models are under development for the coasts of France. The first, covering the Channel and Bay of Biscay (43°N - 52°N, 8.5°W - 4°E) with a 5′ latitude – longitude grid and open boundary input of 16 tidal harmonics, will be operational by the end of 1999. A second model for the Mediterranean coast will follow in 2000. The Météo France mesoscale atmospheric model will drive the models.

2.4.8 Spain - Tides and Storm Surges

The "Nivmar" storm surge prediction system, developed and run at Clima Marítimo, predicts sea level for Spanish coasts. It is based on the HAMSOM ocean circulation model (Backhaus, 1985; Alvarez *et al*, 1998) applied in 2D vertically-integrated mode on a grid with resolution reducing to 1/4º in longitude by 1/6º in latitude. The model is

driven by surface wind and pressure fields from the HIRLAM atmospheric model run by the INM (Instituto Nacional de Meteorología). Two runs are carried out per day, each consisting of a hindcast from T-12 to T+00 forced by analysed met. data, and forecast to T+48h. Since the continental shelf is narrow, with shallow water confined to a coastal strip, atmospheric pressure effects dominate the sea level response to storms. Also because the water is generally deep, interactions between tide and surge components are weak and can be neglected. Thus the model is used to predict the surge component driven by met. forcing only. Water levels are computed as the sum of model predicted surge and tide predicted using the harmonic method from analyses of data from tide gauges of the REDMAR network (Perez and Rodriguez, 1994). Predictions are stored and distributed on the web (http://www.puertos.es/Nivmar). Figure 2.6 shows an example.

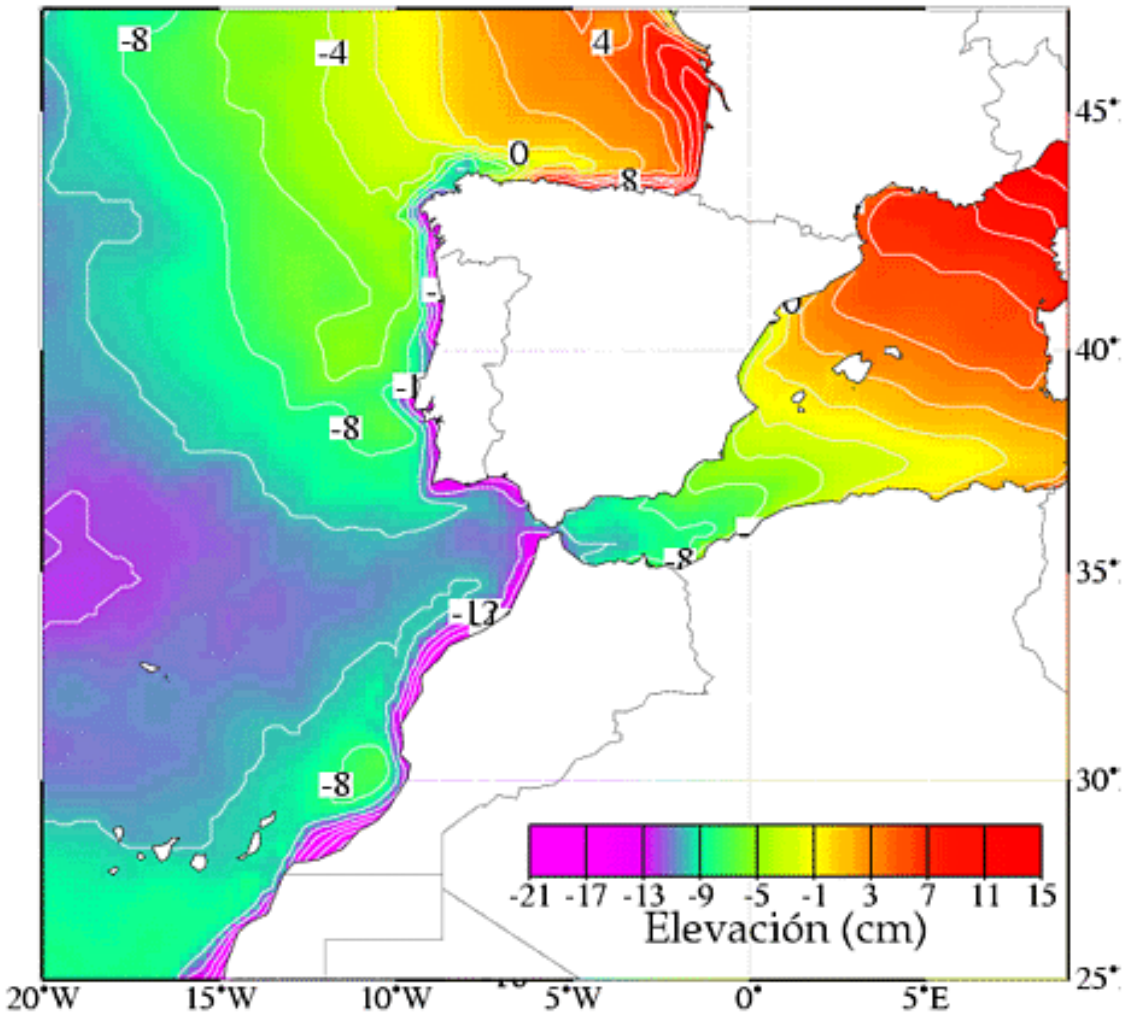

Figure 2.6 Predicted Surge Residual at 06:00 GMT 8 December 1999 Produced by the Nivmar Surge Forecast System at Clima Maritimo. Note the Rapid Variation in Surge on the Narrow Continental Shelf (source: Flather (2000))

3. NUMERICAL MODELLING

3.1 The Depth-Averaged Equations and Their Alternatives

The motion of an incompressible viscous fluid (such as water) can be described by the Navier-Stokes equations, which express the conservation of mass and momentum in three dimensions. Although in principle they describe both laminar and turbulent flows, in practice their solution for turbulent flows is impracticable in all but the very simplest of situations. Solving the Navier-Stokes equations is particularly difficult in the field of hydraulics which deals with very high Reynolds number flows in regions of complex shape, (such as rivers, estuaries, lakes and coastal seas), where in addition there is the complication of a free surface. Roberts (1994) stated that the difficulties encountered, when applying the Navier-Stokes equations to turbulent flows (see Rodi, 1984) stem from the non-linearity of the equations and the large range of scales over which significant flow phenomena occur in turbulent motion.

In order to progress, the equations are usually time-averaged over a period which is long compared to that of the turbulent fluctuations but still sufficiently short compared to the time scale of the mean flow. This results in the Reynolds equations. When modelling shallow seas and estuaries where the length scale is an order of magnitude larger than the depth scale, further simplifications can be made by depth-averaging. The resulting depth-averaged Reynolds equations, also known as the shallow water equations, consist of two equations describing the conservation of momentum in the x- and y- directions and a continuity equation describing the conservation of mass. The equations are once again non-linear but can now be solved satisfactorily using a variety of numerical methods. Often what is gained in the simplification of the Navier-Stokes equations is lost in the requirement for empirical information about internal stresses within the fluid.

However the two-dimensional depth-averaged equations are not the only equation system used for hydraulic modelling. By assuming that the flow is planar, and ignoring one space dimension, the Navier-Stokes equations can be used directly. The two-dimensional Navier-Stokes equations have the advantage that they do not have recourse to empiricism and thus describe the flow exactly. The criteria of planar flow in a fluid stretching in all directions is better satisfied in other areas of computational fluid dynamics, and the Navier-Stokes equations are a popular starting point for modelling flow around aerofoils and other two-dimensional structures (Thames *et al.*, 1977). For hydraulic modelling, the Navier-Stokes equations suffer from an inability to represent free surface gradients as they must assume a horizontal "rigid lid" free surface. Nevertheless, some investigators have opted to use the two-dimensional Navier-Stokes equations to represent the hydrodynamics of shallow water flows. An example of this is the computer program, ODYSSEE, developed jointly between Delft Hydraulics Laboratory in The Netherlands and the Laboratoire National d'Hydraulique in France which solves the time-averaged Navier-Stokes equations on an orthogonal curvilinear grid (Officier *et al.*, 1986). The model has been applied to small scale hydraulic flows over which the "rigid lid" approximation was justified, such as around harbour breakwaters and at river bifurcations.

As well as depth-averaged equations in which the independent variables are x, y and t, width-averaged x, z, t and section-averaged x, t equations may be derived. Weare (1982) discussed the scope of application of each of these types of model, while

Hinwood and Wallis (1975) reviewed existing tidal models and classified them in this way. One-dimensional x, t equations assume that all flow is predominantly along one axis, possibly curved, and are suitable for describing flow in rivers or open channels. The advantage of such an equation set is its simplicity and minimal computing requirements. Rossiter and Lennon (1965) provided a detailed description of their one-dimensional model of the Thames Estuary. The x, z, t equations describe flow with significant variations in the vertical but only in one horizontal dimension and as such are less applicable to natural water bodies.

A quasi three-dimensional shallow water model was developed by Jin and Kranenburg (1993) which incorporated two modules; the first solved the depth-averaged equations of flow; the second determined the vertical velocity distribution. Most fully three-dimensional hydraulic models draw on the techniques of atmospheric modelling (for example Arakawa and Lamb, 1977), and use the spectral method in which the vertical dimension is split into a number of layers over which the depth-averaged equations are assumed applicable. A number of parallel two-dimensional shallow water equation models are therefore solved, whose interface shear stresses are given by empirical formulae depending on the velocity difference between the layers. Such models are thus an extension of depth-averaged models. They are computationally very expensive and therefore have only been viable in recent years, but will certainly become more popular since they allow a greater variety of hydraulic flows to be studied and admit a more detailed description of turbulent processes. The most commonly used methods for splitting the flow into horizontal layers is to employ a ó-transformation in the vertical which ensures that the layer thickness is proportional to the local water depth. Yin and Chen (1982) used this approach in a two-layer tidal model of the Taiwan Strait. Sheng (1986) used a ó-transformation in the vertical and a curvilinear finite-difference grid in the horizontal. Davies and Lawrence (1994) used a multi-layer model to study the interaction of tidal- and wind-induced currents, and Stansby and Lloyd (1995) found that by using a ó-stretched model which simulated the vertical velocity profile, the use of an empirical formula for the bed shear stress could be avoided. Huang and Spaulding (1995) argued that having layer thickness proportional to water depth was not always desirable if significant flow occurred in a surface layer of constant thickness, and they introduced a ã-coordinate to cope with this. Meanwhile Chau and Jin (1995) and Johnson *et al.* (1993) divided the layers at fixed values of z in the vertical, a method suited to regions of rapidly varying bathymetry. The model of Johnson *et al.* (1993) CH3-WES represents the current state of the art in three-dimensional modelling of tidal hydrodynamics, coupling a layered vertical model with a general curvilinear coordinate system in the horizontal, and has been used to study the hydrodynamics of Chesapeake Bay, Maryland. Multi-layer models of tidal flow represent an advance on depth-averaged models but are expensive and complex.

The shallow water equations are usually expressed in primitive variables, i.e. the Cartesian velocity components U and V in the x- and y- directions respectively, and the elevation of the water surface, æ, but the equations may also be written in terms of stream function, ø, and vorticity, ù. Hydraulic models based on these equations have been presented by Codell (1975), Ball *et al.* (1982), Kaar (1991) and Borthwick and Kaar (1993).

3.2 Numerical Solution Methods

The shallow water equations are second-order non-linear partial differential equations in the variables U, V and æand only admit analytical solution for simple geometrical cases when the non-linear terms are ignored. The use of numerical methods permits a far greater range of situations to be considered, and since the emergence of electronic computers in the 1940s increasing research has been devoted to the development of new numerical techniques. A great number and variety of numerical methods have been researched. Liggett and Cunge (1975) considered that the advantages of adopting a particular method for universal application are considerable, since programs could be exchanged, users would not have to learn a variety of methods, and results could be easily compared. However, there is no "best" solution since each method has its advantages and disadvantages and each can be considered appropriate in certain circumstances. Most numerical methods rely on approximating the governing differential equations by a set of algebraic equations at a finite number of fixed points throughout the solution domain, and at a series of timesteps. Most widely used amongst these Eulerian "grid based" techniques are the finite-difference and the finite-element methods. However the grid-based finite-volume method and the Lagrangian method of characteristics must also be considered, since these both have their particular strengths.

3.2.1 The Methods of Characteristics

The characteristics of a system of partial differential equations are defined as those lines or surfaces (functions of time and space) which join all points on the boundary of the domain of influence of some disturbance. The method of characteristics describes the motion of the fluid by following the flow along the characteristic lines. The shallow water equations, normally written as partial differential equations, are rewritten in their characteristic form as ordinary differential equations containing total derivatives of the hydrodynamic variables. Starting from a known initial solution at a selection of points throughout the flow domain, the characteristics emanating from these points form a lattice in the graph of space and time. Where two characteristics cross, the values of the hydrodynamic variables can be determined from known values at previous times by numerical integration and simultaneous equation solution. The method is described in detail by Abbott (1975, 1979) and formed the basis of much of the early DHI code for solving the shallow water modelling problems.

The points at which the solution is known in the future are therefore not fixed in space, but move with the fluid. Likewise the times at which the solution is known vary from one point to another. This is often seen as a disadvantage of the method of characteristics compared to the fixed space interval/fixed time interval numerical methods, but it can be argued that in many problems it is in fact an advantage. Often the net becomes most dense in regions of rapid change exactly where the analysis needs closely spaced points for accurate computation (Abbott, 1975). Other advantages are that relatively few approximations need be made to obtain the numerical solution, and that the non-linear advective terms, so troublesome in other numerical methods, are properly treated. However, the method becomes considerably more difficult to implement in two-dimensional regions of complex geometry, and trivial changes in the form of the governing equations can result in major changes in the solution method. In view of this, methods have been developed which combine characteristics with the use

of a fixed space/time grid. Matsoukis (1992) presented a two-dimensional tidal model using such a characteristics method which he applied to the Bristol Channel. The solution at a grid node at the new time level was found by following five characteristics passing through that node back to the old time level, and interpolating for the flow solution at those points. Similar methods have been used by many researchers (Benque *et al.*, 1982, Li and Falconer, 1995, Hervouet, 1989, Stansby and Lloyd, 1995) to treat the advective terms within a finite-difference or finite-element scheme. The momentum equations are split into advection and propagation parts, and the advection equation is solved separately by characteristics. This technique is particularly popular when solving the species equation for the transport of pollutants where accurate simulation of advection is paramount, and many variations have been developed (Li, 1990, Holly and Preissmann, 1977).

3.2.2 Finite-Volume Methods

In the finite-volume method the flow domain is decomposed into elemental control volumes of quadrilateral or triangular plan form. The governing equations are then integrated around the perimeter of each element as the sum of the flux contributions along each face. The advantages of the method are that complex geometries may be treated accurately and mass and momentum fluxes are conserved exactly. However, although the finite-volume method is well established in the field of aeronautics for solving the Navier-Stokes equations (Periæ *et al.*, 1988) only a small number of studies have applied the technique to the shallow water equations. Alcrudo and Garcia-Navarro (1993) showed that the finite-volume method may be a powerful technique for hydrodynamic modelling since both subcritical and supercritical flows may be dealt with simultaneously, whilst Guillou and Nguyen (1995) developed a finite-volume model for the shallow water equations in general curvilinear coordinates and applied it successfully to the study of jet-forced reservoir flow.

3.2.3 Finite -Differences Versus Finite Elements

Finite-elements were proposed by Zienkiewicz at Swansea University and have found rapid acceptance particularly in the field of aeronautics (Zienkiewicz, 1977). In the finite-element approach the flow domain is covered with an unstructured mesh of triangular or quadrilateral elements. On each element the partial differential equations to be solved (the host equations) are approximated by a linear combination of simple shape functions of the space variable whose coefficients are the nodal values of the solution variables. The shape function approximations are substituted back into the host equations and the resulting discretised equations are minimised. Minimisation can be achieved by a number of integration methods depending on the form of the host equations, and results in a non-space matrix coupling the nodal values of the solution variables which is solved at each timestep. There are few constraints on the configuration of the finite-element mesh, thus the method allows for rapid cell size variation and alignment of the mesh to complex boundary shapes. The ability to concentrate cells in areas of particular interest means that it is ideal for studying features such as boundary layers and shock waves, and it has found regular application to the study of flow around aerofoils and turbines.

Several tidal models have been written using the finite-element method. Hervouet *et al.* (1994) give an overview of the finite-element TELEMAC code developed at Laboratoire National d'Hydraulique in France which is now a very popular shallow water equation model marketed by HR Wallingford in Great Britain. Other finite-element models for the shallow water equations have been written by Peraire (1986) who studied an area of the Bristol Channel, by Kodama and Kawahara (1994) who applied a finite-element code to Tokyo Bay, by Anagnostopoulis and Mpimpas (1995b) who studied wind-driven circulation in the Gulf of Thermaikos, and by Tabuenca and Vila (1995) who modelled hydrodynamics and pollution transport in the Bay of Santander.

The finite-difference method relies on reducing the host partial differential equations to algebraic equations at each node of a structured grid. Partial derivatives in the independent variables are replaced by algebraic difference expressions between neighbouring grid nodes. At a particular computation point, a derivative in a particular independent variable depends on the value at nodes in the grid which lie in the direction of the independent variable. The majority of systems of equations in the field of fluid dynamics are most conveniently expressed in Cartesian coordinates. It therefore follows that the derivatives in those equations are most simply discretised on a Cartesian mesh (an equispaced, rectilinear, orthogonal mesh) whose grid lines are aligned with the directions of the independent coordinates. When modelling flow in a rectangular domain, this choice of mesh is so intuitive that the computational modeller is unlikely to consider consciously the characteristics of the grid best suited to his purpose beyond the question of the cell size required to obtain a sufficiently accurate solution. In many applications of the shallow water equations to large scale natural water bodies (Leendertse, 1967, Reid and Bodine, 1968) the choice of finite-difference mesh was likewise taken to be Cartesian. However, the motivation to choose such a computational grid for the modelling of seas and estuaries is not so strong, because although the square-celled grid provides an excellent network on which to solve the governing equations in the interior of the flow domain, the Cartesian coordinate lines will not in general coincide with the arbitrarily curved coastal boundary. This raises the problem of implementation of boundary conditions.

If the physical boundary of the region being modelled does not pass through the nodes of the grid, the best the Cartesian grid can do is approximate the boundary by a series of steps. When solving the shallow water equations authors have taken two different approaches to this problem. Leendertse (1967) and Flather and Heaps (1975) straddled the physical boundary with the stepped boundary in order to reduce the discrepancy. Kuipers and Vreugdenhil (1973) and then Falconer (1976) included the entire physical flow domain inside their stepped boundary and introduced false depths to satisfy the continuity equation on the physical boundary. The latter procedure requires interpolation between near perimeter points and in both methods the sharp corners of the non-physical stepped boundary generate spurious vorticity. Pedersen (1986) also showed that a wave in incidence with a stepped saw-tooth boundary will undergo a quantifiable phase shift. However, in many applications the boundary conditions determine the nature of the entire flow solution. In other studies the boundary is the area of highest solution gradient and often it is at the boundaries that model predictions are of most interest for the purposes of the study. In each case it can be said that the need for interpolation at the boundary, when employing a Cartesian grid, introduces inaccuracies in the very region where accuracy is of the greatest importance.

Why then persist with finite-differences when the unstructured meshes of the finite-element method would appear to offer the answer to the problems of accurate boundary representation? One reason is historical. The finite-element method was only introduced in the 1960s and its application to shallow flow modelling is relatively recent. By this time the numerical techniques for solution of the shallow water equations by the finite-difference method were well developed. Another reason is the relative complexity of finite-element codes compared with finite-difference codes when applied to the same problem, both for the computer programmer and the end user. The use of structured meshes for finite-difference solutions means that each grid node has a well-defined set of nearest neighbours on which the solution at that point will depend. This admits an explicit solution in which the relationship can be clearly seen between the computer code for the calculation of the governing hydrodynamic variables and the original partial differential equations on which it is based. This is not the case with finite-element codes. The implicit integral solution by shape functions results in a complex matrix-based calculation which is not so clearly related to the host equations. Additionally, when applied to the shallow water equations, the finite-element approach must use a special minimisation method because the equations cannot be written in a variational form. The method of Galerkin (1915) is the most commonly used but the equations solved thus are only an approximation to the shallow water equations. Finally, as stated by Weare (1976a) the finite-element method is computationally more expensive because the number of calculations required per grid point per timestep increased with the band-width of the computational mesh, whereas for the finite-difference method this cost is independent of the size of the model.

In order to overcome the limitations of Cartesian finite-difference schemes while retaining their essential simplicity, curvilinear-grid difference schemes were developed. The basis of these methods is the use of a set of general *curvilinear* coordinates in which the boundaries of the flow domain follow a coordinate line. For this reason such curvilinear grids are often referred to as boundary-fitted. By taking this approach the boundaries may be followed by the mesh as closely as desired. However, the mesh lines are now curved, and intersect, in general, non-orthogonally. Thus partial differential equations which depend on a set of Cartesian coordinates, cannot be easily discretised. The governing hydrodynamic equations must therefore be transformed from being dependent on the Cartesian coordinates to being dependent on the new curvilinear coordinates. In the general curvilinear coordinate space (sometimes termed the logical space or the transformed domain) where the general coordinates themselves form a Cartesian system, the *transformed* host equations may then be discretised, as desired, on a regular celled mesh. Having solved the transformed equations in the transformed domain, results can be related back to the original physical flow domain. What remains to be done in order to transform the governing equations is to find a suitable reversible mapping between the two coordinate systems. This is the task of grid generation.

The transformed partial differential equations are longer than the original equations because they contain terms dependent on both curvilinear coordinates for each original spatial derivative. The transformed equations also require knowledge of the relationships between the two coordinate systems. In effect the problem has been changed from one of solving the relatively simple Cartesian hydrodynamic equations on a curvilinear grid with curved coordinate lines and a complex boundary, to solving the more lengthy transformed hydrodynamic equations on a square-celled grid with straight coordinate lines and a rectilinear boundary.

Barber (1990) offered the opinion that "boundary-fitted coordinate systems provide an approach which combines the best aspects of finite-difference discretisation with the grid flexibility usually attributed to finite-element procedures". Certainly the boundary-fitted methodology can be applied to fit complex boundaries as desired and indeed grids may be generated which concentrate grid lines into areas of particular interest, be they around sewage outfalls, in regions of deep water, or in areas of high solution gradient. However, the grid must retain a certain degree of orthogonality and smoothness if unacceptable truncation errors are to be avoided. Coordinate lines cannot be completely manipulated at will without regard for these factors. The issue to be decided is whether the advantages of increased accuracy at the boundary outweighs the disadvantages of increased complexity of the governing equations. In modelling tidal surges it probably does not whilst in modelling mixing processes it probably does!

3.3 Finite-Difference Solutions to the Shallow Water Equations

Within the field of finite-difference solutions to the shallow water equations there exists a wide variety of different approaches. The literature suggests different types of solution procedure; explicit, implicit, or semi-implicit, the use of conservative or non-conservative equations, different treatment of the advective and diffusive terms and different schemes for the treatment of flooding and drying. These early models are reviewed and the merits of the different approaches are discussed in terms of both boundary-fitted and Cartesian grid solutions.

3.3.1 Cartesian Shallow Water Models

Probably the first numerical solution of the shallow water equations was made by Hansen (1956) who derived the full non-linear equations in two and one dimensions by depth-averaging and then width-averaging the Navier-Stokes equations. The internal fluid stresses and the terms describing the advection of momentum were neglected in the two-dimensional numerical scheme, but the effects of bed friction, surface wind stress and the Coriolis force were modelled. An explicit solution procedure was employed. The depth-averaged model was used to study a storm surge in the North Sea and the one-dimensional model was used to simulate the tides in the River Ems. Later a similar model was used to study the M_2 tidal component in the North Sea (Hansen, 1962).

The work of Leendertse is quoted as the basis for many Cartesian grid solutions to the shallow water equations since in his report (Leendertse, 1967) he presented in detail the difference expressions, boundary conditions and solution procedure used, in a way that could be reproduced by future researchers. The alternating-direction-implicit scheme he employed to solve the shallow water equations is in common use today. Leendertse argued that the stresses introduced by the vertical integration could be neglected if the vertical velocity distribution was fairly constant, but he included the troublesome advective terms. The motivation for the work was the simulation of water waves generated by submarine nuclear explosions as they approached the shore. The resulting model was also used to study the tides of the River Rhine and the North Sea, and was

later developed into a water quality simulation model for well-mixed estuaries and coastal seas (Leendertse, 1970, Leendertse and Gritton, 1971).

Reid and Bodine (1968) developed an explicit tidal model for the simulation of hurricane flooding in Galveston Bay, Texas. Their mode ignored the non-linear terms of advection and diffusion but included the effects of wind and rain and was one of the first to allow for the inundation of dry land at times of flood. All these techniques were brought together by Abbott *et al.* (1973) to produce a computer package for solution of the shallow water equations which was claimed to be capable of modelling "any region of two-dimensional nearly-horizontal flow". The model System 21 "JUPITER" (2 dimensions, 1 layer) used a fractional step solution method and included such features as local grid refinement and flooding and drying of sub-regions. Early applications of the model were to study the effect of bridge construction in Denmark and to simulate tides in the Penang Strait.

In the same year, Kuipers and Vreugdenhill (1973) and Vreugdenhill (1973) carried the study of the shallow water equations forward by discussing the role of all terms in the full non-linear equations and by presenting a solution to these complete equations based on the alternating-direction-implicit scheme of Leendertse (1967). They also sought a better representation of curved coastlines with the restrictions of a square-celled grid by the use of near-boundary interpolation. Falconer (1976) developed this research further. His model of flow in a circular reservoir tackled the simulation of high non-linear flow for the first time. This required a detailed treatment of the effective stresses and inclusion of the advective accelerations, both of which had previously been ignored or considered of little importance (Hansen, 1956, Leendertse, 1967). Falconer (1976) also studied the accuracy and stability of various finite-difference schemes, although his chosen solution method was again the alternating-direction-implicit scheme of Leendertse (1967).

3.3.2 Finite-Difference Schemes

As can be seen from this early work, one of the major differences in approach is the type of finite-difference scheme used to solve the discretised equations. The scheme depends upon the time level at which the hydrodynamic variables are expressed within the discretised equations relative to one another. Falconer (1976, 1994) suggests four solution methods (ranging from fully explicit to fully implicit) for time-dependent equations but further variations on these are possible.

In an explicit scheme the governing equations are discretised in such a way that the hydrodynamic variables at the new time-level can be expressed solely in terms of known values of the hydrodynamic variables at the old time-level. For each flow variable at every node there is a difference equation, and these equations can be solved independently of each other. In contrast, in an implicit scheme, the difference equations for the variables at the new time-level involve values of other unknown variables at the new time-level. The equations can no longer be solved independently but must be treated as a system of simultaneous equations and solved iteratively or using matrix methods.

Implicit schemes may be backward in time if all spatial derivatives are approximated at the new time level, or time-centred if these derivatives use average values of old and new variables. Likewise explicit schemes can be forward in time or time-centred. Falconer (1976, 1994) showed that if all derivatives are evaluated at the old time level (the forward in time explicit scheme) the solution is unconditionally unstable. Most explicit methods overcome this by solving the continuity equation to find the new values of surface elevation, then using these *updated* values of elevation when solving the momentum equations at that timestep. Alternatively the momentum equations can be solved first and the new values of velocity used when evaluating the continuity equation. The effect of this technique is to time-centre the scheme. Values of elevation, æ are known at odd half timesteps, and values of velocity, (U,V), are known at even half timesteps, or vice versa. Hence the method is often referred to as a leapfrog solution. Although the dominant elevation derivatives in the momentum equations are centred in time, it must be noted that the scheme is not perfectly time-centred since the non-linear terms remain at the old time level. This technique was employed in the Cartesian shallow water equation models of, amongst others, Reid and Bodine (1968) Banks (1974) and Flather and Heaps (1975). Other explicit schemes are possible. The Rossiter and Lennon (1965) model of the section-averaged equations fully time-centred the continuity equation by iterating to find the time-centred cross-sectional area. Boericke and Hall (1974) used a two-step predictor-corrector method for the shallow water equations, and Roache (1972) and Mahmood and Yevjevich (1975) describe many possible solution schemes, both explicit and implicit.

Explicit schemes are characterised by the fact that the timestep of the solution is strictly limited by the Courant-Friedriche-Lewy criterion. The explicit scheme will only allow disturbances to propagate the distance of one cell per timestep. Thus the maximum timestep is determined by the speed of the gravity wave. If the timestep exceeds the maximum (i.e. the Courant number is greater than one) then the model solution breaks down catastrophically. This condition makes explicit models slow to run and has a punitive effect on computation time if the mesh resolution is increased. In contrast when using implicit methods there is no such restriction. Thus, theoretically, there are few limits on the timestep which may be employed. The disadvantage of implicit finite-difference schemes is that, in two-dimensions, the updated values to be calculated are related to many other unknown values. The difference equations are therefore exceedingly cumbersome to solve using matrix methods since their solution requires the inversion of large band-width matrices coupling the flow equations in two dimensions (Weare 1976a). Alternatively, implicit schemes can be solved by iterating to arrive at the correct values of the updated variables at each timestep, but in doing so the computational advantages over explicit schemes may be lost. Cheong *et al.* (1991) and Yakimiw and Robert (1986) used fractional timestep methods to reduce the complexity of the matrix inversion when solving the shallow water equations implicitly.

A popular compromise between the implicit and explicit methods is the alternating-direction-implicit (ADI) method developed by Peaceman and Rachford (1955) and Douglas (1955) and first employed for shallow water equation modelling by Leendertse (1967). This method reduces the complexity of the matrix solution of fully implicit methods while avoiding the timestep restriction of explicit schemes. The solution of the two-dimensional equations is performed over two half-timesteps during each of which the derivatives in one coordinate direction are taken at the new (implicit) time, and the derivatives in the other coordinate are taken at the old (explicit) time. Thus at each half-

timestep the unknown variables only depend on other unknowns on one coordinate direction and the matrices to be solved are tri-diagonal. This greatly reduces the amount of computation required in comparison with fully implicit schemes (Peaceman and Rachford, 1955). Following Leendertse (1967) the ADI method has been used in many Cartesian shallow water equation models (Kuipers and Vreugdenhil, 1973, Falconer, 1976, Stelling *et al.*, 1986) and has been modified for use with orthogonal coordinates (Willemse *et al.*, 1985) and non-orthogonal coordinates (Spaulding, 1984, Borthwick and Barber, 1992).

Although the timestep is not limited by the Courant stability criterion, considerations of accuracy mean that very large timesteps cannot be used with ADI schemes. Chandler-Wilde and Lin (1992) found that their model of the Bristol Channel only gave accurate results when the timestep was less than eight times the Courant number. Stelling *et al.* (1986) showed that in a "zigzag" stepped channel, as is commonplace in studies such as the Severn Estuary, the ADI method will not be accurate for Courant numbers greater than 4 2. Another drawback was highlighted by Leendertse (1979) who discovered that the truncation error associated with the ADI scheme tends to diffuse the spurious vorticity generated at stepped boundaries into the rest of the flow solution.

An alternative semi-implicit method was used by Johnson (1980) in his curvilinear grid solution to the shallow water equations and has since been employed by Hwang (1991) and Pearson (1996). In this method the momentum equations are solved explicitly and the continuity equation is solved implicitly by iterating to the new time level. The model also avoids the explicit time restriction, but for large timesteps on non-smooth grids the number of iterations to convergence may become prohibitive or the process may not even converge at all (Johnson *et al.*, 1982).

As well as solving the continuity and momentum equations by different schemes it is possible to combine different solution methods for use with different parts of the momentum equations. Split-operator techniques in which the advective terms are modelled by the method of characteristics have been developed and Benque *et al.* (1982) solved advection by characteristics, diffusion implicitly and propagation by an ADI scheme, while Guillou and Nguyen (1995) included advection, diffusion, propagation and correction steps in their finite-volume model.

3.3.3 The Advective and Diffusive Terms

Another major area of difference between numerical schemes for the shallow water equations is the inclusion or otherwise of the non-linear terms representing advection and diffusion of momentum. These terms can be difficult and time consuming to model and their importance relative to the gravitational and frictional forces may not be great. Linearised models which omit these terms can provide a simple solution to the depth-averaged equations and may be sufficient in many cases. Hansen (1956), Reid and Bodine (1968) and Häuser *et al.* (1985) studied the equations in this way, as did Prandle and Crookshank (1974) who declared that the non-linear terms were small over most of the tidal cycle.

However, it is commonly accepted that the advective terms must be included if the model is to reproduce circulatory motion. Vreugdenhil (1973) showed that the advective

accelerations (sometimes called the convective accelerations) and the effective stresses (which give rise to the diffusive terms) are the only sources of vorticity within the governing equations in the absence of wind stresses. He suggested that the advective terms were vital to a full representation of secondary flow but that the effective stresses might be of importance only for strongly curved flows. Jovanovic and Officier (1984) modelled the full non-linear equations for a stretch of the River Danube and concluded that for large watercourses the flow was dominated by bottom friction and the diffusive terms were negligible. Matsoukis (1992) stated that in coastal regions containing rapid expansions and contractions of flow the non-linear terms are no longer negligible and that a careful numerical treatment of advection and diffusion must be made if circulatory effects are to be properly simulated.

Unfortunately including the advective terms often introduces non-linear instability to the numerical scheme. The instability is characterised by the development of grid scale oscillations (decoupling) within the velocity field. Although Leendertse (1967) included the advective accelerations without encountering instability, he ignored the advective terms within the neighbourhood of the land / water boundary, which Flather and Heaps (1975) argue is where the water is shallow and non-linear effects are likely to be most important. Abrupt changes in the coastline may also serve to generate vorticity and advection is vital in this region in order to transport vorticity throughout the flow. Barber (1990) suggests that the stability of Leendertse's scheme may also be attributable to the fairly uniform hydraulic conditions modelled. Using an ADI scheme similar to that of Leendertse, and including advection everywhere, Falconer (1976) found that it was necessary to resort to first-order upwind difference expressions for the advective terms in order to achieve stable finite-difference solutions of momentum-driven reservoir flow.

The use of upwind differences for the advective derivatives is a popular technique for overcoming non-linear instability (Johnson, 1980, Zech *et al.*, 1983, Guillon and Nguyen, 1995). In this method forward or backward differences are used instead of central differences, with the direction of the difference determined by the local flow direction. Johnson (1980) found that decoupling effects were removed when upwind rather than central differences were used in evaluating the advective derivatives. Other researchers have found a combination of upwind and central differences sufficient to counteract instability (Stelling, 1983, Willemse *et al.*, 1985, Borthwick and Barber, 1992).

The success of the upwind scheme may be attributed to the fact that the non-centred differences introduce numerical diffusion into the solution. Indeed it can be argued that the diffusive terms play an important role in controlling non-linear instability within a numerical model of the turbulent flow. Kuipers and Vreugdenhil (1973) explained the occurrence of non-linear instability in terms of the transfer of energy in turbulent motion. Energy is fed into the flow at quite large scales of motion. The energy is transferred by non-linear interactions towards smaller and smaller scales, until finally at the smallest scales (much smaller than the computational grid size) it is dissipated by viscous friction. Kuipers and Vreugdenhil (1973) argued that this instability can be avoided by introducing diffusion within the numerical scheme to simulate the energy transfer towards smaller scales.

Diffusion is therefore often modelled in conjunction with advection as a method to stabilise the numerical scheme. This is instead of including diffusion in an attempt to simulate accurately the effective stresses which may themselves be negligible. Some authors have swamped the solution with large amounts of diffusion (controlled by the magnitude of the eddy viscosity coefficient) to produce a stable scheme. Johnson (1980) used a value of the eddy viscosity coefficient, í $_t$, of 10 m^2 s^{-1} and Anagnostopoulos and Mpimpas (1995a) used a viscosity of 400 m^2 s^{-1}, compared with a typical theoretical value of 0.1 m^2 s^{-1} for tidal flows (Kuipers and Vreugdenhil, 1973). However Barber (1990) argued that the eddy viscosity coefficient is determined by the properties of the flow and should not be manipulated at will. Kuipers and Vreugdenhil (1973) showed that, for a Cartesian model, spatially averaging the velocity variables at each timestep is directly equivalent to modelling the diffusive terms. They omitted diffusive terms and introduced an amount of spatial averaging such that the effective viscosity was exactly in line with the theoretical value of eddy viscosity. The same technique was employed by Wu and Tsanis (1994) in their model of the hydrodynamics and pollutant transport of Windermere Basin, Canada. Averaging filters have also been used to achieve stability in addition to the diffusive terms. Butler (1978a) used a temporal filter on the elevation, æ and Barber (1990) used a temporal filter on æas well as a degree of upwinding.

A final method of addressing the problem of non-linear instability is to time-centre the advective terms. Weare (1976b) showed that instability arises in the ADI method of Leendertse (1967, 1970) due to imperfect time-centring of the non-linear terms. Falconer's ADI models use central differences for the advective terms and iterate at each timestep to time-centre both the advective accelerations and diffusive terms (Falconer and Owens, 1984, 1987, Falconer and Chen, 1991).

3.3.4 Curvilinear Shallow Water Models

Several of the numerical models solve the governing equations on a curvilinear rather than a Cartesian grid. The techniques used for each method are predominantly the same. However, curvilinear models share some common characteristics in addition to the more complex techniques of grid generation.

A number of quasi boundary-fitted models have been developed which utilised non-Cartesian grids. The schemes of Boericke and Hall (1974) used interpolation in one direction to model more accurately a tidal channel with an irregular shoreline. Butler (1978b) used a stretched rectangular grid to increase locally the mesh resolution when studying tidal inundation, and Houston and Butler (1979) generalised this method to allow grid stretching in both the x- and y-directions. More recently Johns *et al.* (1982) employed interpolation techniques to model the movement of the coastline during flooding and Vemulakonda *et al.* (1985) used an orthogonal rectilinear grid to study wave-induced currents.

The first investigators to consider the application of boundary-fitted grid methods to the modelling of shallow flow were Johnson and Thompson (1978) who transformed the shallow water equations into a general curvilinear coordinate system. However, it was left to Johnson (1980) to develop the first numerical solution to the transformed equations in his model VAHM (Vertically Averaged Hydrodynamic Model). He solved the equations on a non-orthogonal mesh generated using the elliptic grid generation

techniques of Thompson *et al.* (1974). The model also included a transformed transport equation for salinity. Unlike Cartesian grid models in which the three hydrodynamic variables are stored at differing locations on the solution mesh, Johnson stored both velocity components at the same locations. This storage system reduces the amount of averaging required for velocities in the numerical scheme. This is desirable since averaging is not strictly compatible with the varying cell size and curved coordinate lines of the boundary-fitted grid. Johnson (1980) showed the potential of the boundary-fitted method by successfully modelling the flow in a hypothetical estuary geometry, and later VAHM was used to model the hydrodynamics of the Susquehanna River (Johnson *et al.*, 1982).

Since the development of VAHM, several other shallow water equation models have been written using the same elliptic grid generation technique. Häuser *et al.* (1985) solved the transformed shallow water equations explicitly and compared predictions of normal model oscillations in an annular ring with analytical values. They omitted the advective and diffusive terms and enforced a "rigid lid" by assuming that the changes in surface elevation were negligible in comparison with the water depth. Häuser *et al.* (1986) and Raghunath *et al.* (1987) used the same model to study the hydrodynamics of Hamburg harbour, and rotating flow in a parabolic container. Following this work, Nielsen and Skovgaard (1990a) developed a shallow water model for the hydrodynamics of a shallow fjord. They subsequently studied the errors resulting from non-orthogonality when using a general curvilinear coordinate model (Nielsen and Skovgaard, 1990b). All the above schemes located the velocity variables at the same nodes, in line with Johnson (1980). Cruz Leon (1991) used an explicit model to solve the transformed equations on a non-orthogonal mesh and compared the effect of Johnson's layout for the hydrodynamic variables with a Cartesian grid storage method. The latter method was used in the non-orthogonal grid models of Spaulding (1984) and Borthwick and Barber (1992).

An ADI solution scheme was used by Spaulding (1984) and Muin and Spaulding (1994) to solve the shallow water equations in general curvilinear coordinates. Their models allowed for the curvature of the earth's surface but omitted the non-linear terms and were validated against a number of theoretical test cases before application to the study of tidal flows. Unlike most boundary-fitted models which retain the Cartesian components of velocity as the dependent variables, the model of Muin and Spaulding (1994) employed contravariant velocities which are locally aligned to the curvilinear grid. Contravariant velocity components were also used by Borthwick and Akponasa (1993) in their ADI non-orthogonal grid model. They argued that the contravariant shallow water equations model the mass and momentum fluxes correctly across cell faces, independently of the grid curvature, unlike the transformed equations with Cartesian velocity components. However, the contrvariant momentum equations contain many more terms, particularly for advection and diffusion, and as a result Borthwick and Akponasa (1993) found non-linear instabilities hard to suppress. Sheng and Hirsh (1984) and Sheng (1986) used contravariant velocity components in combination with a boundary-fitted mesh as the horizontal part of a three-dimensional model of coastal waters. Thompson's elliptic grid generation technique was also used in the shallow water equation model of Johnson *et al.* (1993).

A number of solutions to the shallow water equations in orthogonal coordinates have been made at Delft Hydraulics in the Netherlands. Wijbenga (1985a) used an ADI

technique similar to that of Leendertse (1967) to solve the non-linear equations on an orthogonal boundary-fitted grid. The velocity variables were located separately as for a Cartesian grid and the model was used to study flow in the River Waal (Wijbenga, 1985b). Willemse *et al.* (1985) used a similar scheme but with covariant velocities to simulate the hydrodynamics of the River Rhine. More recently Chau and Jin (1995) used an orthogonal boundary-fitted grid in the horizontal part of their three-dimensional model. The shallow water equations were solved in conformal coordinates by Hamilton (1979) for a linearised model of storm surges in the North Sea, and Chandler-Wilde and Lin (1992) who studied the Bristol Channel.

Thacker (1977) developed an altogether different approach to the problem of accurate boundary representation within the finite-difference method. He generated an unstructured grid composed of triangular elements and approximated the derivatives in the hydrodynamic equations by the average slope of planar surfaces. Bauer and Schmidt (1983) later employed this method to model storm surges in Lake Geneva. Recently, curvilinear grid shallow water equation models have been developed by Barber (Barber, 1990, Borthwick and Barber, 1992). This approach included advection and diffusion and solved the hydrodynamic equations using an ADI algorithm on a Cartesian type staggered grid. Its practicality for studying flows in irregular water bodies was also demonstrated (Barber, 1992). This lead to the development of a non-orthogonal boundary-fitted model to simulate the hydrodynamics of the Humber Estuary by Pearson and Barber (1993a,b,c). Pearson's model solved the transformed equations using the semi-implicit technique of Johnson (1980) and included an Eulerian-Lagrangian solution of the transformed pollutant transport equation (Pearson, 1996). The model described in Scott (1996) is the latest in this line of shallow water equation simulations. It is an explicit curvilinear coordinate solution to the full non-linear equations. An overview of the model and early results for the study of the Severn Estuary using the linearised equations may be found in Scott and Barber (1994a,b,c) Barber *et al.* (1994) and Barber and Scott (1995).

3.3.5 Simulation of Intertidal Zones

The majority of numerical solutions of the shallow water equations, both Cartesian and boundary-fitted, were developed in order to study the hydrodynamics of coastal waters - whether for the simulation of tides and currents (Flather and Heaps, 1975, Falconer and Owens, 1984, Spaulding, 1984) or the prediction of storm surges and flooding (Reid and Bodine, 1968, Mathisen and Johansen, 1983, Verboom *et al.*, 1992). However, modelling shallow coastal regions presents a number of special problems. Flather and Hubbert (1989) list these as : the prevalence of tidal flats, the related problem of inundation of low-lying coastal land during storm surge events, and the non-linear effects in general, which are enhanced with decreasing water depth.

Estuaries in general are characterised by wide expanses of intertidal sandbanks and mudflats generated by fluvial deposits. Such areas are submerged at high tide and are gradually uncovered as the tide ebbs until, typically, water remains only in narrow deep channels. Thus at low tide the area to be modelled may differ greatly in size and shape from that at high water. In effect the boundary of the flow domain is not fixed but is continuously moving dependent on the elevation of the sea surface and the bathymetry of the estuary bed. This presents a major challenge to the numerical modeller.

Cartesian grid models of coastal regions allow for the changing shape of the flow domain by discretely adding or removing grid cells from the computation (the "wet or dry point" method). As the water level falls over a grid cell checks are performed to determine whether the cell should be "dried", and as the water level rises in cells surrounding a dry cell checks are performed to determine whether the cell should be "flooded". These checks are typically performed at the beginning of every timestep. The discretised equations are then solved only at points which are currently "wet". This method is not ideal since, as Falconer and Owens (1987) point out, "the discretisation process associated with the numerical solution method generally results in the need for a smoothly varying process - such as an ebbing tide receding over a smoothly varying bed - to be modelled as a discretely varying form".

Probably the first such "flooding and drying" scheme was used by Reid and Bodine (1968) who allowed dry land to be inundated, and calculated the discharge into dry cells using formulae for the overtopping and submergence of weirs. Leendertse and Gritton (1971) developed a flooding and drying algorithm to cope with the simulation of tidal flats in estuaries. They dried a cell if either the volume of water in the cell or the water depth at one of the four cell faces dropped to zero, and flooded a cell when all cell face depths were positive and the average flow was into the cell from surrounding wet cells. These flooding and drying checks were performed at intervals larger than the timestep.

The complex flooding and drying scheme of Leendertse and Gritton (1971) was designed to minimise the amount of computational noise. This noise arises for a variety of reasons. Waves are generated by discrete jumps in the location of the boundary, and by the discrete parcels of water which are added to, and subtracted from, the flow domain as cells flood and dry. In addition, if flooding and drying checks are performed at each timestep, there is a possibility that some cells will alternately flood and dry and flood and dry, creating spurious noise. Other problems occur when water levels are very low. Empirical formulae may lead to excessive values of bed friction, and negative depths must be avoided since these could lead to the collapse of the numerical scheme.

Some authors have avoided excessive values of bed friction by setting a minimum depth in the bed stress calculation. Flather and Heaps (1975) specified a minimum depth H_0 in their tidal model of Morecambe Bay and Zech *et al.* (1983) did not allow this depth to fall below 1 m. In the model of Zech *et al.* (1983) cells were dried when the water depth was less than 2 cm which was sufficient to preclude negative depths. Benque *et al.* (1982) and Chau and Jin (1995) used the value of bed friction to indicate which cells were dry. By increasing the bed friction coefficient to very high values in cells which satisfied the drying conditions, they were able to achieve zero flow over the dry cells without removing them from the computation.

Following the work by Leendertse and Gritton (1971) Falconer has devoted considerable effort to the development of a flooding and drying algorithm which will accurately replicate the actual motion of the land / sea boundary while minimising the amount of computational noise. His initial scheme (Falconer and Owens, 1984) was later improved (Falconer and Owens, 1987) and refined further (Falconer and Chen, 1991). In the final method the minimum permissible depth of water in a grid square is given by the roughness height k_s (used in the Colebrook-White bed friction formula) and is thus directly related to the physical roughness of the bed. A check was also

introduced such that a cell may dry once the water depth has fallen below a shallow depth. Pearson and Barber (1993a) borrowed the techniques of Falconer and Chen (1991) for use with their boundary-fitted grid model of the Humber Estuary.

However the use of boundary-fitted grids opens up new possibilities for the accurate simulation of flooding and drying. Whereas Cartesian grid schemes can only ever represent the natural coastline in a stepped fashion using square cells of the chosen resolution, the boundary-fitted grid technique allows varying cell size and curved coordinate lines such that a grid can be generated to fit the shape of the flow domain wherever the coastline falls. Thus one can imagine the boundary-fitted grid moving with the flow, the location of the grid boundary being determined by the physics of the problem rather than a set of empirical rules. A dense grid covering the area of water at low tide would expand and stretch with the tide to give a sparser grid at high tide. Both Johnson (1982) and Barber (1992) looked forward to the use of such a self-adaptive grid to simulate the process of flooding and drying within their curvilinear coordinate models.

A few self-adaptive grid models have been developed. Johns *et al.* (1982) simulated the inundation of the coastline of Andhra Pradesh, India, during a cyclone using a model with one moving boundary. The location of three sides of the solution mesh were fixed and the fourth shoreline boundary was determined by model predictions. Interpolation was then used to specify the location of the coordinate lines in the direction parallel to the shore. Recently Shi and Sun (1995) presented a storm surge model of the Bohai Sea, China, which represents the closest attempt to date at a completely free moving boundary simulation. They used a non-orthogonal grid and concentrated the cells near areas of the coast where flooding was expected to occur. The grid was then allowed to expand only in certain areas as the flooding occurred. This addressed one of the major drawbacks of an ideal moving boundary model, i.e. the need for re-interpolation of variables as the grid moves.

If the grid was completely free to move, then at each timestep it would be necessary to re-interpolate for depth at the new node positions, re-evaluate the metric derivatives at every node and interpolate for the hydrodynamic variables at the new node positions. This would be very expensive in terms of computing time for a grid of reasonable resolution. Further problems would arise if islands emerged in the middle of the flow domain, for then the grid required would not be topologically equivalent to its original shape. In this case a new transformed domain would be necessary, requiring re-indexing of nodes and regeneration of the boundary-fitted grid. Regeneration of the mesh would also be necessary if the cells became too stretched or too skewed as the grid moved. These problems have not yet been solved. Hence boundary-fitted models currently must rely on the discrete "wet and dry point" method of Cartesian grids.

3.3.6 One-Dimensional and Coupled Models

The study by Scott (1996) included a one-dimensional model that was coupled to a two-dimensional depth-averaged model in order to study the flow in the riverine upper reaches of the Severn Estuary. The one-dimensional scheme closely followed that of Rossiter and Lennon (1965) who developed a numerical solution to the section-averaged equations to model the Thames Estuary. An earlier numerical model of the

one-dimensional equations was presented by Hansen (1956) who studied the estuary of the River Ems. Stability was easier to achieve with the one-dimensional equations and although the effective stresses were usually neglected the advective terms were nearly always modelled. Rossiter and Lennon (1965) thus included advection and solved the equations explicitly, using iteration to fully time-centre the continuity equation.

With increases in computer power and the development of two-dimensional models of the depth-averaged equations it became possible to model river/sea systems. Banks (1974) combined the Thames Estuary model of Rossiter and Lennon (1965) with a Cartesian grid model of the North Sea. Banks solved the linearised two-dimensional equations by a leapfrog explicit method and the one-dimensional equations with advection as for Rossiter and Lennon, using the same timestep for each model. The join of the two numerical schemes was located at a discharge point in the one-dimensional model and a line of velocity nodes in the two-dimensional model. These values of discharge and velocity were calculated independently using the momentum equations for the one- and two-dimensional schemes respectively. They were then blended together to eliminate any discrepancies. Prandle (1975) used the same model to investigate the hydrodynamics of the Thames Estuary in advance of the construction of the Thames Barrier.

Another coupled two-dimensional / one-dimensional model was written by Prandle and Crookshank (1974) to study the St. Lawrence River Estuary. As well as a one-dimensional representation of the St. Lawrence River the program included one-dimensional models of side tributaries. Unlike Rossiter and Lennon (1965) the scheme allowed for unequal section lengths in the one-dimensional model, but otherwise followed Banks (1974) in using the work of Reid and Bodine (1968) for the two-dimensional part of the model.

3.4 Estuarial Storm Surge Modelling

Many new studies on the propagation of tides are now available and increase the knowledge base that currently exists. What is clear is that the hydrodynamics of rivers affected by tides is dominated by the dampening and the distortion induced by the quadratic bottom friction. Godin (1999) has shown that a compact and accurate approximation to the deceleration term, standing for the frictional effect, allows the retention of the concept of harmonics and separation of the time and space variations. It then becomes possible to explain, in terms of basic physics, the transformation of the tide from the estuary, to the zone where it becomes extinct. Godin's theoretical reasoning is supported by pertinent observations collected in the St Lawrence river and numerical relationships were derived to demonstrate the existence of non-linear effects and to quantitatively link various relevant physical parameters.

Applications of such modelling strategies are now available around the world. Unnikrishnan *et al.* (1997) have studied tidal propagation in the Mandovi-Zuari estuarine network on the west coast of India. This estuary consists of shallow strongly converging channels, that receive large seasonal influxes of fresh water due to the monsoons. The main channels, the Mandovi and Zuari estuaries, connect the network to the Arabian Sea. Observations showed that tidal amplitude in the channels remained unchanged over large distances (

channels and then decayed rapidly over approximately 10 km near the head. To understand the dynamics behind this behaviour, a numerical model for tidal propagation was used that simulated the observed tidal elevations well. Much of this work is being directed at the 'ultimate' numerical solution that involves a three-dimensional modelling strategy.

Lin and Falconer (1997) have developed a three-dimensional layer-integrated numerical model of tidal circulation, with the aim of simulating severe tidal conditions for practical engineering applications. The mode splitting strategy has been used in the model. A set of depth-integrated two-dimensional equations were first solved to give the pressure gradient, and the layer-integrated three-dimensional equations were then solved to obtain the vertical distributions of the flow velocities. Attention was given to maintaining consistency of the physical quantities derived from the two-dimensional and three-dimensional equations. A two-layer mixing length turbulence model for the vertical shear stress distribution was included in the model. Emphasis was focused on applying the model to a real estuary, which was geometrically complicated and had large tidal ranges giving rise to extensive flooding and drying.

Doornkamp (1998) reviewed the difficulties associated with the definition of coastal flood frequencies and magnitudes. This led to the recognition that there is considerable doubt in many parts of the world as to the precise nature of this particular hazard. Similarly, a review of the sea-level measurements that have been used to indicate a response to global warming shows that there is uncertainty about the impact of other controlling influences. What is clear, however, is that past management decisions about human endeavours in the coastal zone (including flood defences, occupance of flood-prone lands, extraction of groundwater and natural gas) have had an impact on relative land and sea levels and have done more to increase the risk of coastal flooding than can be assigned so far to global warming. In addition, Doornkamp (1998) argues that these changes induced by human activity may render inappropriate calculations of coastal-flood frequencies based on historical records since the latter relate to a period of time when the controls on flooding may have been very different.

A more interesting approach that has recently been developed in the United Kingdom focuses on the effect of non-stationarity on extreme sea level estimation. The sea level is the composition of astronomical tide and meteorological surge processes. It exhibits temporal non-stationarity due to a combination of long-term trend in the mean level, the deterministic tidal component, surge seasonality and interactions between the tide and surge. Dixon and Tawn (1999) assessed the affect of these non-stationarities on the estimation of the distribution of extreme sea levels. This is important for coastal flood assessment as the traditional method of analysis assumes that, once the trend has been removed, extreme sea levels are from a stationary sequence. They therefore compared the traditional approach with a recently proposed alternative that incorporates the knowledge of the tidal component and its associated interactions, by applying them to twenty-two UK data sites and through a simulation study. Their main finding was that if the tidal non-stationarity is ignored then a substantial underestimation of extreme sea levels results for most sites. In contrast, if surge seasonality and the tide-surge interaction were not modelled, the traditional approach produces little additional bias. Also it needs to be noted that the coincidence of several processes (see Figure 2.1) produce the most extreme cases.

Ultimately many new procedures may be applicable to the general problem area of forecasting extreme water levels in estuaries for flood warning and the current interest in tidal prediction using neural networks may a have a future role. An example of such an approach is that of Deo and Chaudhari (1998) who presented an objective method to predict tides at a subordinate point in the interior of an estuary or bay with the help of a neural network technique. In complex field conditions, this approach may have advantages. Prediction of high water and low water levels as well as that of continuous tidal cycles was made at three different locations. Their results indicated satisfactory reproduction of actual observations. This was further confirmed by the high value of the accompanying correlation coefficient which was better than the one obtained using a statistical linear regression model. The cascade correlation training algorithm produced the shortest training time and hence was found to be most suitable for adaptive training purposes.

Of particular note has been the recent work on the Firth of Clyde Flood Forecasting System by Burns *et al*. (1999). The system utilises a nest of finite difference numerical models for the seaward boundary and a one-dimensional model to take the predictions up the tidal part of the estuary and lower river. The system developed for the Scottish Environmental Protection Agency has been operational since 1999 and performance data will be archived over the next few flood seasons.

4. CONCLUDING REMARKS

The profound difficulty of numerically modelling the sophisticated and highly non-linear characteristics of tidal surge propagation within estuaries makes it unlikely that high dimensional numerical procedures will provide a way forward in the short term. A one-dimensional solution of the St Venant shallow water equations will be applied to the Thames Estuary in the next phase of the work. However, what is clearly emerging is that in many cases simple methods suffice.

On major estuaries it is likely that one-dimensional numerical models which attempt to capture the physics to the best of thier ability will be practicable solutions. Hence the Thames, Humber, Bristol Avon and other similar estuaries are likely to follow this strategy.

Given that most major errors in the surge prediction seem to emanate from the mesoscale forcing of the hydrodynamic model it seems likely that as the mesoscale model improves these errors will reduce. However, they are unlikely to disappear and an error reduction strategy that will be generally applicable to the more simple approaches currently utilised by the Environment Agency may need to be developed.

Appendices 1 and 2 provide a detailed assessment of some of the current procedures adopted in the North West, and South West Regions. In many cases the simple approaches prove to be adequate. However, there remain incidences where large errors in the surge prediction cause problems in the estuarial phase of the flood forecasting procedure. This element forms the focus of the next phase of the study.

5. ACKNOWLEDGEMENTS

Sections 3.1 to 3.3 of this report are based on the recent Ph.D. work of Scott (1996) and Section 3.4 is derived from a contribution to the project by Dr Roger Flather of the Natural Environment Research Council (NERC) Proudman Oceanographic Laboratory (POL) at Bidston, Liverpool.

6. REFERENCES

Abbott, M.B. (1975) Methods of Characteristics. In Mahmood, K. and Yevjevich, V. (eds.) *Unsteady Flow in Open Channels*, 1, pp.63-88, Water Resources Publications, Fort Collins, Colorado, USA.

Abbott, M.B. (1979) Computational Hydraulics. Elements of the Theory Of Free Surface Flows. Pitman, London, UK.

Abbott, M.B., Damsgaard, A. and Rodenhuis, G.S. (1973) System 21, Jupiter (A Design System for Two-Dimensional Nearly-Horizontal Flows. *Journ. of Hydraulics Research*, 11(1) pp.1-28.

Adam, Y. (1979) Belgian Real-Time System for the Forecasting of Currents and Elevations in the North Sea. In Nihoul, J.C.J (ed.) *Marine forecasting,*. (Proceedings of the 10th international Liege colloquium on ocean hydrodynamics, 1978). Elsevier Oceanography Series 25, Amsterdam: Elsevier. pp. 411-425.

Alcrudo, F. and Garcia-Navarro, P. (1993) A High Resolution Scheme for the Simulation of Discontinuous Free Surface Flows in Two Dimensions. Proc. of 1st Internat. Conf. on *Hydro-Science and Engineering*, Washington DC, USA, 1(B), pp.2062-2067.

Alvarez Fanjul, E., Perez Gomez, B., Carretero, J.,C., Rodriguez Sanchez-Arevalo, I. (1998) Tide and Surge Dynamics along the Iberian Atlantic Coast. *Oceanologica Acta*. 21(2) pp.131-143.

Amin, M. and Flather, R.A. (1996) Investigation into the Possibilities of using Bristol Channel Models for Tidal Predictions. In Spaulding, M.L. and Cheng, R.T. (eds.) *Estuarine and Coastal Modeling*, (Proceedings of the 4th International Conference,) New York: American Society of Civil Engineers, pp.41-52.

Anagnostopoulos, P. and Mpimpas, H. (1995a) Numerical Solution of Wind Induced Coastal Circulation - Effect of Time Integration Scheme. Proceedings of the 4th National Congress on *Mechanics*, Xanthi, Greece, 2, pp.897-905.

Anagnostopoulos, P. and Mpimpas, H. (1995b) Finite-Element Solution of Wind-Induced Circulation and Pollutant Dispersion in the Thermaikos Gulf. Proc. 2nd Internat. Conf. on *Computer Modelling of Seas and Coastal Regions*, Cancun, Mexico, pp.133-140.

Arakawa, A. and Lamb, V.R. (1977) Computational Design of the Basic Dynamical Processes of the UCLA General Circulation Model. *Methods in Comp. Physics*, 17, pp.174-265.

Backhaus, J.O. (1985). A Three-Dimensional Model for Simulation of Shelf Sea Dynamics.*Dt. Hydrogr. Z.* 38, H.4, pp.164-187.

Ball, D.J., Penoyre, R.B.S. and O'Connor, B.A. (1982) Numerical Modelling of the Hydrodynamics of Complex Civil Engineering Structures. Internat. Conf. on *The Hydraulics Modelling of Civil Engineering Structures*, Coventry, England, Paper A2, pp.13-32.

Banks, J.E. (1974) A Mathematical Model of a River - Shallow Sea System Used to Investigate Tide, Surge and their Interaction in The Thames - Southern North Sea Region. *Phil. Trans. Royal Society of London*, A275, pp.567-609.

Barber, R.W. (1990) Numerical Modelling of Jet-Forced Circulation in Reservoirs Using Boundary-Fitted Coordinate Systems. PhD Thesis, University of Salford, UK.

Barber, R.W. (1992) Solving the Shallow Water Equations Using a Non-Orthogonal Curvilinear Coordinate System. Proc. 2nd Internat. Conf. on *Hydraulic and Environmental Modelling of Coastal, Estuarine and River Waters*, Bradford, UK, 1, pp.469-480.

Barber, R.W. and Scott, L.J. (1995) Numerical Simulation of Estuarine Hydrodynamics Using a Depth-Averaged Non-Orthogonal Grid. Proceedings of the 3rd Internat. Conf. on *Computational Modelling of Free and Moving Boundary Problems*, Ljubljana, Slovenia, June, pp.39-47.

Barber, R.W., Scott, L.J. and Pearson, R.V. (1994) Numerical Simulation of the Severn Estuary Using a Non-Orthogonal Boundary-Fitted Grid. Proc. of the 5th Internat. Conf. on *Hydraulic Engineering Software*, Porto Carras, Greece, September, 2, pp.167-174.

Bauer, S.W. and Schmidt, K.D. (1983) Irregular-Grid Finite-Difference Simulation of Lake Geneva Surge. *Journ. of Hydraulic Engineering, Proc. ASCE*, 109(10) pp.1285-1297.

Benque, J.P., Cunge, J.A., Feuillet, J., Hauguel, A. and Holly, F.M. (1982) New Method for Tidal Current Computation. *Journ. of Waterway, Port, Coastal and Ocean Engineering*, 108(WW3) pp.396-417.

Bode, L. and Hardy, T. A. (1997) Progress and Recent Developments in Storm Surge Modelling. *J. Hydraulic Engineering* 123(4) pp.315-331.

Boericke, R.R. and Hall, D.W. (1974) Hydraulics and Thermal Dispersion in an Irregular Estuary. *Journ. Hydraulics Div., Proc. ASCE*, 100(HY1) pp.85-102.

Borthwick, A.G.L. and Akponasa, G.A. (1993) On the Contravariant Shallow Water Equations. Proceedings of the 5th Internat. Symposium on *Refined Flow Modelling and Turbulence Measurements*, Paris, pp.719-726.

Borthwick, A.G.L. and Barber, R.W. (1992) River and Reservoir Flow Modelling Using the Transformed Shallow Water Equations. *Internat. Journ. for Numerical Methods in Fluids*, 14, pp.1193-1217.

Borthwick, A.G.L. and Kaar, E.T. (1993) Shallow Flow Modelling Using Curvilinear Depth-Averaged Stream Function and Vorticity Transport Equations. *Internat. Journ. for Numerical Methods in Fluids*, 17, pp.417-445.

Buch, E. (1997) Oceanographic Monitoring Network in the Danish Waters. In Stel *et al.* (eds.) *Operational Oceanography. The Challenge for European Co-operation*. Elsevier Oceanography Series, 62. Amsterdam: Elsevier. pp.344-350.

Burns, J., Becker, M. and Kaya, Y. (1999) Firth of Clyde Flood Warning Scheme. Paper presented at MAFF Winter Meeting, 12p.

Butler, H.L. (1978a) Numerical Simulation of Tidal Hydrodynamics, Great Egg Harbour and Corson Inlets, New Jersey. Technical Report H-78-11, US Army Engineers Waterways Experiment Station Coastal Engineering Research Center, Vicksburg, Mississippi, USA

Butler, H.L. (1978b) Coastal Flood Simulation in Stretched Coordinates. Proceedings of the 16th Coastal Engineering Conference (ASCE) Hamburg, Germany, 1, pp.1030-1048.

Chandler-Wilde, S.N. and Lin, B. (1992) A Finite-Difference Method for the Shallow Water Equations with Conformal Boundary-fitted Mesh Generation. Proceedings of 2nd Internat. Conf. on *Hydraulic and Environmental Modelling of Coastal, Estuarine and River Waters*, 1, pp.507-518.

Chau, K.W. and Jin, H.S. (1995) Numerical Solution of Two-Layer, Two-Dimensional Tidal Flow in a Boundary-Fitted Orthogonal Curvilinear Coordinate System. *Internat. Journ. for Numerical Methods in Fluids*, 21, pp.1087-1107.

Cheong, H.-F., Abdul Khader, M.H. and Yang, C.-J. (1991) On the Numerical Modelling of Tidal Motion in Singapore Strait. *Journ. of Hydraulics Research*, 29(2) pp.229-242.

Codell, R.B. (1975) Two-Dimensional Model of Flow Toward Intakes. Symposium on *Modelling Techniques, ASCE*, San Francisco, September, 2, pp.426-438.

Cruz Leon, S. (1991) Curvilinear Shallow Water Equations on a Parallel Computer. MSc Thesis, Delft University of Technology, Delft, The Netherlands.

Dahlin, H. (1997) Towards a Baltic Operational Oceanograhic System, "BOOS". In Stel *et al.* (eds.) *Operational Oceanography. The Challenge for European Co-operation.* Elsevier Oceanography Series, 62. Amsterdam: Elsevier, pp.331-335.

Daniel, P. (1997) Forecasting Tropical Cyclone Storm Surges at Météo France. In Acinas, J.R. and Brebbia, C.A. (eds.) *Computer Modelling of Seas and Coastal Regions III*, Coastal 97, Southampton: Computational Mechanics Publications, pp.119-128.

Davies, A.M. and Lawrence, J. (1994) Modelling the Non-Linear Interaction of Wind and Tide: Its Influence on Current Profiles. *Internat. Journ. for Numerical Methods in Fluids*, 18, pp.163-188.

Deo, M.C. and Chaudhari, G. (1998) Tide Prediction Using Neural Networks. *Microcomputers in Civil Engineering*, 13(2) pp.113-120.

Dick, S. (1997) Operationelles Modellsystem für Nord- und Ostsee. In: FORUM, Proc. Der Fachtagung "EDV im Seeverkehr und maritimen Umweltschutz", Bremen, pp.22-25.

Dixon, M.J. and Tawn, J.A. (1999) The Effect of Non-Stationarity on Extreme Sea Level Estimation. *Applied Statistics*, 48, Part 2, pp.135-151.

Douglas, J. (1955) On the Numerical Integration of $^2u/\ ^2x+\ ^2u/\ ^2y=\ u/\ t$ by Implicit Methods. *Journ. of the Society of Industrial and Applied Mathematics*, 3(1) pp.42-65.

Doornkamp, J.C. (1998) Coastal Flooding, Global Warming and Environmental Management. *Journal of Environmental Management*, 52, pp.327-333.

Engedahl, H. (1995) Implementation of the Princeton Ocean Model (POM/ECOM3D) at the Norwegian Meteorological Institute. Research Report No. 5, DNMI.

Falconer, R.A. (1976) Mathematical Modelling of Jet-Forced Circulation in Reservoirs and Harbours. PhD Thesis, Imperial College London.

Falconer, R.A. (1993) Application of Numerical Models for Water Quality Studies. *Proceedings of the Institution of Civil Engineers, Civil Engineering*, 93, pp.163-170.

Falconer, R.A. (1994) Finite-Difference Methods for Shallow Water Equations. From *Computational Hydraulics: A Modular Course for Practising Engineers*, February, HR Wallingford, UK.

Falconer, R.A. and Chen, Y. (1991) An Improved Representation of Flooding and Drying and Wind Stress Effects in a Two-Dimensional Tidal Numerical Model. *Proceedings of the Institution of Civil Engineers*, Part 2, 91, pp.659-678.

Falconer, R.A. and Owens, P.H. (1984) Mathematical Modelling of Tidal Currents in the Humber Estuary. *Journ. Institute of Water Engineers and Scientists*, 38(6) pp.528-542.

Falconer, R.A. and Owens, P.H. (1987) Numerical Simulation of Flooding and Drying in a Depth-Averaged Tidal Flow Model. *Proc. Inst. Civ. Eng.*, Part 2, 83, pp.161-180.

Flather, R.A. (1979) Recent Results from a Storm Surge Prediction Scheme for the North Sea. In Nihoul, J.C.J. (ed.) *Marine forecasting*, (Proc. 10th Int. Liege Colloquium on Ocean Hydrodynamics, 1978). Elsevier Oceanography Series 25, pp.385-409.

Flather, R.A. (1984) A Numerical Model Investigation of the Storm Surge of 31 January and 1 February 1953 in the North Sea. *Quarterly Journal of the Royal Meteorological Society*, 110, pp.591-612.

Flather, R.A. (2000) Existing Operational Oceanography. Personal Communication

Flather, R.A. and Heaps, N.S. (1975) Tidal Computations for Morecambe Bay. *Geophys. Journ. of the Royal Astro. Society*, 42, pp.489-517.

Flather, R.A. and Hubbert, K.P. (1989) Tide and Surge Models for Shallow Water - Morecambe Bay Revisited. In Davies, A.M. (ed.) *Modelling Marine Systems*, CRC Press, Boca Raton, Florida, pp.135-166.

Flather, R., Proctor, R. and Wolf, J. (1991) Oceanographic Forecast Models. In Farmer, D.G. and Rycroft, M.J. (eds.) *Computer modelling in the environmental sciences*, Keyworth, April 1990, Oxford: Clarendon Press, pp.15-30.

Flather, R.A. and Smith, J. (1993) Recent Progress with Storm Surge Models - Results for January and February 1993. In *Proceedings of the MAFF Conference of River and Coastal Engineers*, 5-7 July 1993, University of Loughboroough, pp.6.2.1-6.2.16.

Galerkin, B.G. (1915) Series Solution of Some Problems of Elastic Equilibrium of Rods and Plates. (Russian) *Vestn. Inzh. Tech.* 19, pp.897-908.

Gerritsen, H., de Vries, J.W. and Phillippart, **M.E.** (1995) The Dutch Continental Shelf Model. In Lynch, D. and Davies, A.M. (eds.) *Quantitative Skill Assessment for Coastal Ocean Models*, Coastal and Estuarine Studies 47, AGU, pp 425-467.

Godin, G. (1999) The Propagation of Tides up Rivers With Special Considerations on the Upper Saint Lawrence River. *Estuarine, Coastal and Shelf Science*, 48, pp.307-324.

Grönvall, H. (1997) Finnish Operational Oceanographical Service. In Stel *et al.* (eds.) *Operational Oceanography. The Challenge for European Co-operation.* Elsevier Oceanography Series, 62. Amsterdam: Elsevier, pp.336-343

Guillou, S. and Nguyen, K.D. (1995) A Finite-Volume Technique for 2-D Coastal-Flow on a Non-Orthogonal Curvilinear Coordinate System. In Blain, W.R. (ed.) *Proceedings of the 3rd Internat. Conf. on the Planning, Design and Operation of Marinas*, Computational Mechanics Publications, Southampton, UK, pp.261-269.

Hamilton, J. (1979) Finite-Difference Storm Surge Prediction. Deutsche Hydrographische Zeitschrift, Jahrgang 32, Heft 6 (Sonderdruck) pp.267-278.

Hansen, W. (1956) Theorie zur Errechnung des Wasserstandes und der Stromungen in Randmeeren nebst Anwendungen. *Tellus*, 8(3) pp.287-300.

Hansen, W. (1962) Hydrodynamical Methods Applied to Oceanographic Problems. Proceedings of the Symposium on *Mathematical-Hydrodynamical Methods of Physical Oceanography*, Institut fur Meereskunde Der Universitat Hamburg.

Häuser, J., Paap, H.G., Eppel, D. and Mueller, A. (1985) Solution of Shallow Water Equations for Complex Flow Domains via Boundary-Fitted Coordinates. *Internat. Journ. for Numerical Methods in Fluids*, 5, pp.727-744.

Häuser, J., Paap, H.G., Eppel, D. and Sengupta, S. (1986) Boundary Conformed Coordinate Systems for Selected Two-Dimensional Fluid Flow Problems. Part 2: Application of the BFG Method. *Internat. Journ. for Numerical Methods in Fluids*, 6, pp.529-539.

Heemink, A.W. (1988) Two Dimensional Shallow Water Flow Identification. *Applied Mathematical Modelling*, 12, pp.109-118.

Hervouet, J.-M. (1989) Comparison of Experimental Data and Laser Measurements with the Computational Results of the TELEMAC Code (Shallow Water Equations). Proc. Internat. Conference on *Interaction of Comp. Methods and Measurements in Hydrualics and Hydrology*, Dubrovnic, Yugoslavia, pp.107-116.

Hervouet, J.-M., Hubert, J.L. Janin, J.M., Lepeintre, F. and Peltier, E. (1994) The Computation of Free Surface Flows with TELEMAC: An Example of Evolution Towards Hydroinformatics. *Journ. of Hydraulics Research*, 32(3) pp.45-64.

Hinwood, J.B. and Wallis, I.G. (1975) Review of Models of Tidal Waters. *Journ. Hydraulics Div., Proc. ASCE*, 101(HY11) pp.1405-1425.

Holly, F.M. and Preissmann, A. (1977) Accurate Calculation of Transport in Two-Dimensions. *Journ. of Hydrualics Div., Proceedings ASCE*, 103(HY11) pp.1259-1277.

Houston, J.R. and Butler, H.L. (1979) A Numerical Model for Tsunami Inundation. Technical Report HL-79-2, US Army Engineers Waterways Experiment Station Coastal Engineering Research Center, Vicksburg, Mississippi, USA.

Huang, W. and Spaulding, M. (1995) 3D Model of Estuarine Circulation and Water Quality Induced by Surface Discharges. *Journ. of Hydraulic Engineering*, 121(4), pp.300-311.

Hwang, R.R. (1991) Numerical Simulation of Storm Surges Via Boundary-Fitted Coordinates. In Arcilla, A.S., Häuser, J.,, Eiseman, P.R. and Thompson, J.F. (eds.) *Numerical Grid Generation in Computational Fluid Dynamics and Related Fields*. Elsevier Science Publishers B.V.

Jin, X. and Kranenburg, C. (1993) Quasi-3D Numerical Modelling of Shallow Water Circulation. *Journ. of Hydraulic Engineering*, 119(4) pp.458-472.

Johns, B., Dube, S.K., Sinha, P.C. Mohanty, U.C. and Rao, A.D. (1982) The Simulation of a Continuously Deforming Lateral Boundary in Problems Involving the Shallow Water Equations. *Computers and Fluids*, 10(2) pp.105-116.

Johnson, B.H. (1980) VAHM - A Vertically Averaged Hydrodynamic Model Using Boundary-Fitted Coordinates. Misc Paper HL-80-3, US Army Engineers Waterways Experiment Station Coastal Engineering Research Center, Vicksburg, Mississippi, USA

Johnson, B.H. (1982) Numerical Modelling of Estuarine Hydrodynamics on a Boundary-Fitted Coordinate System. In Thompson, J.F. (ed.) *Numerical Grid Generation*, Proceedings of a Symposium on *the Numerical Generation of Curvilinear Coordinate Systems and their Use in the Numerical Solution of Partial Difference Equations*, Nashville, Tennessee, USA, pp.409-436.

Johnson, B.H., Kim, K.W., Heath, R.E., Hsieh, B.B. and Butler, H.L. (1993) Validation of Three-Dimensional Hydrodynamic Model of Chesapeake Bay. *Journ. of Hydraulic Engineering*, 119(1) pp.2-20.

Johnson, B.H., Stein, A.B. and Thompson, J.F. (1982) Modelling of Flow and Conservative Substance Transport on a Boundary-Fitted Coordinate System. Proceedings of the IAHR Symposium on *Refined Modelling of Flows*, Paris, 2, pp.509-518.

Johnson, B.H. and Thompson, J.F. (1978) A Discussion of Boundary-Fitted Coordinate Systems and their Applicability to the Numerical Modelling of Hydraulics Problems. Misc. Paper H-78-9, US Army Engineers Waterways Experiment Station Coastal Engineering Research Center, Vicksburg, Mississippi, USA.

Jovanovic, M.B. and Officier, M.J. (1984) An Example of Application of Curvilinear Coordinates in Numerical Modelling of Complex Flow Patterns. Proceedings of the 1st Internat. Conf. on *Hydraulic Engineering Software*, Portoroz, Yugoslavia, 2, pp.41-51.

Kaar, E.T. (1991) Curvilinear Systems Modelling of Pollutant Transport in Shallow Waters. D.Phil. Thesis, University of Oxford.

Kernkamp, H.W.J. (1992) A Graphical Interactive Orthogonal Grid Generation Program. Presented at the 4th Internat. Conf. on *Hydraulic Engineering Software*, Valencia, Spain.

Kleine, E. (1993) Die Konzeption eines Numerischen Verfahrens für dir Advektionsgleichung – Literatur Übersicht und Details der Methode im Operationelle Modell des BSH für Nordsee und Ostsee: Konzeption und Übersicht. *Techn. Ber. der Bundesamtes für Seeschiffahrt und Hydrogrophie*, 106p.

Kleine, E. (1994) Das operationelle Modell des BSH für Nordsee und Ostsee: Konzeption und Übersicht. *Techn. Ber. der Bundesamtes für Seeschiffahrt und Hydrogrophie*, 126p.

Kodama, T. and Kawahara, M. (1994) Finite Element Tidal Current Analysis with an Open Boundary Condition. *Engineering Computations*, 11, pp.3-24.

Kuipers, J. and Vreugdenhil, C.B. (1973) Calculations of Two-Dimensional Horizontal Flow. Research Report S163, Part 1, Delft Hydraulics Laboratory, The Netherlands.

Leendertse, J.J. (1967) Aspects of a Computational Model for Long-Period Water-Wave Propagation. The Rand Corporation, RM-5294-PR.

Leendertse, J.J. (1970) A Water Quality Simulation Model for Well-Mixed Estuaries and Coastal Seas: Volume 1, Principles of Computation. Rand Corporation, RM-6230-RC.

Leendertse, J.J. and Gritton, E.C. (1971) A Water Quality Simulation Model for Well-Mixed Estuaries and Coastal Seas: Volume 2, Computational Procedures. The Rand Corporation, R-708-NYC.

Li, C.W. (1990) Advection Simulation by Minimax-Characteristics Method. *Journ. of Hydraulic Engineering*, 116(9) pp.1138-1144.

Li, C.W. and Falconer, R.A. (1995) Depth Integrated Modelling of Tide Induced Circulation in a Square Harbour. *Journ. of Hydraulic Research*, 33(3) pp.321-332.

Lin, B. and Falconer, R.A. (1997) Three-Dimensional Layer-Integrated Modelling of Estuarine Flows with Flooding and Drying. *Estuarine, Coastal and Shelf Science*, 44, 737-751.

Liggett, J.A. and Cunge, J.A. (1975) Numerical Methods of Solution of the Unsteady Flow Equations. In Mahmood, K. and Yevjevich, V. (eds.) *Unsteady Flow in Open Channels*, 1, pp.89-182, Water Resources Publications, Fort Collins, Colorado, USA.

Mahmood, K. and Yevjevich, V. (1975) Unsteady Flow in Open Channels. Water Resources Publications, Fort Collins, Colorado, USA.

Mathisen, J.P. and Johansen, Ø. (1983) A Numerical Tidal and Storm Surge Model of the North Sea. *Marine Geodesy*, 6, pp.267-291.

Matsoukis, P.-F.C. (1992) Tidal Model Using Method of Characteristics. *Journ. of Waterway, Port, Coastal and Ocean Engineering*, 118(3) pp.233-248.

Muin, M. and Spaulding, M. (1994) A 2-D Boundary-Fitted Circulation Model in Spherical Coordinates. *Journ. of Hydraulic Engineering*

Nielsen, P. and Skovgaard, O. (1990a) A Scheme for Automatic Generation of Boundary-Fitted Depth- and Depth-gradient Dependent Grids in Arbitrary Two-Dimensional Regions. *Internat. Journ. for Numerical Methods in Fluids*, 10, pp.741-752.

Nielsen, P. and Skovgaard, O. (1990b) The Effect of Using Non-Orthogonal Boundary-Fitted Grids for Solving the Shallow Water Equations. *Internat. Journ. for Numerical Methods in Fluids*, 11, pp.177-188.

Nöhren, I., Duwe, K. and Sündermann, J. (1995) OPMOD: Operational Modelling of Regional Seas and Coastal Waters; Recent Experiences and Developments. Commission of the European Communities (ed.), 2nd MAST days and EUROMAR market 7 – 10 November 1995, Project Reports Vol. 1.

Officier, M.J., Vreugdenhil, C.B. and Wind, H.G. (1986) Applications in Hydraulics of Numerical Solutions of the Navier-Stokes Equations. In Taylor, C., Johnson, J.A. and Smith, W.R. (eds.) *Recent Advances in Numerical Methods in Fluids, Vol. 5*, Pineridge Press, Swansea, UK, pp.115-147.

Ozer, J., Berlamont, J., Van den Eynde, D. and Yu, **C.S.** (1997) Operational Modelling of the Northwest European Continental Shelf. Activity Report No. 5. Report MNECS/O/XX/199710/NL/AR/5, 25p.

Peaceman, D.W. and Rachford, H.H. (1955) The Numerical Solution of Parabolic and Elliptic Differential Equations. *Journ. of the Society of Industrial and Applied Mathematics*, 3(1) pp.28-41.

Pearson, R.V. (1996) Simulation of Shallow Water Hydrodynamics and Species Transport Using Eliptically Generated Non-Orthogonal Boundary-Fitted Coordinate Systems. PhD Thesis, University of Salford, UK.

Pearson, R.V. and Barber, R.W. (1993a) Numerical Simulation of Flooding and Drying in a Depth-Averaged Boundary-Fitted Tidal Model. Proc. 2nd Int. Conf. on *Computational Modelling of Free and Moving Boundary Problems*, Milan, Italy, pp.261-268.

Pearson, R.V. and Barber, R.W. (1993b) Mathematical Modelling of Tidal Currents in the Humber Estuary Using a Non-Orthogonal Boundary-Fitted Coordinate System. Proceedings of the 1st Internat. Conf. on *Hydro-Science and -Engineering*, Washington DC, Part B, 1, pp.1683-1688.

Pearson, R.V. and Barber, R.W. (1993c) Mathematical Simulation of the Humber Estuary Using a Depth-Averaged Boundary-Fitted Tidal Model. In *Numerical Methods in Laminar and Turbulent Flow*, Pineridge Press, Swansea, UK, Vol 8(2) pp.1244-1255.

Pedersen, G. (1986) On the Effects of Irregular Boundaries in Finite Difference Models. *Internat. Journ. for Numerical Methods in Fluids*, 6, pp.497-505.

Peraire, J. (1986) The Solution of Some Convection Dominated Problems by the Finite-Element Method. PhD Thesis, University College of Swansea, UK.

Perez B. and Rodriguez I. (1994) REDMAR. Spanish Harbours Tidal Gauges Network. Processing of Tidal Data. Publicacíon No 57 de Clima Marítimo.

Periæ M., Kessler, R. and Scheurerer, G. (1988) Comparison of Finite-Volume Numerical Methods with Staggered and Colocated Grids. *Computers and Fluids*, 16(4) pp.389-403.

Phillippart, M.E. and Gebraad, **A.** (1997) A New Storm Surge Forecasting System. In Stel *et al.* (eds.) *Operational Oceanography. The Challenge for European Co-operation.* Elsevier Oceanography Series, 62. Amsterdam: Elsevier. pp.487-495.

Phillippart, M.E., Gebraad, A.W., Scharroo, R., Roest, M.R.T., Vollebregt, E.A.H., Jacobs, A., van den Boogaard, H.F.P. and Peters, H.C. (1998) *DATUM2: Data assimilation with Altimetry; Techniques Used in a tidal Model, 2nd program.* Netherlands Remote Sensing Board (BCRS) NRSP-2 Report 98-19.

Prandle, D. (1975) Storm Surges in the Southern North Sea and River Thames. *Proceedings of the Royal Society of London*, A, 344, pp.509-539.

Prandle, D. and Crookshank, N.L. (1974) Numerical Model of the St Laerence River Estuary. *Journ. Hydraulics Div. Proc. ASCE*, 100(HY4) pp.517-529.

Raghunath, R., Sengupta, S. and Häuser, J. (1987) A Study of the Motion in Rotating Containers Using a Boundary-Fitted Coordinate System. *Internat. Journ. for Numerical Methods in Fluids*, 7, pp.453-464.

Reid, R.O. and Bodine, B.R. (1968) Numerical Model for Storm Surges in Galveston Bay. *Journ. Waterway, Port, Coastal and Ocean Div., Proc. ASCE*, 94(WW1) pp.33-57.

Roache, P.J. (1972) Computational Fluid Dynamics. Hermosa, Albuquerque, USA.

Roberts, W. (1994) Theory of Shallow Water Equations. From *Computational Hydraulics: a Modular Course for Practising Engineers*. February, 1994, HR Wallingford, UK.

Rodi, W. (1984) Turbulence Models and their Application in Hydrualics - A State of the Art Review. 2nd Edition, IAHR.

Rossiter, J.R. and Lennon, G.W. (1965) Computation of Tidal Conditions in the Thames Estuary by the Initial Value Method. *Proc. Inst. Civil Engineers*, 31, pp.25-56.

Scott, L.J. (1996) Numerical Modelling of Tidal Propagation in the Severn Estuary Using a Boundary-Fitted Coordinate System. PhD Thesis, Water Resources Research Group, Telford Research Institute, University of Salford, 313p.

Scott, L.J. and Barber, R.W. (1994a) The Effects of Grid Adaptation on Tidal Propagation in a Boundary-Fitted Coordinate System. Proceedings of the 4th Internat. Conf. on *Numerical Grid Generation in Computational Fluid Dynamics and Related Fields*, Pineridge Press, Swansea, UK, PP.603-614.

Scott, L.J. and Barber, R.W. (1994b) Numerical Simulation of Tidal Flow in the Severn Estuary Using a Boundary-Fitted Non-Orthogonal Grid. In Tsakiris, G. and Santos, M.A. (eds.) *Advances in Water Resources Technology and Management*, Balkema Publishers, Rotterdam, The Netherlands, pp.125-132.

Scott, L.J. and Barber, R.W. (1994c) Estuary Modelling on an Adapted Curvilinear Grid. Proceedings of the Internat. Symposium on *Waves: Physical and Numerical Modelling*, Vancouver, Canada. Published by the University of British Columbia, 1, pp.326-335.

Sheng, Y.P. (1986) Numerical Modelling of Coastal and Estuarine Processes Using Boundary-Fitted Grids. Proc. 3rd Internat. Symposium on *River Sedimentation*, Jackson, USA, 3, pp.1426-1442.

Sheng, Y.P. and Hirsh, J.E. (1984) Numerical Solution of Shallow Water Equations in Boundary Fitted Grid. Technical Memo 84-15, Aeronautical Research Associates of Princeton Inc. Princeton, New Jersey, USA.

Shi, F. and Sun, W. (1995) A Variable Boundary Model of Storm Surge Flooding in Generalised Curvilinear Grids. *Internat. Journ. for Numerical Methods in Fluids*, 21, pp.641-651.

Spaulding, M.L. (1984) A Vertically Averaged Circulation Model Using Boundary-Fitted Coordinates. *Journ. of Phys. Oceanography*, 14, pp.973-982.

Stansby, P.K. and Lloyd, P.M. (1995) A Semi-Implicit Lagrangian Scheme for 3D Shallow Water Flow with a Two-Layer Turbulence Model. *Internat. Journ. for Numerical Methods in Fluids*, 20, pp.115-133.

Stelling, G.S. (1983) On the Construction of Computational Methods for Shallow Water Flow Problems. PhD Thesis, Delft University of Technology, Delft, The Netherlands.

Stelling, G.S., Wiersma, A.K. and Willemse, J.B.T.M. (1986) Practical Aspects of Accurate Tidal Computations. *Journ. of Hydraulic Engineering*, 112(9) pp.802-817.

Tabuenca, P. and Vila, J.A. (1995) 2-D Numerical Modelling of Pollution in Estuaries with Application to the Bay of Santander in Spain. Proc. 3rd Internat. Conf. on *Water Pollution-Modelling, Measuring and Prediction*, Porto Carras, Greece, pp.229-236.

Thacker, W.C. (1977) Irregular-Grid Finite-Difference Techniques: Simulations of Oscillations in Shallow Circular Basins. *Journ. Phys. Oceanography*, 7(2) pp.284-292.

Thames, F.C., Thompson, J.F., Mastin, C.W. and Walker, R.L. (1977) Numerical Solutions for Viscous and Potential Flow about Arbitrary Two-Dimensional Bodies Using Body-Fitted Coordinate Systems. *Journ. of Comp. Physics*, 24, pp.245-273.

Thompson, J.F., Thames, F.C. and Mastin, C.W. (1974) Automatic Numerical Generation of Body-Fitted Curvilinear Coordinate System for Field Containing any Number of Arbitrary Two-Dimensional Bodies. *Journ. of Comp. Physics*, 15, pp.299-319.

Unnikrishnan, A.S., Shetye, S.R. and Gouveia, A.D. (1997) Tidal Propagation in the Mandovi-Zuari Estuarine Network, West Coast of India: Impact of Freshwater Influx. *Estaurine, Coastal and Shelf Science*, 45, pp.737-744.

Van den Eynde, D., Malisse, J.-P., Ozer, J. and Scory, S. (1998) Operational Modelling of the Northwest European Continental Shelf: Gebruikershandleiding. Report OMNECS/O/XX/199809/NL/TR/3.1, 83p.

Vemulakonda, S.R., Swain, A., Houston, J.R., Farrar, P.D., Chou, L.W. and Ebersole, B.A. (1985) Coastal and Inlet Processes Numerical Modelling System for Oregon Inlet, North Carolina. Technical Report CERC-85-6, US Army Engineers Waterways Experiment Station Coastal Engineering Research Center, Vicksburg, USA.

Verboom, G.K., de Ronde, J.G. and Van Dijk, R.P. (1992) A Fine Grid Tidal Flow and Storm Surge Model of the North Sea. *Continental Shelf Research*, 12, pp.213-233.

Vested, H.J., Nielsen, J.W., Jensen, H.R., and Kristensen, K.B. (1995) Skill Assessment of an Operational Hydrodynamic Forecast System for the North Sea and Danish Belts. In Lynch, D. and Davies, A.M. (eds.) *Quantitative Skill Assessment for Coastal Ocean Models*, Coastal and Estuarine Studies 47, AGU, pp.373-396.

Vreugdenhil, C.B. (1973) Secondary Flow Computations. Proceedings of the 15th Congress of the IAHR, Istanbul, Paper B20, pp.153-160. Reprinted as Publication No.114, November, Delft Hydraulics Laboratory, Delft, The Netherlands.

Weare, T.J. (1976a) Finite-Element or Finite-Difference Methods for the Two-Dimensional Shallow Water Equations? *Computer Methods in Applied Mechanics and Engineering*, 7, pp.351-357.

Weare, T.J. (1976b) Instability in Tidal Flow Computational Schemes. *Journ. Hydraulics Div. Proc. ASCE*, 102(HY5) pp.569-580.

Weare, T.J. (1979) Errors Arising From Irregular Boundaries in ADI Solutions of the Shallow Water Equations. *Internat. Journ. for Numerical Methods in Engineering*, 14, pp.921-931.

Weare, T.J. (1982) Mathematical Models. In *Hydraulic Modelling in Maritime Engineering*, Thomas Telford, London, pp.15-31.

Weatherill, N.P., Eiseman, P.R., Häuser, J. and Thompson, J.F. (1994) Numerical Grid Generation in Computational Fluid Dynamics and Related Fields. Pineridge Press, Swansea, UK.

Wijbenga, J.H.A. (1985a) Determination of Flow Patterns in Rivers with Curvilinear Coordinates. Proceedings of 21st IAHR Congress, Melbourne, Australia, August. Reprinted as Publication No.352, October, Delft Hydraulics Laboratory, Delft, The Netherlands.

Wijbenga, J.H.A. (1985b) Steady Depth-Averaged Flow Calculations on Curvilinear Grids. 2nd Internat. Conf. on *The Hydraulics of Floods and Flood Control*, Cambridge, England, September, pp.373-387.

Willemse, J.B.T.M., Stelling, G.S. and Verboom, G.K. (1985) Solving the Shallow Water Equations with an Orthogonal Coordinate Transformation. Presented at the Internat. Symposium on *Computational Fluid Dynamics*, Tokyo, September. Reprinted as Delft Hydraulics Communication No.356, January 1986, Delft Hydraulics Laboratory, Delft, The Netherlands.

Woods, J.D., Dahlin, H., Droppert, L., Glass, M. Vallerga, S. and Flemming, N.C. (1996) The Strategy for EuroGOOS, EuroGOOS Publication No. 1, Southampton Oceanography Centre, Southampton. ISBN 0-904175-22-7.

Woods, J.D., Dahlin, H., Droppert, L., Glass, M. Vallerga, S. and Flemming, N.C. (1997) The Plan for EuroGOOS, EuroGOOS Publication No. 3, Southampton Oceanography Centre, Southampton. ISBN 0-904175-26-X.

Wu, J. and Tsanis, I.K. (1994) Pollutant Transport and Residence Time in a Distorted Scale Model and a Numerical Model. *Journ. of Hydraulics Research*, 32(4) pp.583-598.

Yakimiw, E. and Robert, A. (1986) Accuracy and Stability Analysis of a Fully Implicit Scheme for the Shallow Water Equations. *Monthly Weather Review*, 114, pp.240-244.

Yin, F. and Chen, S.-H. (1982) Tidal Computation on Taiwan Strait. *Journ. Waterway, Port, Coastal and Ocean Div., Proc. ASCE*, 108(WW4) pp.539-553.

Zech, Y., Sorel, M.C. and Vansnick, M. (1983) Mathematical Modelling of Floods in Rivers; Flooding and Uncovering of Flood Plains. Internat. Conf. on *The Hydraulic Aspects of Floods and Flood Control*, London, UK, pp.217-227.

Zienkiewicz, O.C. (1977) The Finite-Element Method (3rd Edition). McGraw-Hill, London.

APPENDIX 1

RESULTS FROM EXISTING MODELS IN THE NORTH WEST REGION

1.1 Formulation of the Simple Model

The Simple Model is expressed as follows:

Forecast Tide Level = *Astronomic Tide* + *STFS Surge*

Error = *Forecast Level* - *Actual Level*

In the North West Region this simple model is enhanced by the ***Operation Neptune*** scheme.

- This operates at four forecasting sites:

  Liverpool (Gladstone Dock)
  Heysham
  Blackpool
  Workington

- The *Tide Level* for this scheme is defined as:

  Tidal Level = *Astronomic High Tide at Liverpool (Gladstone Dock)*
  + STFS Forecast Surge Residual for Liverpool at High Tide

- If either of the following conditions is fulfilled, then a minimum of a **Yellow Warning** is issued.

  1. The *Forecast Tide* at Liverpool **> 5.0 m A.O.D.** with a *Wind Forecast* of **Force 8** with a direction of between north and south west at any time in the 12 hours before high water.

  2. The *Forecast Tide* at Liverpool **> 5.5 m A.O.D.**

- **Amber Warnings** are issued on the same basis as yellow warnings as a confirmation of the situation nearer to the actual peak tide.

- If the *Forecast Tide* at Liverpool **> 6.0 m A.O.D.** then a **Red Warning** is to be issued.

- The lead times for the above warnings are as follows:

Yellow Warning	**> 8 hours**	NB These are to be replaced by a new national system of warnings from September 2000.
Amber Warning	**> 6 hours**	
Red Warning	**> 4 hours**	

1.2 Review of Forecast Accuracy

This review focuses on the accuracy of both the forecasting of the astronomic tide and the surge component at Liverpool. Fourteen events were considered and seventeen high tides were analysed. Seven of these events resulted in the issuing of a flood warning, however, only one of them (23/11/1995) reached the *Neptune* trigger level and even in this case there were no reports of flooding. An Amber Warning was issued for the event of 24/02/1997 although the *Forecast Tide* at Liverpool (4.5 m) did not meet the model criteria. Again no flooding was reported. The warnings issued may be summarised as follows:

- 1 event produced a Red Warning, 6 events produced an Amber Warning and there was no information available for a further 6 events.
- Of the 8 events for which surge information was available, 5 resulted in a large (±0.2 m) surge forecast error.
- Of the 7 events for which warnings were issued, 5 were shown to have a forecast error ±0.2 m
- For the 17 high tides, there were 7 forecasts for which the error was ±0.2 m

The full set of results for the 14 events is presented in Table A1-1.1.

1.3 Forecast Accuracy Test Results

The data used in these tests were from the period 04/10/98 - 31/12/98 and were recorded at the following three sites:

Liverpool	Gauged Tide;	Astronomic Tide;	STFS Surge at Liverpool
Heysham	Gauged Tide;	Astronomic Tide;	STFS Surge at Heysham
Fleetwood	Gauged Tide;	Astronomic Tide;	STFS Surge at Blackpool

The criteria used to select events was that the *Actual Tide* was **> 4.5 m** and the *Forecast Lead Time* was **6 hours**.

Of the fourteen events used in this test and recorded at Liverpool, four were accompanied by medium to large surges. Errors in the *Peak Value* exceeded ±0.2 m for only three events, one of which (24/10/1998) was affected by a high surge (see Table A1-1.2 for further details). Only one of the events was affected by a *Peak Value* error of more than ±0.3 m.

Of the twelve events used in this test and recorded at Heysham, four were accompanied by medium to large surges. Errors in the *Peak Value* exceeded ±0.2 m for only two events, one of which (24/10/1998) was affected by a high surge (see Table A1-1.3 for further details). There were no occasions on which the error in *Peak Value* exceeded ±0.3 m.

Of the thirteen events used in this test and recorded at Fleetwood, four were accompanied by medium to large surges. Errors in the *Peak Value* exceeded ±0.2 m for six events, two of which (24/10/1998 and 05/11/1998) were affected by a medium or

high surge (see Table A1-1.4 for further details). For only one event did the error in the *Peak Value* exceed ±0.3 m.

These results (the plots for which may be found in Figures A1-1.13 - A1-1.51 at the end of this Appendix) show that there is not necessarily a connection between the magnitude of the surge and the error in the tidal forecast, although the error often arises from estimation errors in the surge forecasts. In order to investigate further this relationship, the correlation coefficients between the *STFS Surge Forecast* and the *Tide Forecast Error* were calculated. As shown in Table A1-1.5, no significant correlation was found and the mean of the error at the three sites is small enough to be thought of as zero (Table A1-1.6).

1.4 Conclusions

The following conclusions can be drawn from the analysis undertaken.

I. For all three sites, the *Simple Model* exhibits a sufficient degree of accuracy when forecasting tide level.

II. No systematic errors exist and the errors are normally distributed (see Figures A1-1.1 - A1-1.6)

Table A1 1.1 The Accuracy of High Tide and Surge Forecasts at Liverpool

Date	Wind Direction	Wind Speed (Force)	Predicted Surge (m)	Actual Surge (m)	Surge Error (m)	Forecast Tide (m)	Actual Tide (m)	Tide Error (m)	Warning
231195	SW	7-8	0.20	0.00	0.20	5.27	5.00	0.27	
290996	SSE	7	0.36	0.11	0.25	5.63	5.38	0.25	Amber
291096	W	7-8	0.41	0.00	0.41	4.71	5.18	-0.47	Amber
090297	SW	5-6 to 4-5	0.12	0.41	-0.29	5.49	5.30	0.19	Amber
100297	SSW-W	6-7 to 8	0.73	0.77	-0.04	6.20	6.00	0.20	Red
110297	SW	7	0.30	0.20	0.10	5.20	4.90	0.30	Amber
240297	SW	7-8	0.60	0.40	0.20	4.50	4.50	0.00	Amber
150997		5-6	0.10			4.90	4.88	0.02	
160997	SW SW	6-7 6	0.10 0.27			4.90 5.44	4.52 5.30	0.38 0.14	
170997		3	-0.11 -0.08			4.96 5.39	4.67 5.25	0.29 0.14	
180997	SW	2	-0.13			5.06	4.92	0.14	
190997			-0.22 -0.30			5.25 4.77	5.15 4.60	0.10 0.17	
200997			-0.20			5.17	5.00	0.17	
030198	W	9-10	1.30	1.20	0.10	5.40	5.50	-0.10	Amber

Table A1 1.2 Results for Forecast Tidal Peak Errors at Liverpool

Event	STFS Surge (m)	Astronomic Tide (m)	Forecast Peak Tide (m)	Actual Peak Tide (m)	Peak Error (m)	Timing Error (hours)
061098	-0.17/-0.17	4.9/5.2	4.73/5.03	4.60/4.93	0.13/0.10	0.0/0.0
071098	-0.16/-0.23	5.0/5.2	4.84/4.97	4.79/5.12	0.05/-0.15	0.0/0.0
081098	-0.22/0.16	4.8/5.0	4.58/5.16	4.48/4.88	0.10/0.28	0.0/0.0
091098	0.05	4.6	4.65	4.63	0.02	0.0
201098	0.66	4.2	4.86	4.67	0.19	0.0
241098	0.53/0.66	3.8/3.6	4.33/4.26	4.55/4.55	-0.22/-0.29	0.0/0.0
021198	0.17	4.5	4.67	4.60	0.07	0.0
031198	0.11/-0.03	4.7/5.0	4.81/4.97	4.40/4.73	0.41/0.24	0.0/0.0
041198	0.06/0.02	4.9/5.2	4.96/5.22	4.69/5.23	0.27/-0.01	0.0/0.0
051198	0.34/0.17	4.9/5.1	5.24/5.27	5.27/5.38	-0.03/-0.11	-1.0/0.0
061198	-0.11/0.0	4.9/4.8	4.79/4.80	4.84/4.85	-0.05/-0.05	0.0/0.0
071198	0.09/0.31	4.7/4.4	4.79/4.71	4.78/4.75	0.01/-0.04	0.0/0.0
031298	-0.14	4.8	4.66	4.60	0.06	0.0
041298	-0.17/-0.09	4.8/4.8	4.63/4.71	4.54/4.54	0.09/0.17	0.0/0.0

(See also Figures A1-1.7 & A1-1.8)

Table A1 1.3 Results for Forecast Tidal Peak Errors at Heysham

Event	STFS Surge (m)	Astronomic Tide (m)	Forecast Peak Tide (m)	Actual Peak Tide (m)	Peak Error (m)	Timing Error (hours)
061098	-0.13/-0.13	5.2/5.5	5.07/5.37	4.85/5.20	0.22/0.17	0.0/0.0
071098	-0.13/-0.17	5.4/5.6	5.27/5.43	5.18/5.39	0.09/0.04	0.0/0.0
081098	-0.19/-0.11	5.2/5.5	5.01/5.39	4.93/5.27	0.08/0.12	0.0/0.0
091098	0.06/0.02	4.9/5.0	4.96/5.02	4.91/4.93	0.05/0.09	0.0/0.0
201098	0.65	4.4	5.05	4.96	0.09	0.0
241098	0.60/0.58	4.1/3.8	4.70/4.38	4.93/4.52	-0.23/-0.14	0.0/0.0
041198	0.05/0.03	5.2/5.6	5.25/5.63	5.05/5.56	0.20/0.07	0.0/0.0
051198	0.31/0.09	5.3/5.6	5.61/5.69	5.67/5.80	-0.06/-0.11	0.0/0.0
061198	-0.08/0.00	5.2/5.3	5.12/5.30	5.13/5.31	-0.01/-0.01	0.0/0.0
071198	0.09/0.36	5.0/4.7	5.09/5.06	5.17/4.99	-0.08/0.07	0.0/0.0
031298	-0.11	5.3	5.19	5.00	0.19	0.0
041298	-0.14/-0.06	5.1/5.2	4.96/5.14	4.78/4.96	0.18/0.18	0.0/0.0

(See also Figures A1-1.9 & A1-1.10)

Table A1 1.4 Results for Forecast Tidal Peak Errors at Fleetwood

Event	STFS Surge (m)	Astronomic Tide (m)	Forecast Peak Tide (m)	Actual Peak Tide (m)	Peak Error (m)	Timing Error (hours)
061098	-0.17/-0.19	5.0/5.2	4.83/5.01	4.84/5.12	-0.01/-0.11	0.0/0.0
071098	-0.13/-0.22	5.2/5.4	5.07/5.18	5.12/5.39	-0.05/-0.21	0.0/0.0
081098	-0.19/-0.09	5.0/5.3	4.81/5.21	4.84/5.21	-0.03/0.00	0.0/0.0
091098	-0.06/0.00	4.7/4.8	4.64/4.80	4.91/4.85	-0.27/-0.05	0.0/0.0
201098	0.66	4.1	4.76	4.94	-0.18	0.0
241098	0.52/0.63	4.0/3.7	4.52/4.33	4.85/4.61	-0.33/-0.28	0.0/0.0
031198	0.09/-0.03	4.7/5.0	4.79/4.97	4.58/4.91	0.21/0.06	0.0/0.0
041198	0.05/0.02	5.0/5.4	5.05/5.42	4.99/5.53	0.06/-0.11	0.0/0.0
051198	0.34/0.08	5.1/5.4	5.44/5.48	5.57/5.74	-0.13/-0.26	0.0/0.0
061198	-0.11/0.00	5.0/5.1	4.89/5.10	5.12/5.26	-0.23/-0.16	0.0/0.0
071198	0.09/0.38	4.8/4.6	4.89/4.98	5.11/4.97	-0.22/0.01	0.0/0.0
031298	-0.11	5.1	4.99	4.82	0.17	0.0
041298	-0.17/-0.06	4.9/5.0	4.73/4.94	4.64/4.78	0.09/0.16	0.0/0.0

(See also Figures A1-1.11 & A1-1.12)

Table A1 1.5 Correlation Coefficients for STFS Surge Predictions and Forecast Errors

Correlation Coefficient R	All Point Samples on the Tidal Cycle	Point Samples with a Tide Level >0.0 m AOD	Point Samples with a Tide Level >4.0 m AOD
Liverpool	-0.176	-0.177	-0.175
Heysham	-0.345	-0.344	-0.342
Fleetwood	-0.340	-0.340	-0.335

Table A1 1.6 The Mean and the Standard Deviation of the Forecast Errors

	Liverpool		**Heysham**		**Fleetwood**	
	Tide>0m	**Tide>4m**	**Tide>0m**	**Tide>4m**	**Tide>0m**	**Tide>4m**
Mean Of Error	0.059	0.058	0.031	0.030	-0.044	-0.048
Standard Deviation	0.149	0.149	0.141	0.140	0.151	0.148

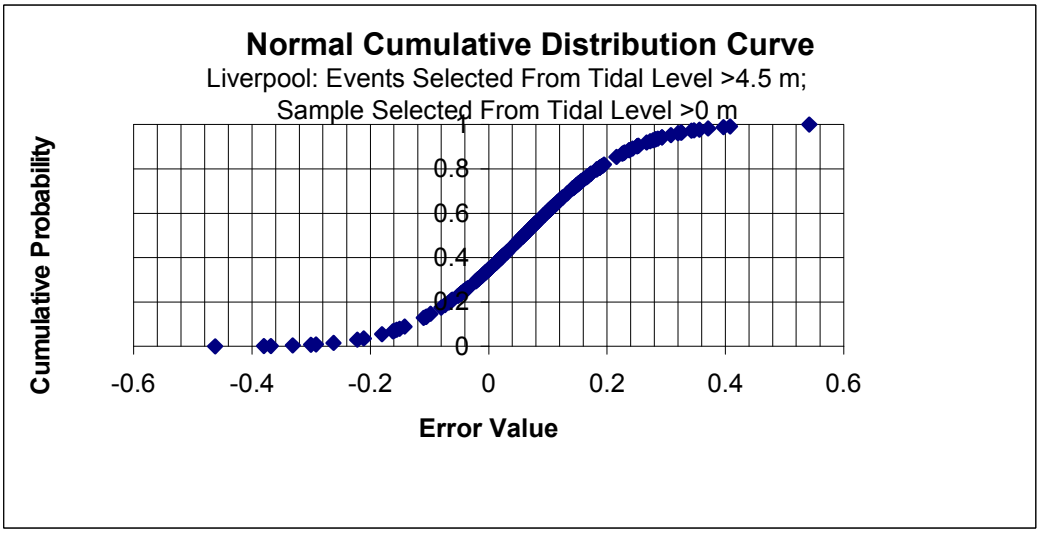

Figure A1 1.1 Error Distribution Analysis at Liverpool (peak > 4.5 m; tide level > 0.0 m)

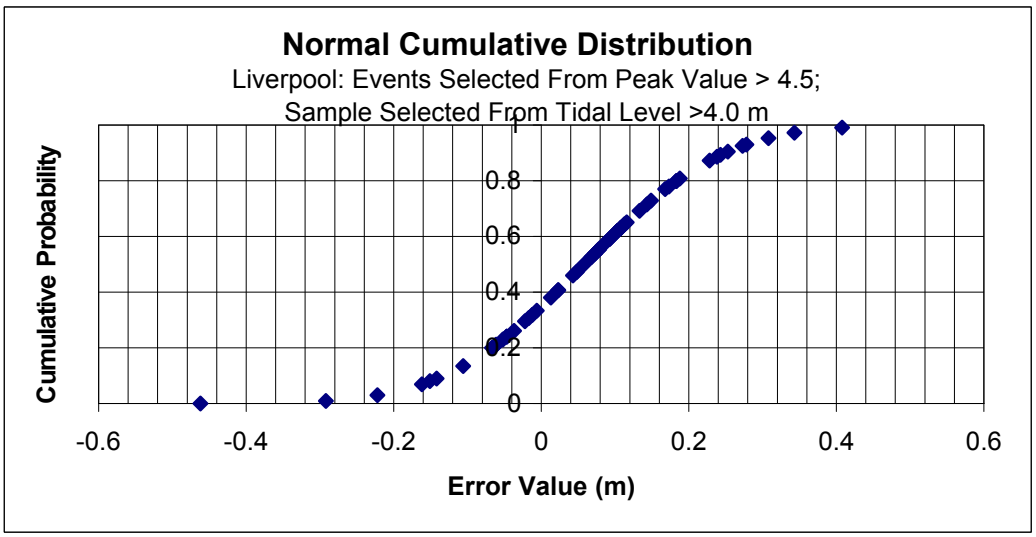

Figure A1 1.2 Error Distribution Analysis at Liverpool (peak > 4.5 m; tide level > 4.0 m)

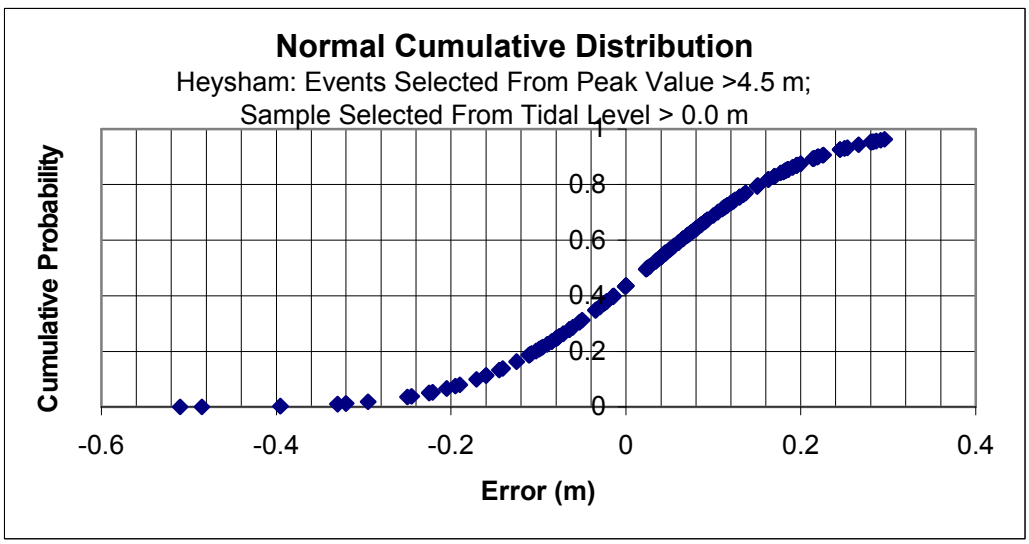

Figure A1 1.3 Error Distribution Analysis at Heysham (peak > 4.5 m; tide level > 0.0 m)

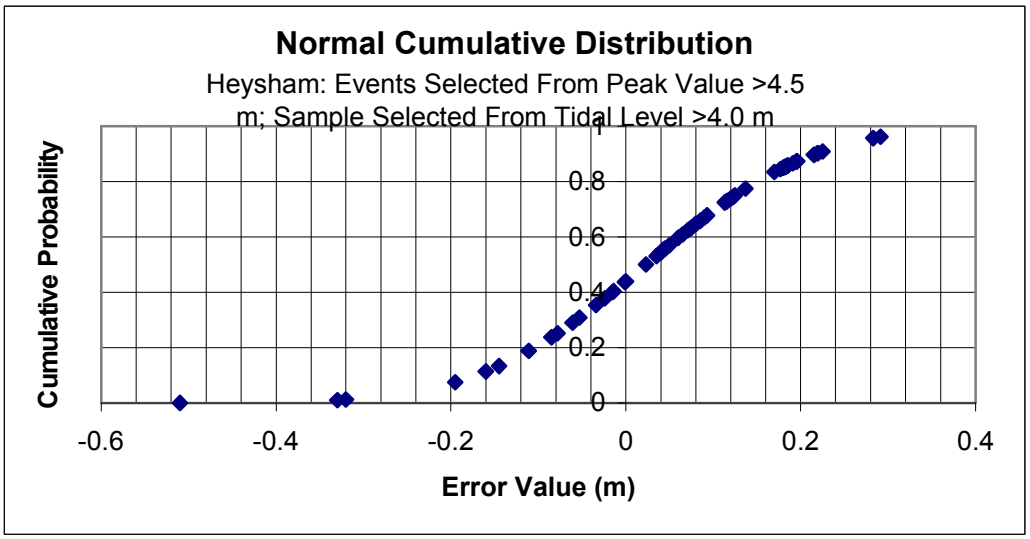

Figure A1 1.4 Error Distribution Analysis at Heysham (peak >4.5 m; tide level > 4.0 m)

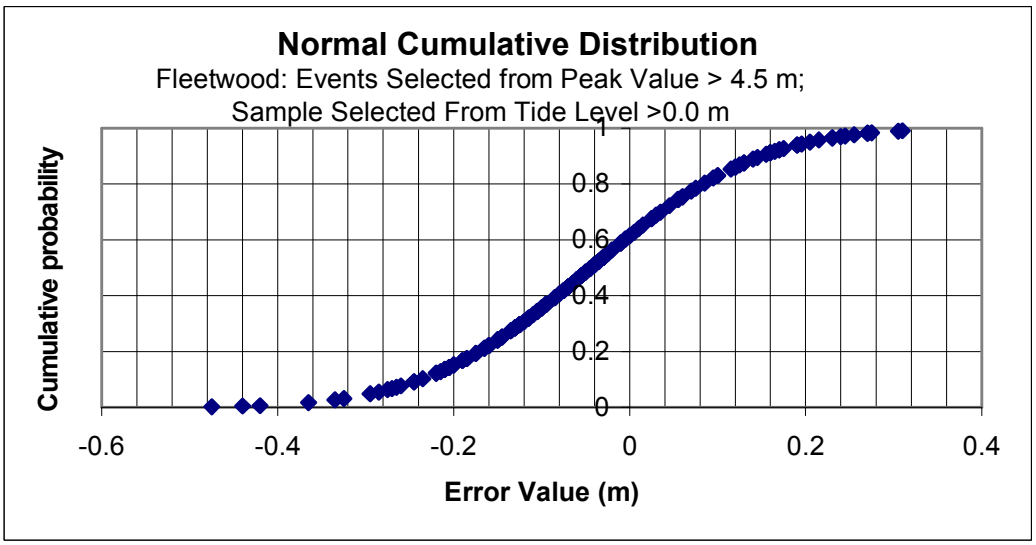

Figure A1 1.5 Error Distribution Analysis at Fleetwood (peak >4.5 m; tide level > 0.0 m)

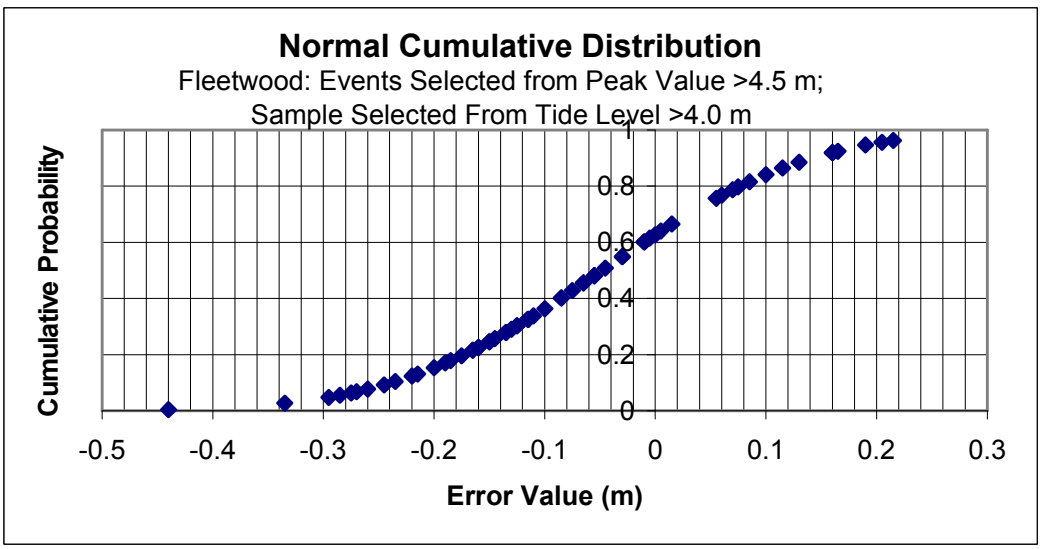

Figure A1 1.6 Error Distribution Analysis at Fleetwood (peak >4.5 m; tide level > 4.0 m)

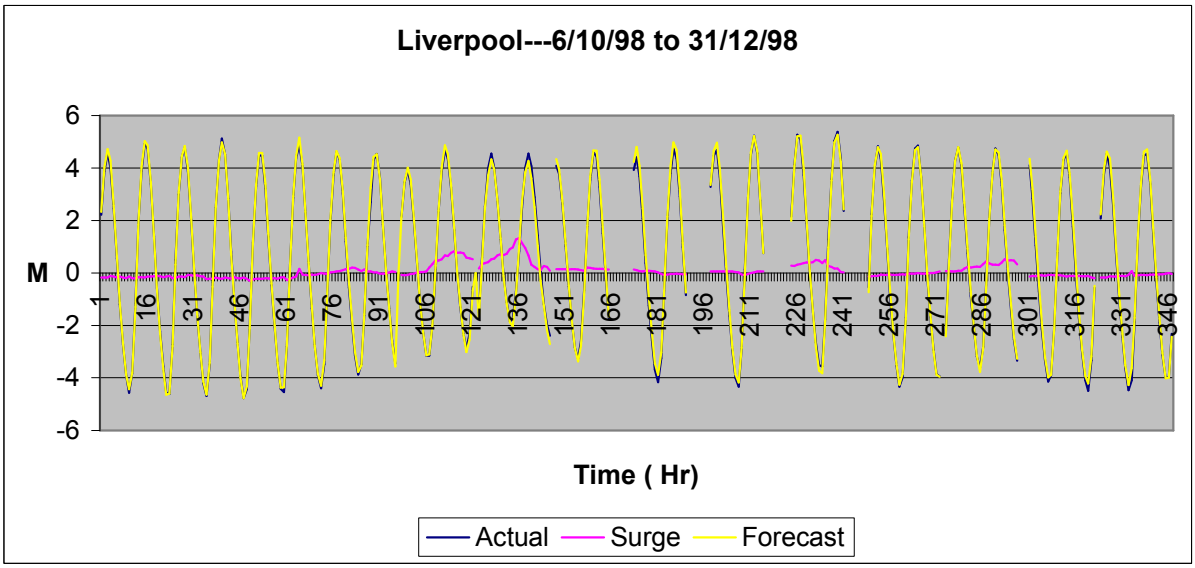

Figure A1 1.7 Tide Level, Surge and Forecast Tide at Liverpool for 061098 - 311298 (non-continuous)

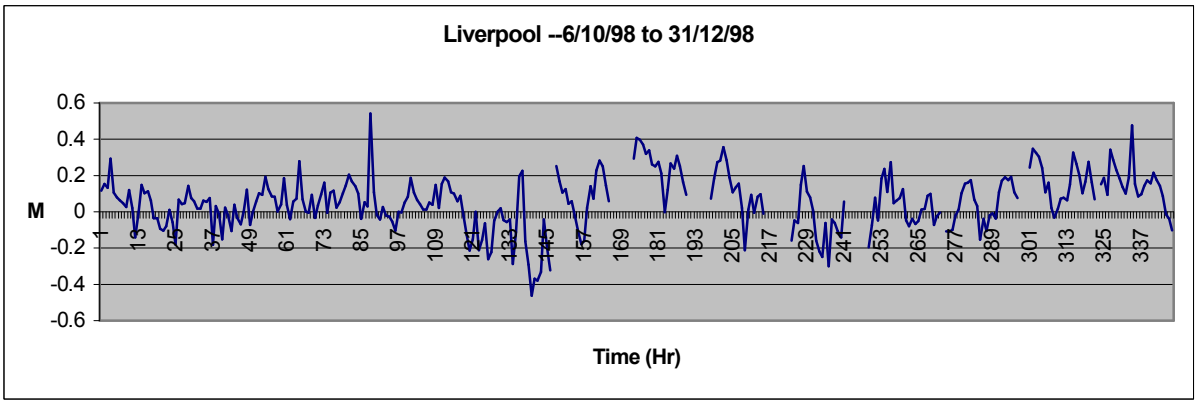

Figure A1 1.8 Errors in Forecast Tides at Liverpool for 061098 - 311298 (non-continuous)

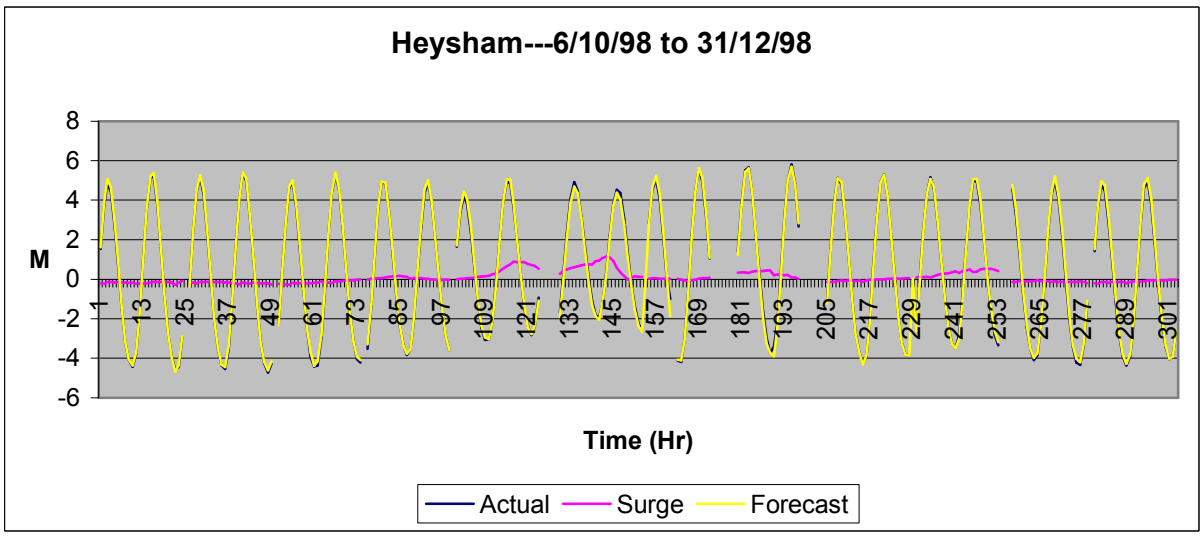

Figure A1 1.9 Tide Level, Surge and Forecast Tide at Heysham for 061098 - 311298 (non-continuous)

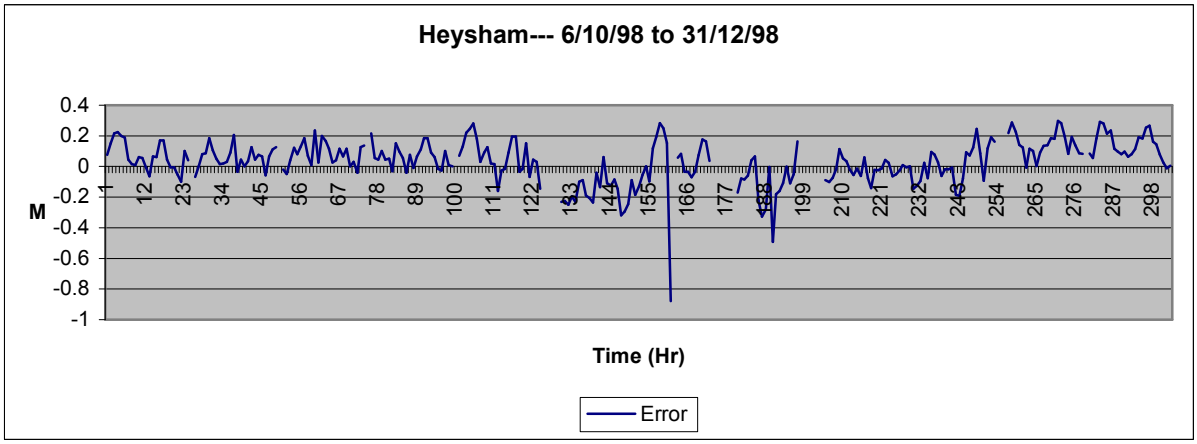

Figure A1 1.10 Errors in Forecast Tides at Heysham for 061098 - 311298 (non-continuous)

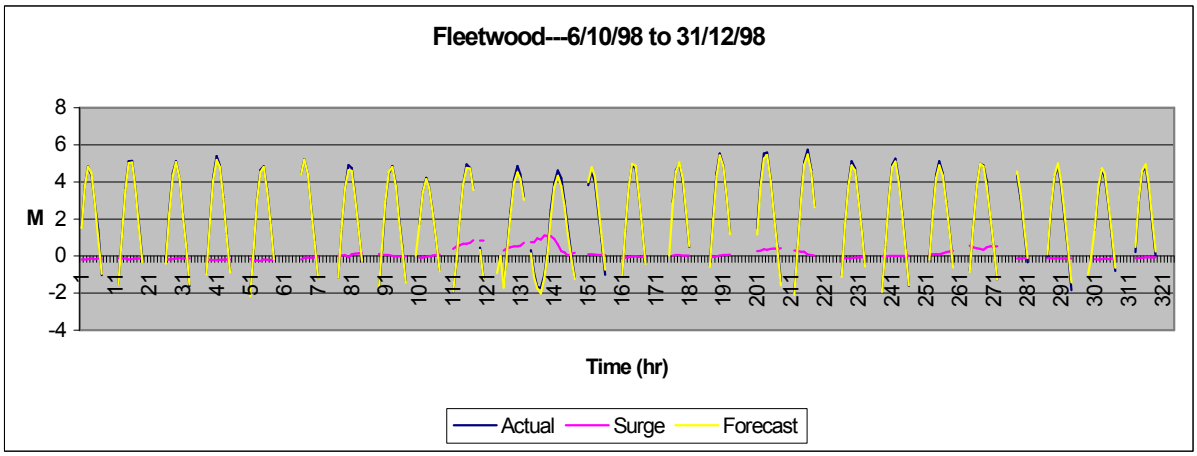

Figure A1 1.11 Tide Level, Surge and Forecast Tide at Fleetwood for 061098 - 311298 (non-continuous)

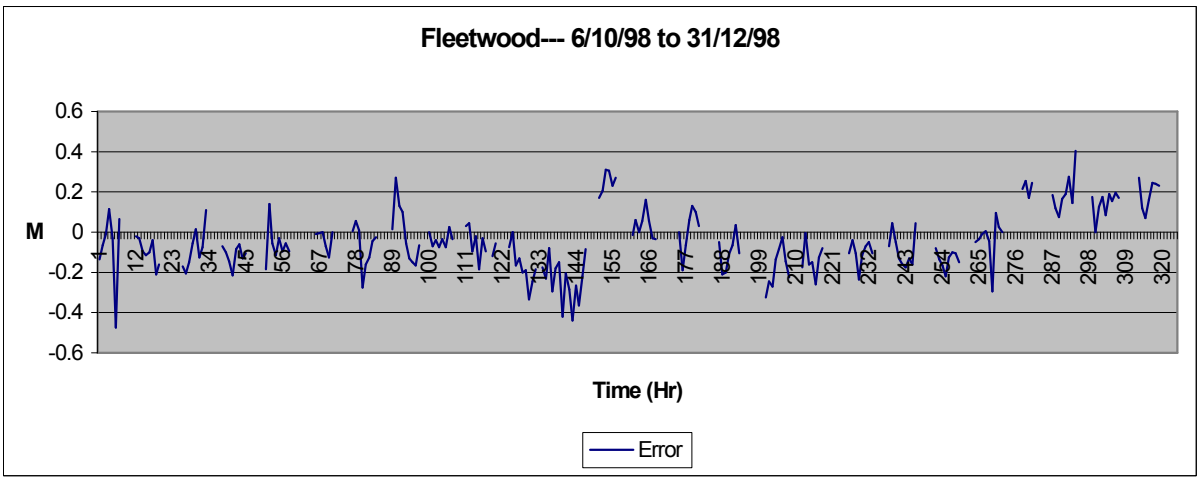

Figure A1 1.12 Errors in Forecast Tides at Fleetwood for 061098 - 311298 (non-continuous)

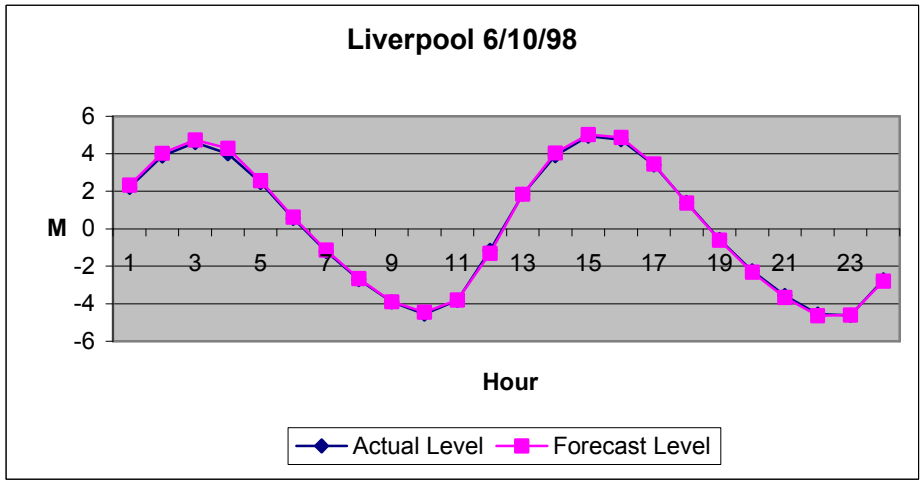

Actual Peak Value: 4.60 m & 4.93 m; Forecast Peak Value: 4.73 m & 5.03 m
Error: 0.13 m & 0.10 m; Time Error: 0 h & 0 h

Figure A1 1.13 Tide Forecast at Liverpool on 061098

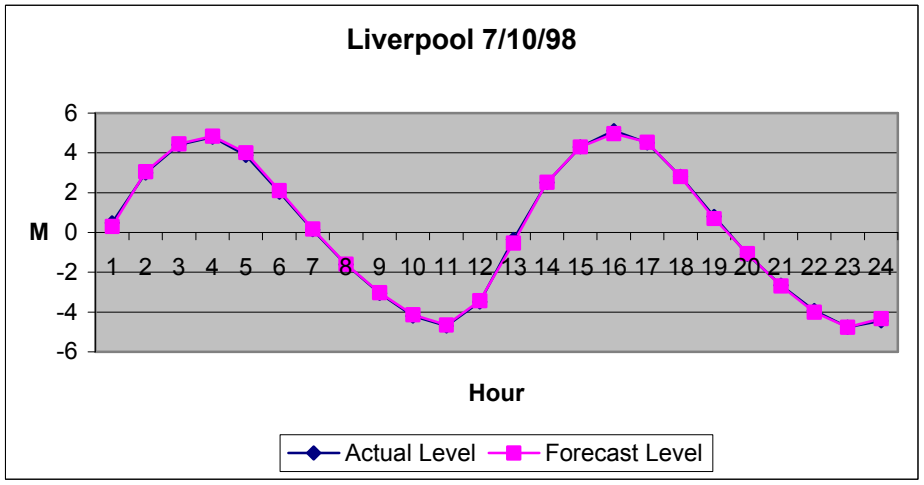

Actual Peak Value: 4.79 m & 5.12 m; Forecast Peak Value: 4.84 m & 4.97 m
Error: 0.05 m & -0.15 m; Time Error: 0 h & 0 h

Figure A1 1.14 Tide Forecast at Liverpool on 071098

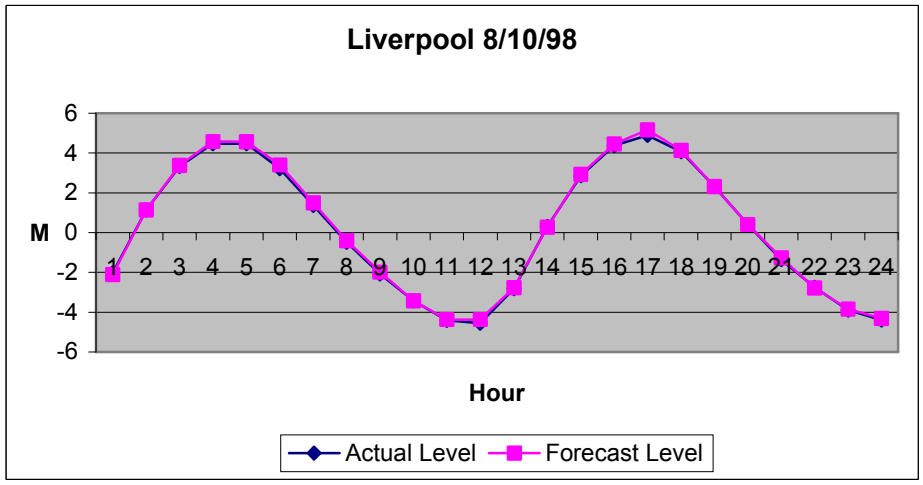

Actual Peak Value: 4.48 m & 4.88 m; Forecast Peak Value: 4.58 m & 5.16 m
Error: 0.10 m & 0.28 m; Time Error: 0 h & 0 h

Figure A1 1.15 Tide Forecast at Liverpool on 081098

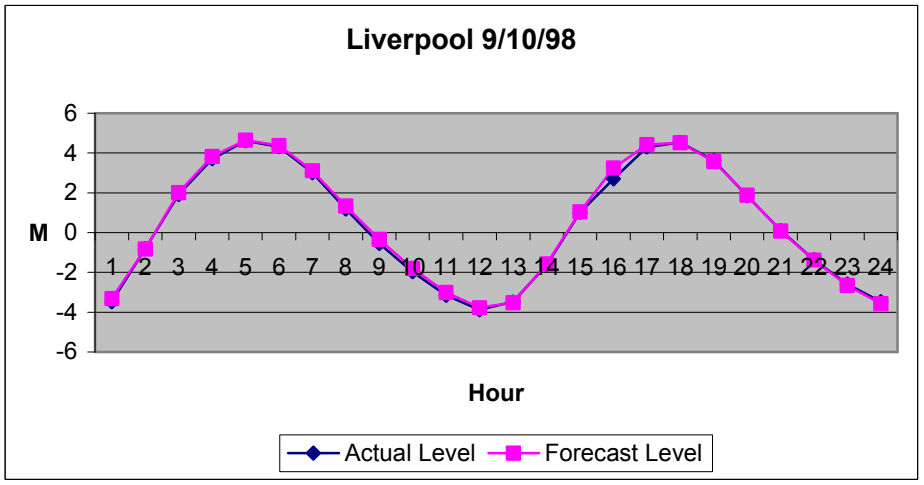

Actual Peak Value: 4.63 m & 4.54 m; Forecast Peak Value: 4.65 m & 4.52 m
Error: 0.02 m & -0.02 m; Time Error: 0 h & 0 h

Figure A1 1.16 Tide Forecast at Liverpool on 091098

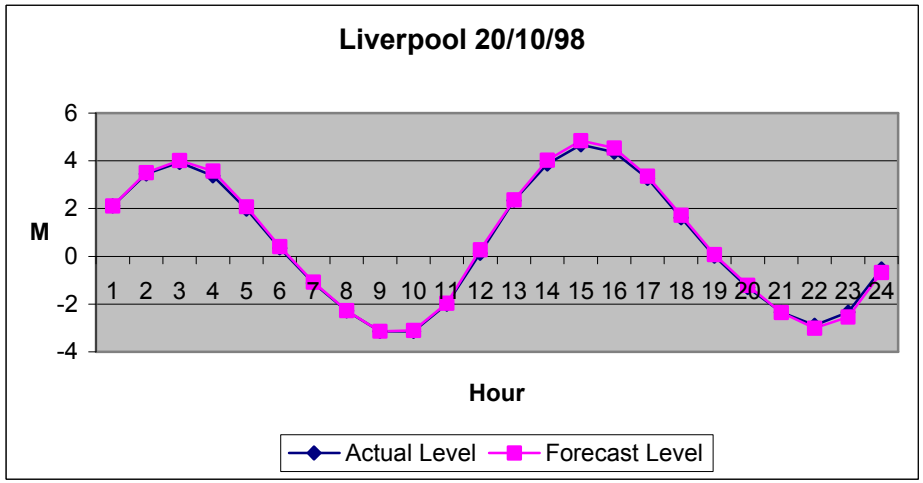

Actual Peak Value: 4.67 m; Forecast Peak Value: 4.86 m
Error: 0.19 m; Time Error: 0 h

Figure A1 1.17 Tide Forecast at Liverpool on 201098

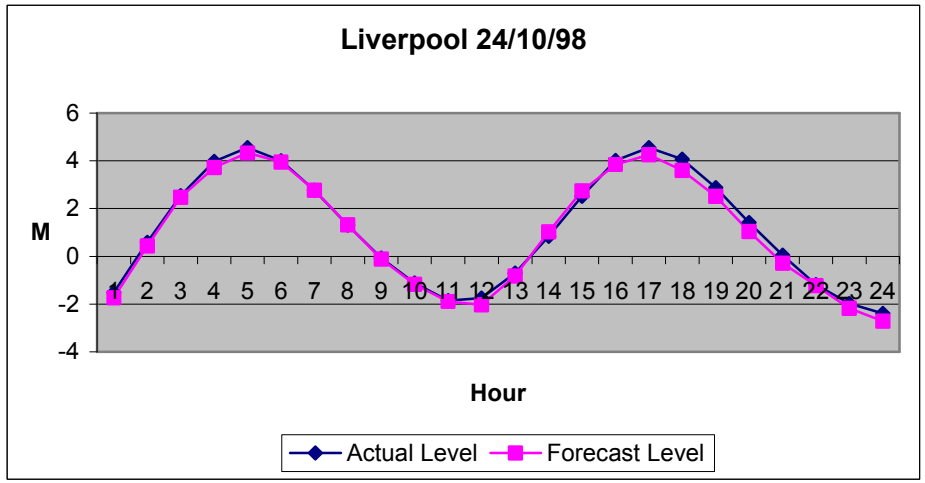

Actual Peak Value: 4.55 m & 4.55 m; Forecast Peak Value: 4.33 m & 4.26 m
Error: -0.22 m & -0.29 m; Time Error: 0 h & 0 h

Figure A1 1.16 Tide Forecast at Liverpool on 241098

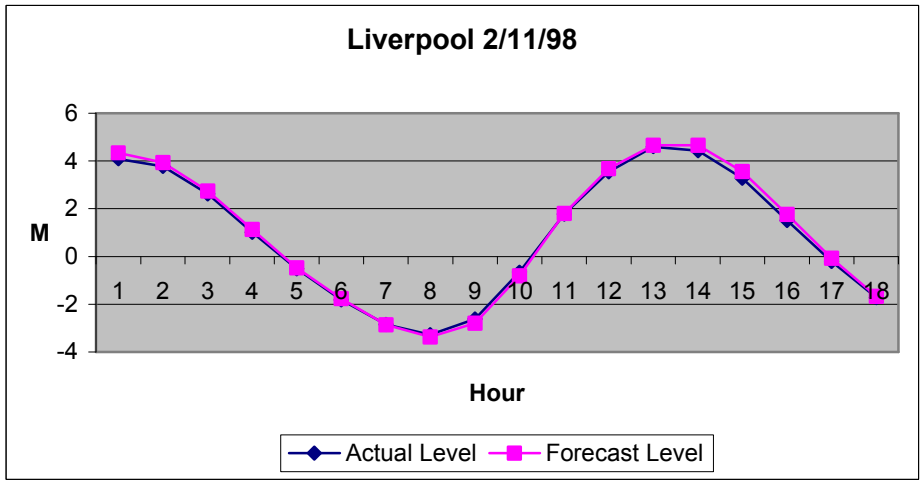

Actual Peak Value: 4.60 m; Forecast Peak Value: 4.67 m
Error: 0.07 m; Time Error: 0 h

Figure A1 1.19 Tide Forecast at Liverpool on 021198

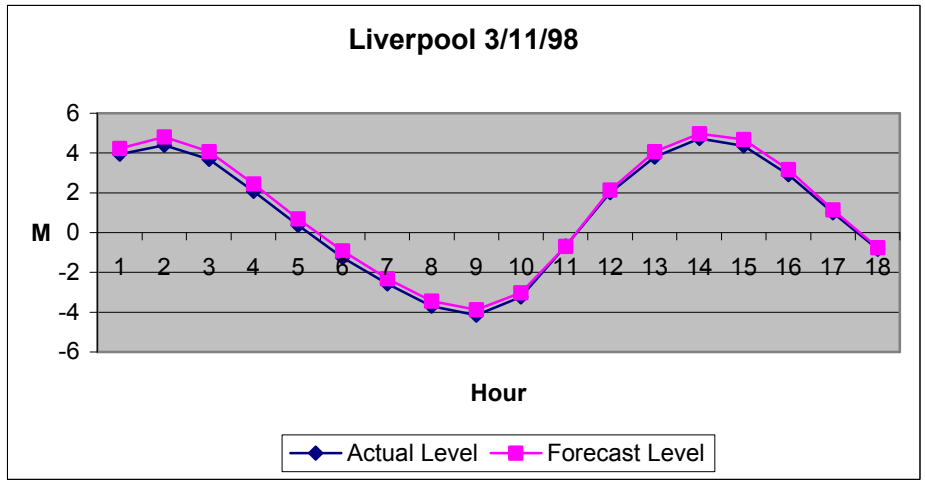

Actual Peak Value: 4.40 m & 4.73 m; Forecast Peak Value: 4.81 m & 4.97 m
Error: 0.41 m & 0.24 m; Time Error: 0 h & 0 h

Figure A1 1.20 Tide Forecast at Liverpool on 031198

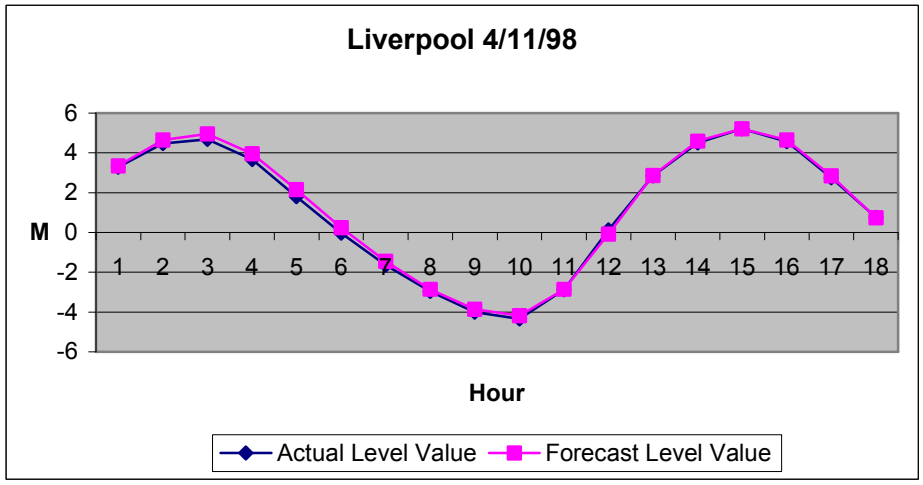

Actual Peak Value: 4.69 m & 5.23 m; Forecast Peak Value: 4.96 m & 5.22 m
Error: 0.27 m & -0.01 m; Time Error: 0 h & 0 h

Figure A1 1.21 Tide Forecast at Liverpool on 041198

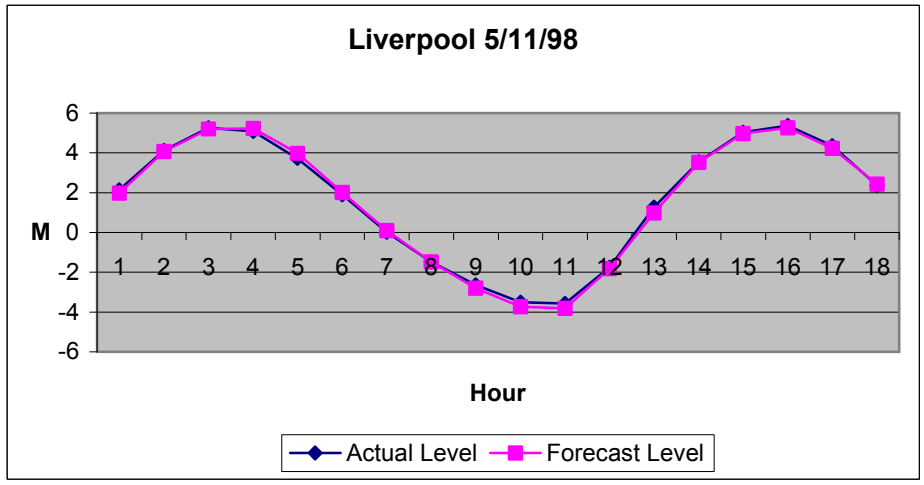

Actual Peak Value: 5.27 m & 5.38 m; Forecast Peak Value: 5.24 m & 5.27 m
Error: -0.03 m & -0.11 m: Time Error: -1 h & 0 h

Figure A1 1.22 Tide Forecast at Liverpool on 051198

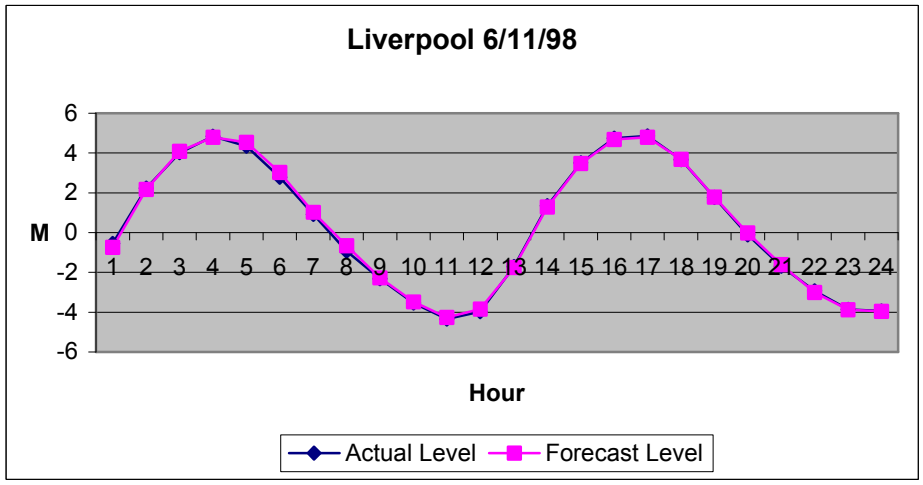

Actual Peak Value: 4.84 m & 4.85 m; Forecast Peak Value: 4.79 m & 4.80 m
Error: -0.05 m & -0.05 m; Time Error: 0 h & 0 h

Figure A1 1.23 Tide Forecast at Liverpool on 061198

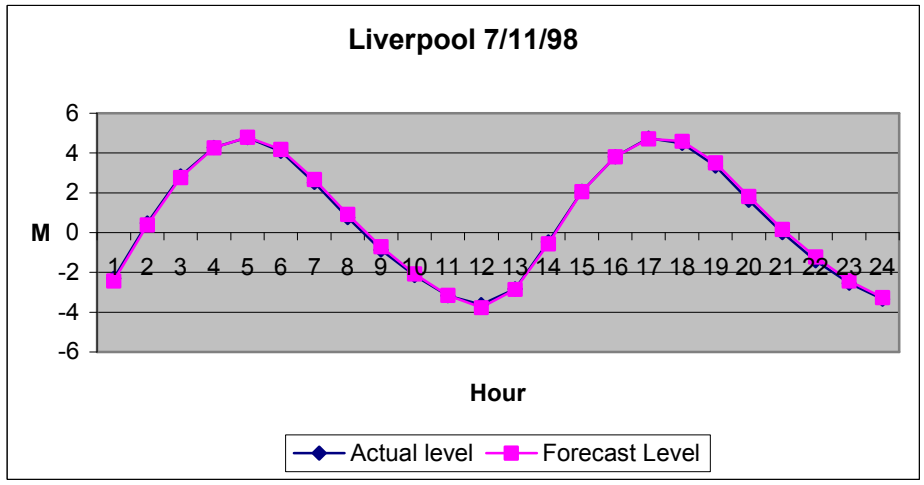

Actual Peak Value: 4.78 m & 4.75 m; Forecast Peak Value: 4.79 m & 4.71 m
Error: 0.01 m & -0.04 m; Time Error: 0 h & 0 h

Figure A1 1.24 Tide Forecast at Liverpool on 071198

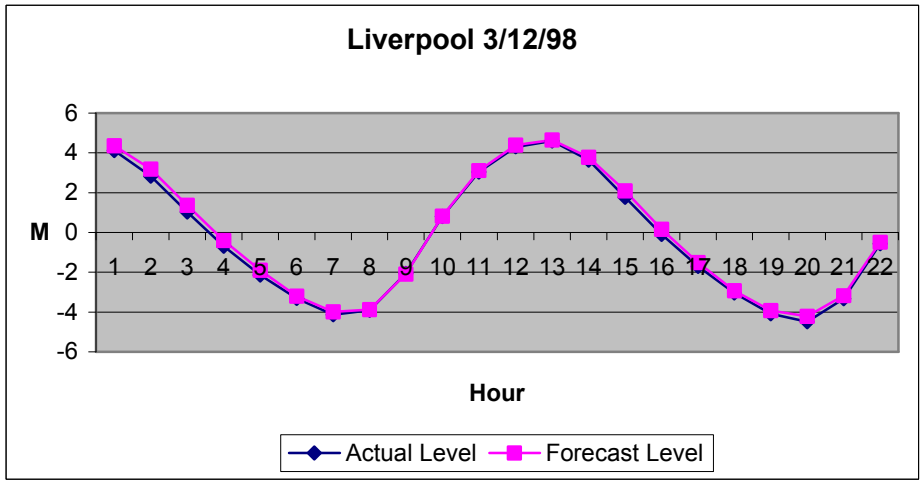

Actual Peak Value: 4.60 m; Forecast Peak Value: 4.66 m
Error: 0.06 m; Time Error: 0 h

Figure A1 1.25 Tide Forecast at Liverpool on 031298

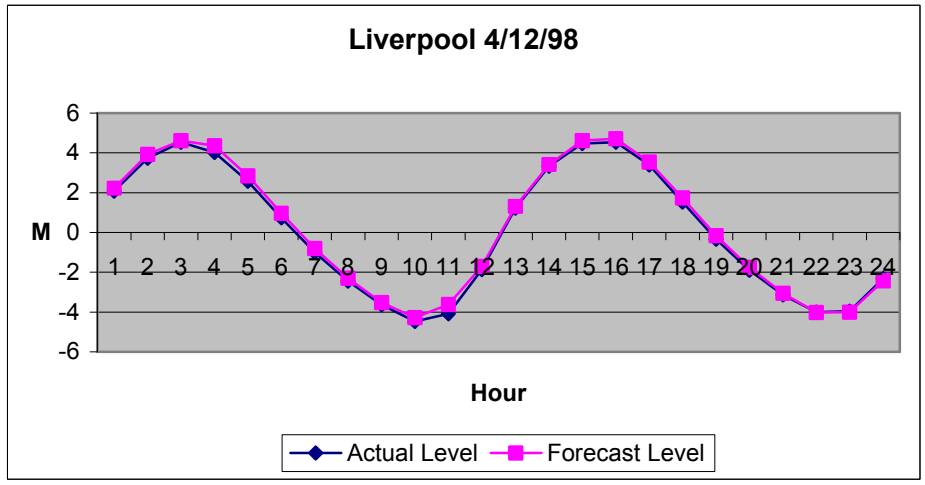

Actual Peak Value: 4.54 m & 4.54 m; Forecast Peak Value: 4.63 m & 4.71 m
Error: 0.09 m & 0.17 m; Time Error: 0 h & 0 h

Figure A1 1.26 Tide Forecast at Liverpool on 041298

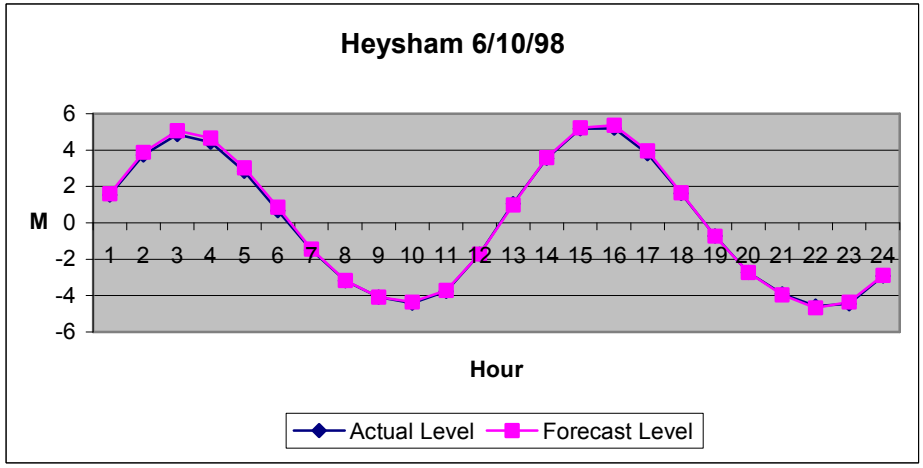

Actual Peak Value: 4.85 m & 5.20 m; Forecast Peak Value: 5.07 m & 5.37 m
Error: 0.22 m & 0.17 m; Time Error: 0 h & 0 h

Figure A1 1.27 Tide Forecast at Heysham on 061098

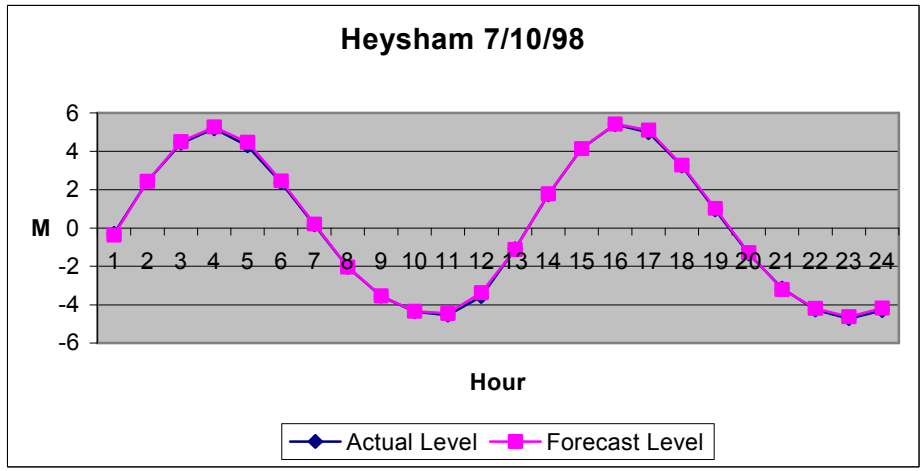

Actual Peak Value: 5.18 m & 5.39 m; Forecast Peak Value: 5.27 m & 5.43 m
Error: 0.09 m & 0.04 m; Time Error: 0 h & 0 h

Figure A1 1.28 Tide Forecast at Heysham on 071098

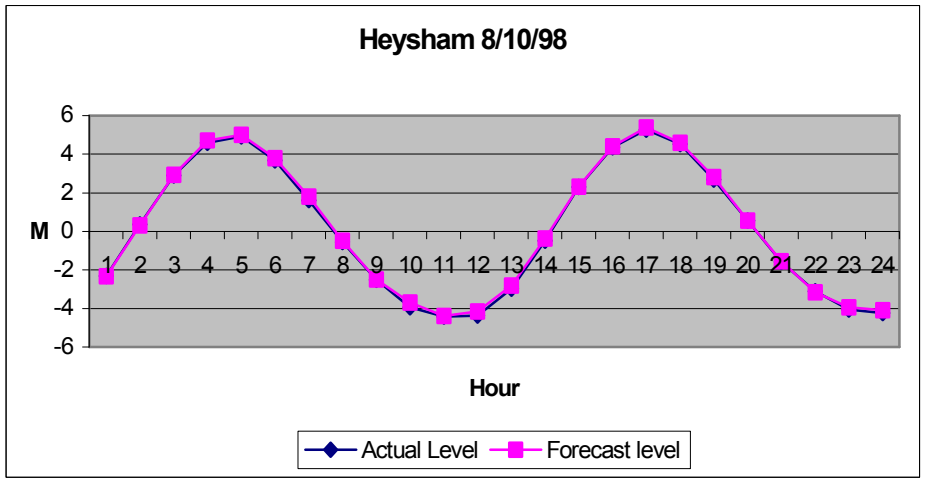

Actual Peak Value: 4.93 m & 5.27 m; Forecast Peak Value: 5.01 m & 5.39 m
Error: 0.08 m & 0.12 m; Time Error: 0 h & 0 h

Figure A1 1.29 Tide Forecast at Heysham on 081098

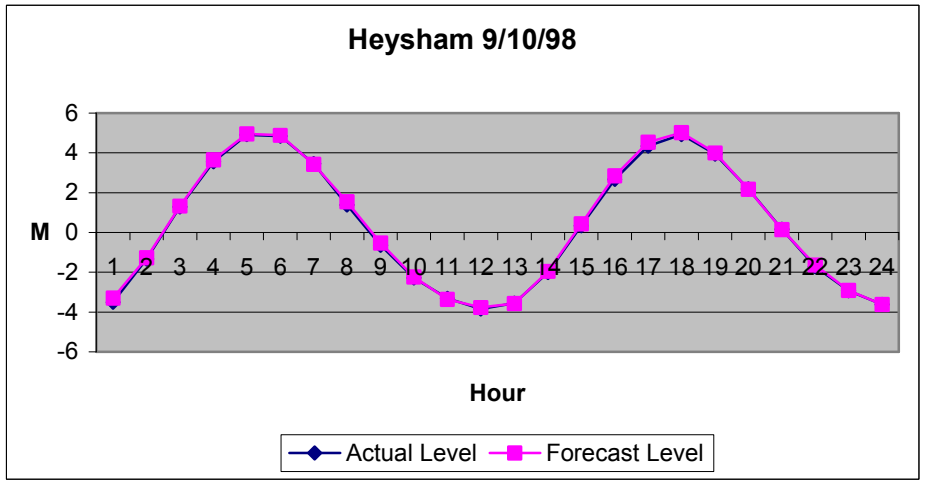

Actual Peak Value: 4.91 m & 4.93 m; Forecast Peak Value: 4.96 m & 5.02 m
Error: 0.05 m & 0.09 m; Time Error: 0 h & 0 h

Figure A1 1.30 Tide Forecast at Heysham on 091098

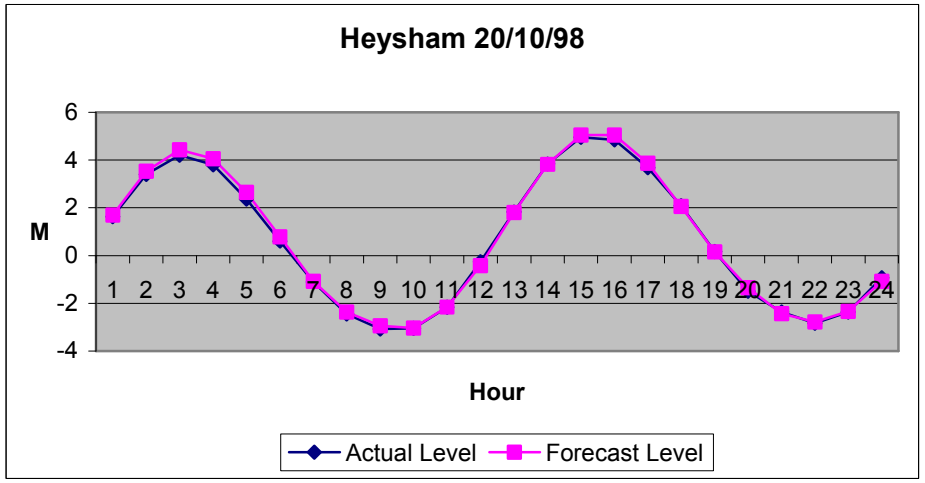

Actual Peak Value: 4.96 m; Forecast Peak Value: 5.05 m
Error: 0.09 m; Time Error: 0 h & 0 h

Figure A1 1.31 Tide Forecast at Heysham on 201098

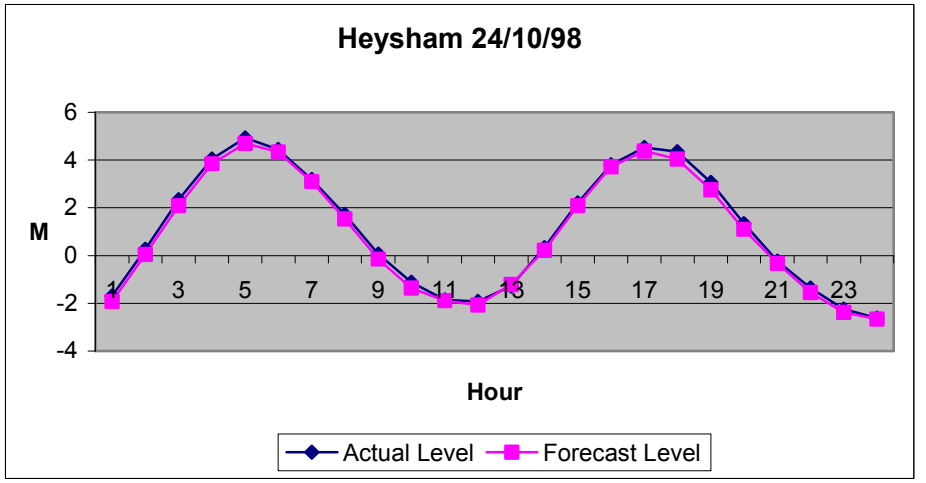

Actual Peak Value: 4.93 m & 4.52 m; Forecast Peak Value: 4.70 m & 4.38 m
Error: -0.23 m & -0.14 m; Time Error: 0 h & 0 h

Figure A1 1.32 Tide Forecast at Heysham on 241098

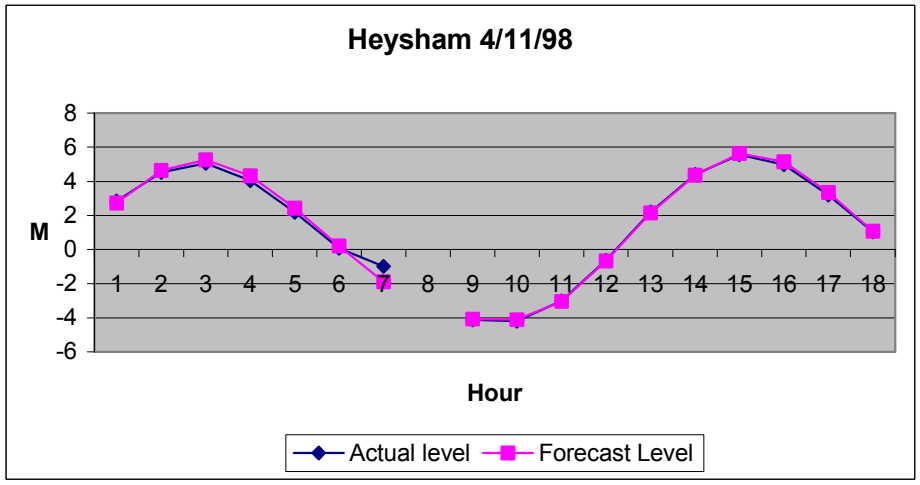

Actual Peak Value: 5.05 m & 5.56 m; Forecast Peak Value: 5.25 m & 5.63 m
Error: 0.20 m & 0.07 m; Time Error: 0 h & 0 h

Figure A1 1.33 Tide Forecast at Heysham on 041198

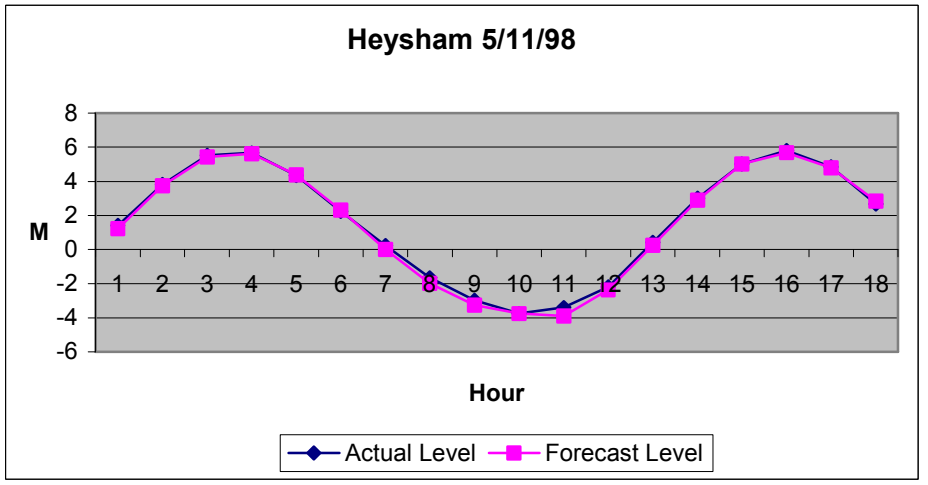

Actual Peak Value: 5.67 m & 5.80 m; Forecast Peak Value: 5.61 m & 5.69 m
Error: -0.06 m & -0.11 m; Time Error: 0 h & 0 h

Figure A1 1.34 Tide Forecast at Heysham on 051198

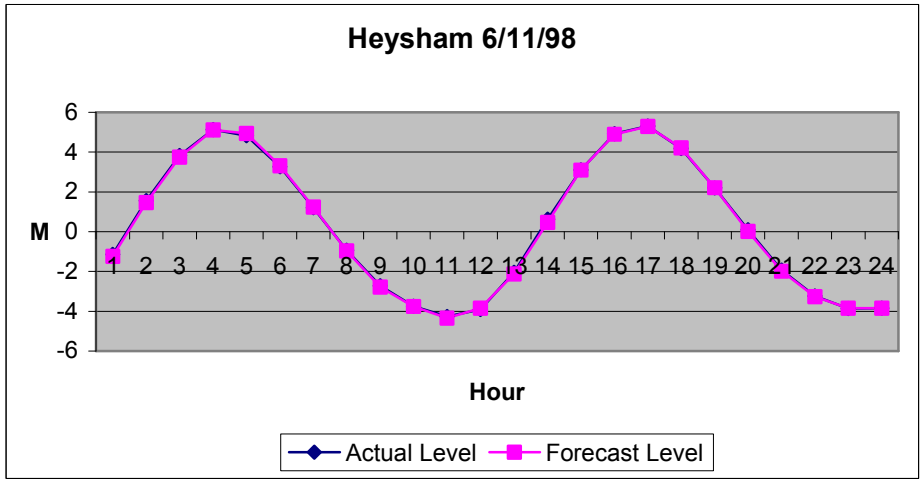

Actual Peak Value: 5.13 m & 5.31 m; Forecast Peak Value: 5.12 m & 5.30 m
Error: -0.01 m & -0.01 m; Time Error: 0 h & 0 h

Figure A1 1.35 Tide Forecast at Heysham on 061198

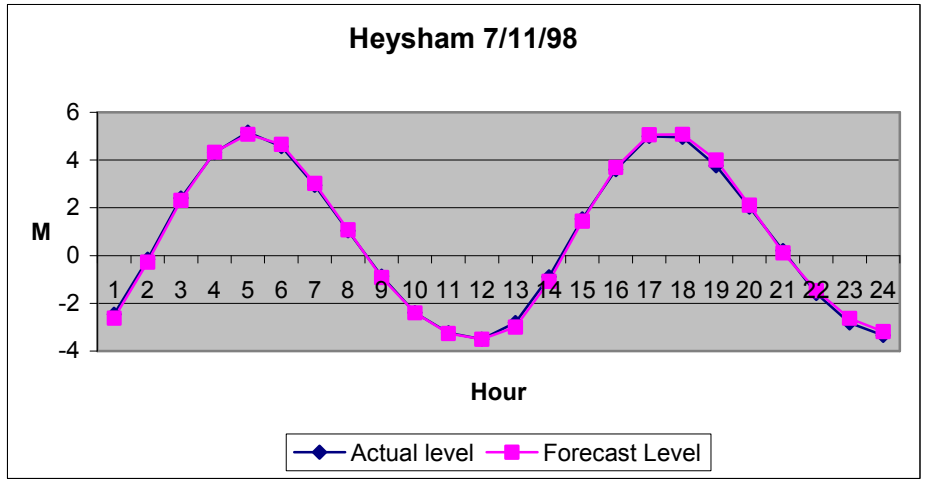

Actual Peak Value: 5.17 m & 4.99 m; Forecast Peak Value: 5.09 m & 5.06 m
Error: -0.08 m & 0.07 m; Time Error: 0 h & 0 h

Figure A1 1.36 Tide Forecast at Heysham on 071198

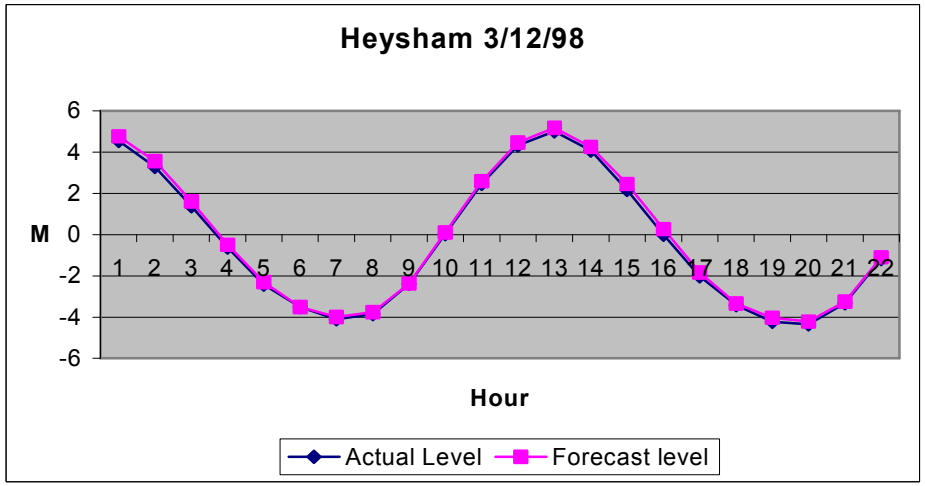

Actual Peak Value: 5.00 m; Forecast Peak Value: 5.19 m
Error: 0.19 m; Time Error: 0 h

Figure A1 1.37 Tide Forecast at Heysham on 031298

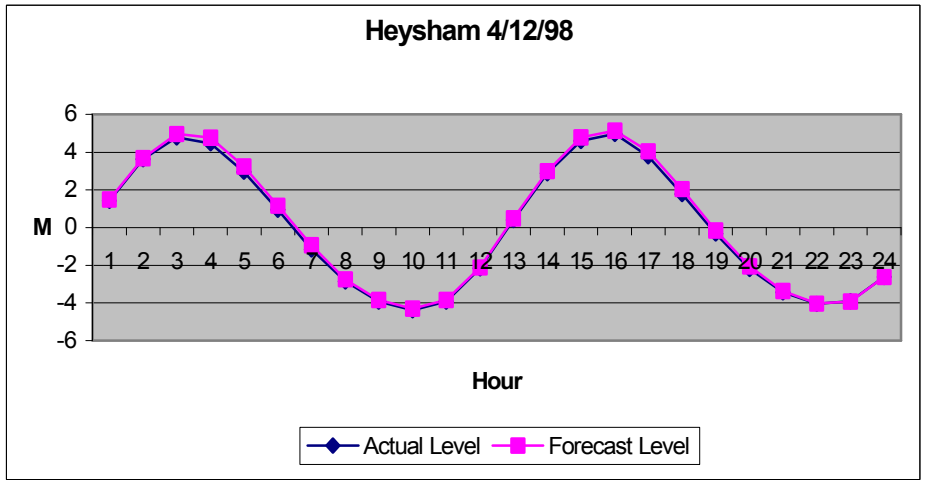

Actual Peak Value: 4.78 m & 4.96 m; Forecast Peak Value: 4.96 m & 5.14 m
Error: 0.18 m & 0.18 m; Time Error: 0 h & 0 h

Figure A1 1.38 Tide Forecast at Heysham on 041298

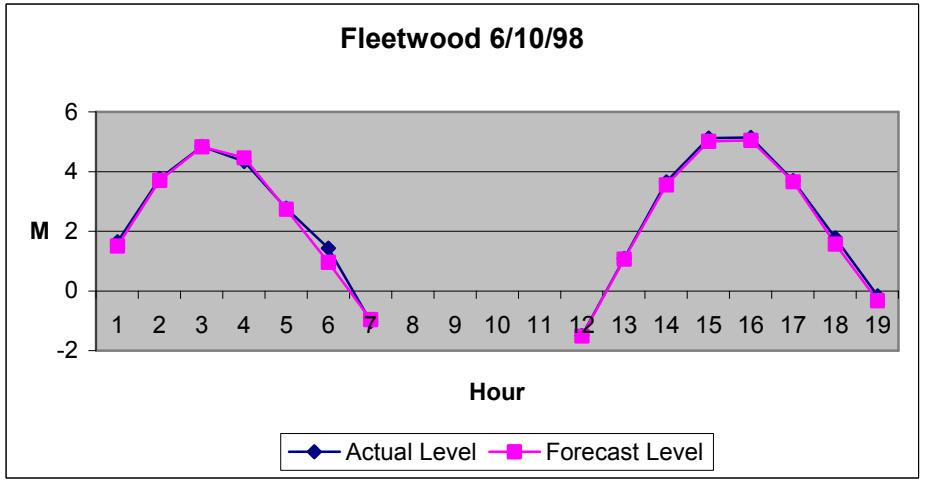

Actual Peak Value: 4.84 m & 5.12 m; Forecast Peak Value: 4.83 m & 5.01 m
Error: -0.01 m & -0.11 m; Time Error: 0 h & 0 h

Figure A1 1.39 Tide Forecast at Fleetwood on 061098

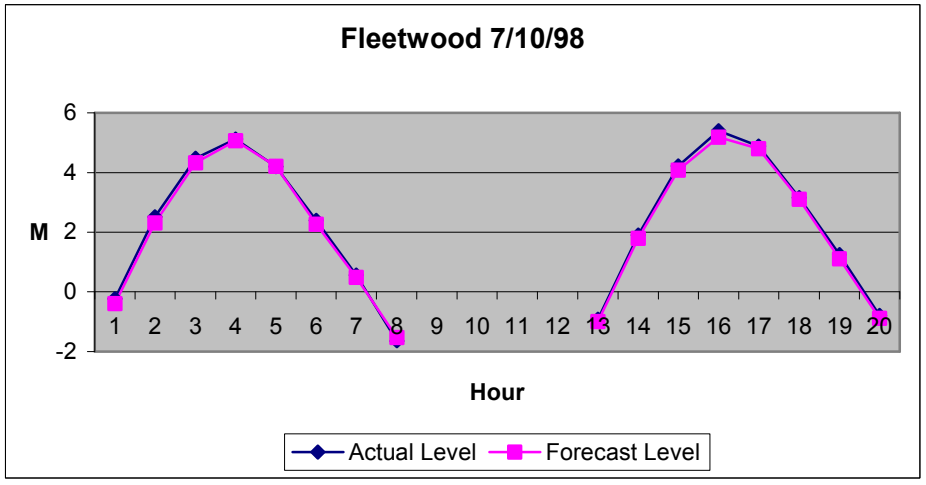

Actual Peak Value: 5.12 m & 5.39 m; Forecast Peak Value: 5.07 m & 5.18 m
Error: -0.05 m & -0.21 m; Time Error: 0 h & 0 h

Figure A1 1.40 Tide Forecast at Fleetwood on 071098

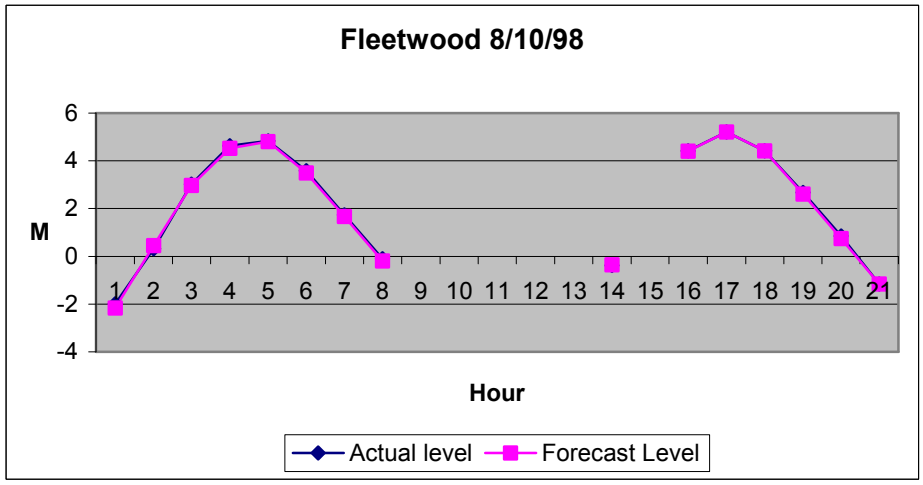

Actual Peak Value: 4.84 m & 5.21 m; Forecast Peak Value: 4.81 m & 5.21 m
Error: -0.03 m & 0.00 m; Time Error: 0 h & 0 h

Figure A1 1.41 Tide Forecast at Fleetwood on 081098

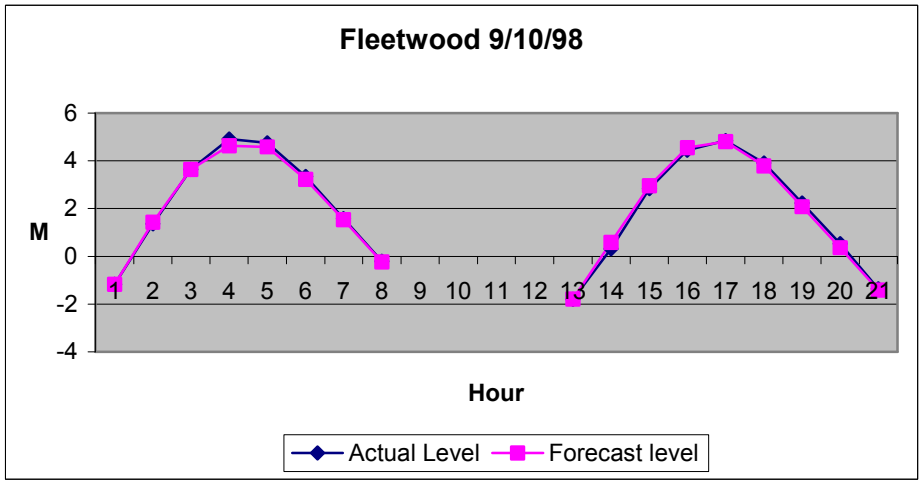

Actual Peak Value: 4.91 m & 4.85 m; Forecast Peak Value: 4.64 m & 4.80 m
Error: -0.27 m & -0.05 m; Time Error: 0 h & 0 h

Figure A1 1.42 Tide Forecast at Fleetwood on 091098

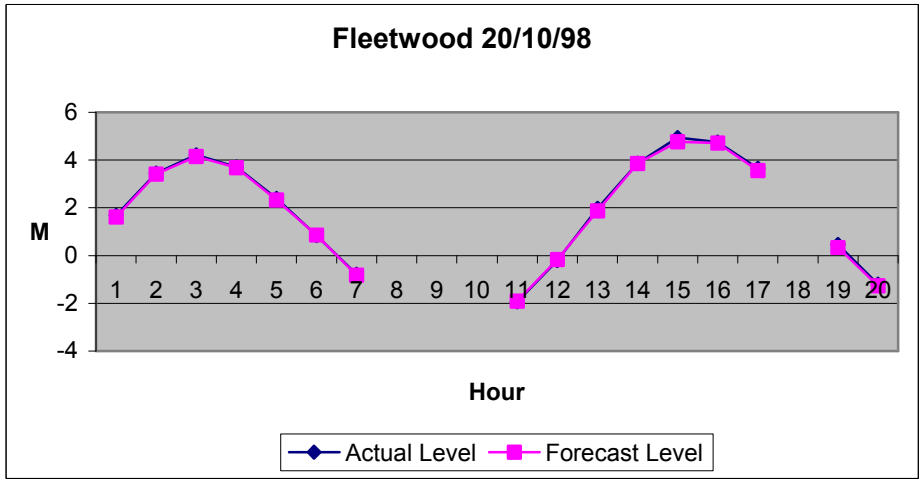

Actual Peak Value: 4.94 m; Forecast Peak Value: 4.76 m
Error: -0.18 m; Time Error: 0 h

Figure A1 1.43 Tide Forecast at Fleetwood on 201098

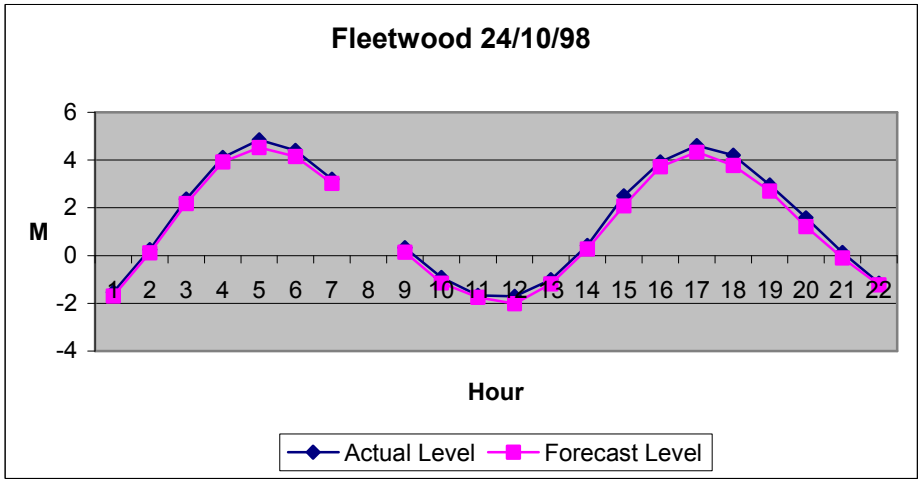

Actual Peak Value: 4.85 m & 4.61 m; Forecast Peak Value: 4.52 m & 4.33 m
Error: -0.33 m & -0.28 m; Time Error: 0 h & 0 h

Figure A1 1.44 Tide Forecast at Fleetwood on 241098

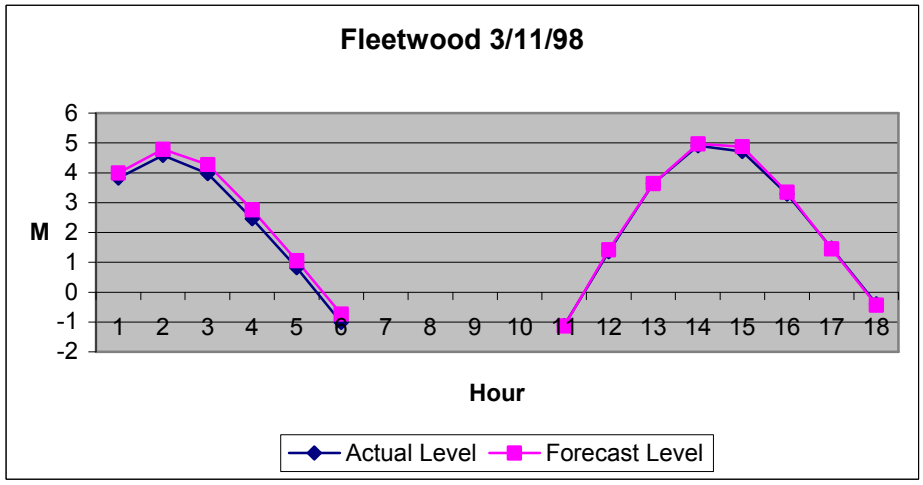

Actual Peak Value: 4.58 m & 4.91 m; Forecast Peak Value: 4.79 m & 4.97 m
Error: 0.21 m & 0.06 m; Time Error: 0 h & 0 h

Figure A1 1.45 Tide Forecast at Fleetwood on 031198

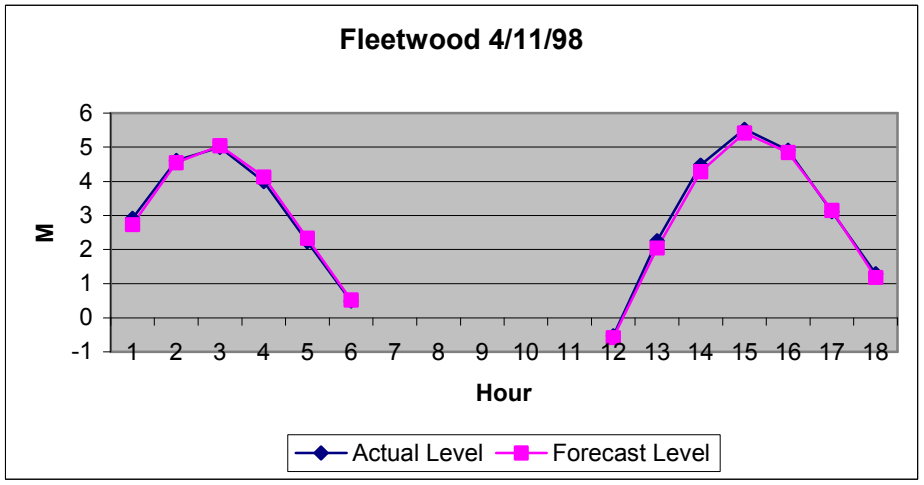

Actual Peak Value: 4.99 m & 5.53 m; Forecast Peak Value: 5.05 m & 5.42 m
Error: 0.06 m & -0.11 m; Time Error: 0 h & 0 h

Figure A1 1.46 Tide Forecast at Fleetwood on 041198

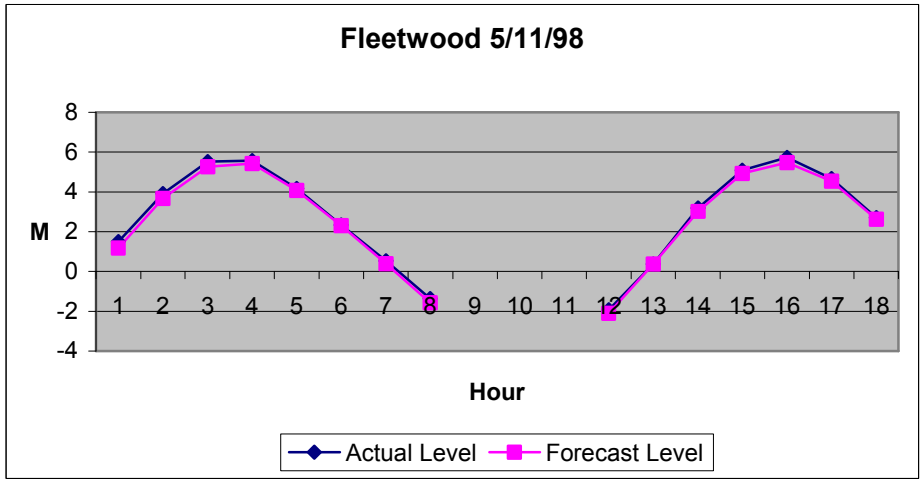

Actual Peak Value: 5.57 m & 5.74 m; Forecast Peak Value: 5.44 m & 5.48 m
Error: -0.13 m & -0.26 m; Time Error: 0 h & 0 h

Figure A1 1.47 Tide Forecast at Fleetwood on 051198

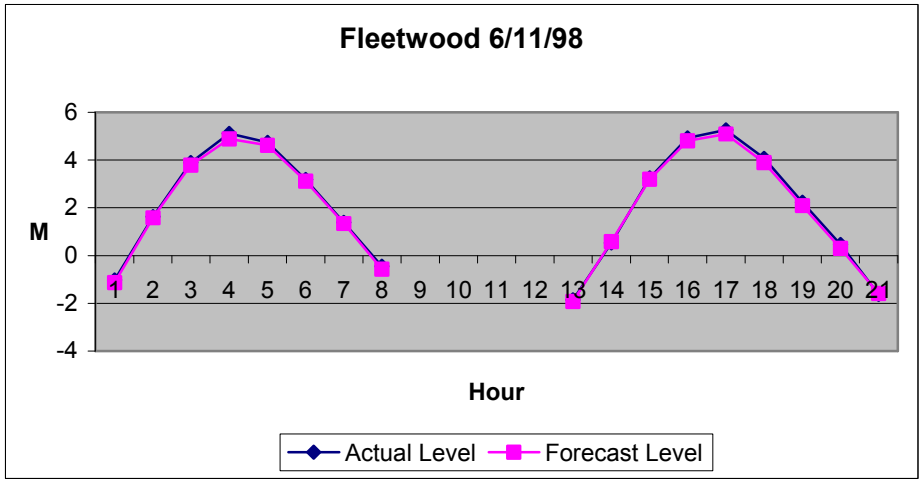

Actual Peak Value: 5.12 m & 5.26 m; Forecast Peak Value: 4.89 m & 5.10 m
Error: -0.23 m & -0.16 m; Time Error: 0 h & 0 h

Figure A1 1.48 Tide Forecast at Fleetwood on 061198

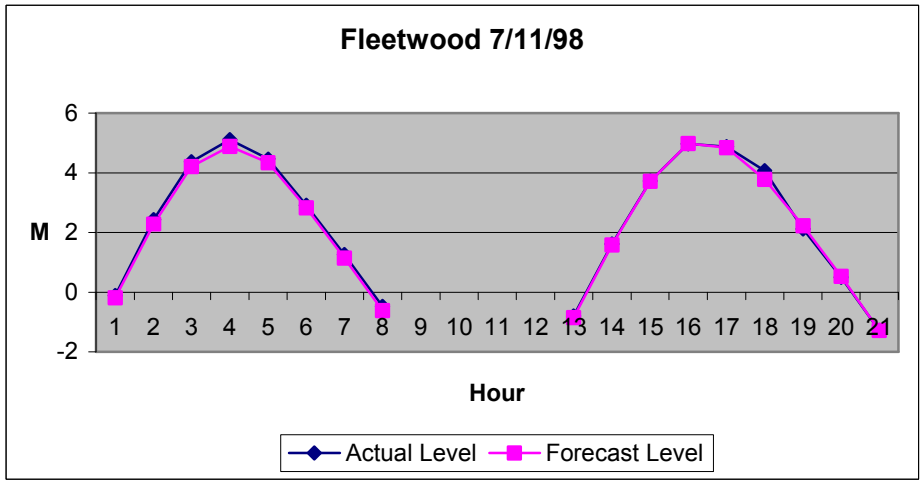

Actual Peak Value: 5.11 m & 4.97 m; Forecast Peak Value: 4.89 m & 4.98 m
Error: -0.22 m & 0.01 m; Time Error: 0 h & 0 h

Figure A1 1.49 Tide Forecast at Fleetwood on 071198

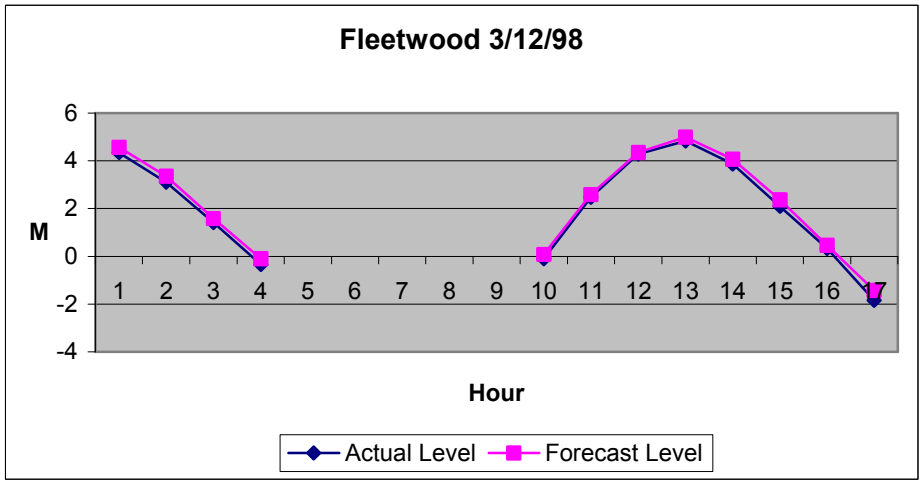

Actual Peak Value: 4.82 m; Forecast Peak Value: 4.99 m
Error: 0.17 m; Time Error: 0 h

Figure A1 1.50 Tide Forecast at Fleetwood on 031298

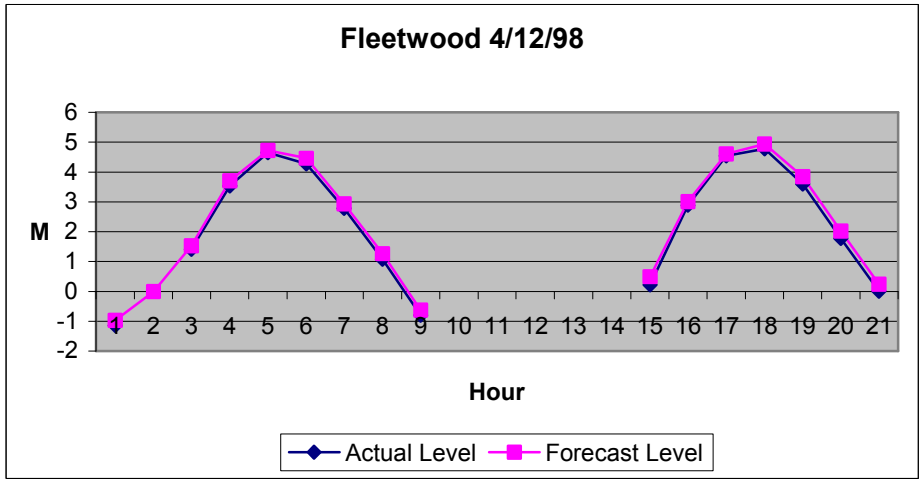

Actual Peak Value: 4.64 m & 4.78 m; Forecast Peak Value: 4.73 m & 4.94 m
Error: 0.09 m & 0.16 m; Time Error: 0 h & 0 h

Figure A1 1.51 Tide Forecast at Fleetwood on 041298

APPENDIX 2

RESULTS FROM EXISTING MODELS IN THE SOUTH WEST REGION

2.1 Avonmouth

The tidal levels are all computed on the basis of mean level in metres above chart datum. The chart datum correction for Avonmouth is 6.5 m, which must be added to the levels cited in order to give a level relative to Ordnance Datum at Newlyn, Cornwall.

2.1.1 Forecast Model

The Forecast model used at Avonmouth may be defined as:

Forecast Tide Level = *Astronomic Tide* + *STFS Forecast Surge Residual* (At Avonmouth)

2.1.2 Tidal Flood Warning Procedures

The tidal flood warning procedure is as follows

- If the *Tide Level (Astronomic + Surge)* **< 7.2 m** then *Tide Watch* = **None**; *Action to be Taken* = **None**
- If the *Tide Level (Astronomic + Surge)* = **7.2 m** then *Tide Watch* = **Provisional**; *Action to be Taken* = **Keep Situation Under Review**
- If the *Tide Level (Astronomic + Surge)* = **7.7 m** then *Tide Watch* = **Definite**; *Action to be Taken* = **Issue YELLOW WARNING**
- If the *Tide Level (Astronomic + Surge)* = **8.0 m** then *Tide Watch* = **Definite**; *Action to be Taken* = **Issue AMBER WARNING**
- If the *Tide Level Astronomic + Surge)* = **8.7 m** then *Tide Watch* = **Definite**; *Action to be Taken* = **Issue RED WARNING**

NB These actions apply for all wind conditions.

2.1.3 Data Used in the Tests

The data used in the testing of the Avonmouth model was taken from the period 010194 - 311298. The events selected were determined by compliance with the condition that the *High Tide Level* > 7.5 m. The forecast lead time considered was 6 hours.

2.2 Forecast Accuracy at Avonmouth

- Of 40 tidal cycles considered, 30 cycles triggered flood warnings correctly based upon the associated forecast. The accuracy of the flood warning issued is 72.5% with a lead time of 6 hours.

- Of 40 tidal cycles considered, 28 had a peak error of less than 0.2 m. The accuracy of the peak forecast is 75% with a 0.2 m error.

- Of 40 tidal cycles considered, 36 had a peak error of less than 0.3 m. The accuracy of the peak forecast is 90% with a 0.3m error.

The details of the events used in these tests are listed in Table A2-2.1.

2.3 Error Analysis at Avonmouth

9 tidal cycles should have resulted in the issuing of a yellow warning based upon the forecast. However their actual high tide levels did not reach the flood warning threshold of 7.70 m. One event (061094 evening tide) should have resulted in the issuing of a flood warning but this did not occur. The largest errors are to be found in these events, details of which are given in Table A2-2.2. Three of these events have obvious errors, These being the 090994 (morning tide); 031194 (morning tide); and 100297 (evening tide). The peak tide levels for these three events exhibit obvious differences between the two peaks for the day. The biggest difference was 0.73 m on 031194. This characteristic is not observable in other events at Avonmouth and thus could result from gauge errors.

2.4 Error Statistical Tests

The correlation coefficients between the error and forecast surge, and the error and astronomic tide at Avonmouth are very small (see Table A2-2.3). This shows that there is not a strong correlation within these results. The mean of the error is sufficiently small to be thought of as zero. The error fits a normal distribution without generating a significant cumulative error. This shows that there are no systematic errors within the data (see Table A2-2.4 and Figures A2-2.1 - A2-2.3). The complete set of forecasts and actual tides for Avonmouth are displayed graphically in Figures A2-2.4 - 2.23

Table A2 2.1 List of Tide Events Used in Tests at Avonmouth

Event	Wind Direction	Wind Speed (Force)	Forecast Surge (m)	Astron. Tide (m)	Forecast Tide (m)	Actual Tide (m)	Peak Error (m)	Warning
080994	SW	7	0.23	7.6	7.83	7.84	-0.01	Yellow
	SW-W	7-8	0.27	7.6	7.87	7.71	0.16	Yellow
090994	SSW	6-7	0.22	7.6	7.82	7.13	0.69	Yellow*
	SW	6	0.25	7.5	7.75	7.53	0.22	Yellow*
061094	SSE	6	-0.22	7.6	7.38	7.53	-0.15	
	SSE	5	-0.16	7.7	7.54	7.72	-0.18	Missed
071094		3	-0.14	7.7	7.56	7.37	0.19	
			-0.11	7.6	7.49	7.57	-0.08	
031194	SW	4	0.05	7.7	7.75	7.02	0.73	Yellow*
	SWW	5-6	0.20	7.5	7.70	7.64	0.06	Yellow*
041194		3	0.06	7.8	7.86	7.79	0.07	Yellow
		4-5	0.09	7.7	7.79	7.52	0.27	Yellow*
051194	S	5	0.11	7.7	7.81	7.73	0.08	Yellow
			0.05	7.6	7.65	7.64	0.01	
180395	S	5-6	0.19	7.6	7.79	7.47	0.32	Yellow*
	SSW-W	5-6	0.23	7.4	7.63	7.65	-0.02	
190395		4	0.03	7.6	7.63	7.47	0.16	Yellow
			0.05	7.6	7.65	7.65	0.00	
170495		3	0.02	7.6	7.62	7.46	0.16	
	SW	7-8	0.25	7.6	7.85	7.72	0.13	Yellow
241095	SW	6	0.19	7.6	7.79	7.42	0.37	Yellow*
	W	6	0.30	7.5	7.80	7.77	0.03	Yellow
01896		4	0.00	7.6	7.60	7.41	0.19	Yellow
			-0.03	7.8	7.77	7.76	0.01	Yellow
090297		4	-0.02	7.9	7.88	7.69	0.19	Yellow
			0.02	7.8	7.82	7.72	0.10	Yellow
100297	W-NW	7-8	0.55	7.9	8.45	8.22	0.23	Amber
	S	7	0.17	7.7	7.87	7.33	0.54	Yellow*
100397	SE	6	-0.22	7.9	7.68	8.02	-0.34	Yellow
	SE	7	-0.25	7.7	7.45	7.50	-0.05	
280298		4	-0.06	7.8	7.74	7.70	0.04	Yellow
		3	0.06	7.7	7.76	7.87	-0.11	Yellow
010398		3	0.05	7.8	7.85	8.05	-0.20	Amber
			0.13	7.7	7.83	7.61	0.22	Yellow
300398	SW	6	0.13	7.9	8.03	8.20	-0.17	Amber
			0.10	7.7	7.80	7.70	0.10	Yellow
041198			0.09	7.7	7.79	7.72	0.07	Yellow
			0.03	7.9	7.93	7.94	-0.01	Yellow
051198	S	5-6	0.11	7.7	7.81	7.94	-0.13	Amber
			0.08	7.9	7.98	8.24	-0.26	Amber

* Warning level that should have been issued but was not.

Table A2 2.2 Events that Should have Resulted in a Flood Warning at Avonmouth but Did Not and Their Peak Error

Event	090994 am	090994 pm	061094 pm	031194 am	031194 pm	041194 pm	180395 am	241095 am	100297 pm
Surge (m)	0.22	0.25	-0.16	0.05	0.20	0.06	0.09	0.19	0.3
Forecast Peak (m)	7.82	7.75	7.54	7.75	7.70	7.79	7.79	7.79	7.87
Actual Peak (m)	7.13	7.53	7.72	7.02	7.64	7.52	7.47	7.42	7.33
Error (m)	0.69	0.22	-0.18	0.73	0.06	0.27	0.32	0.37	0.54

Table A2 2.3 Correlation Coefficient R Between Error and Forecast Surge; and Error and Astronomical Tide

	Avonmouth
R (error and Forecast Surge)	**0.022**
R (error and Astronomic Tide)	**0.123**

Table A2 2.4 The Mean of the Error and Its Standard Deviation

	Avonmouth
Mean of The Error	0.013
Standard Deviation	0.119

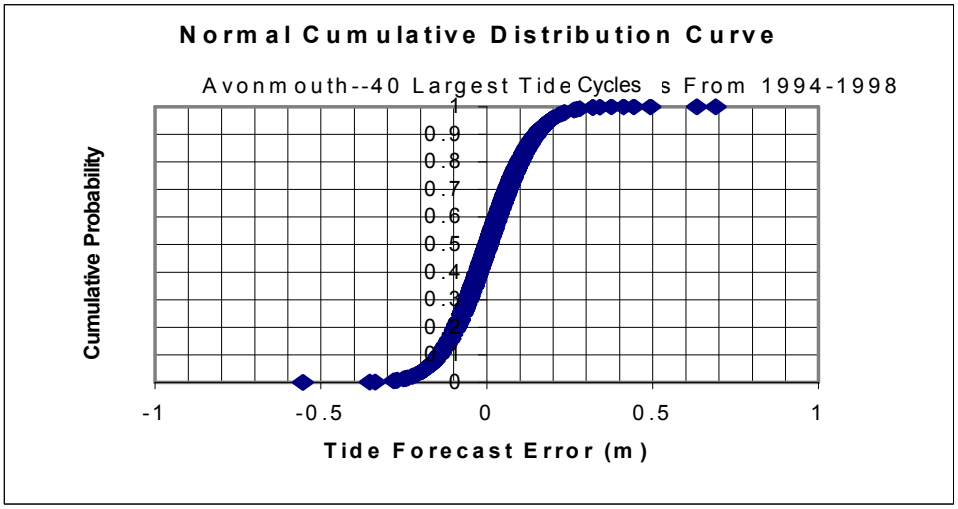

Figure A2 2.1 Error Distribution Analysis at Avonmouth

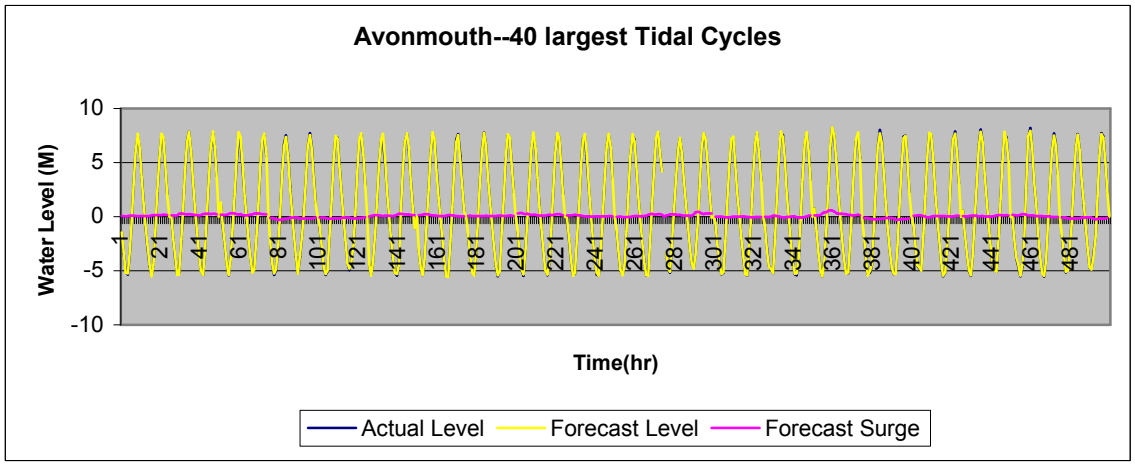

Figure A2 2.2 Tide Level, Surge and Forecast Tide at Avonmouth for the 40 Largest Tidal Cycles

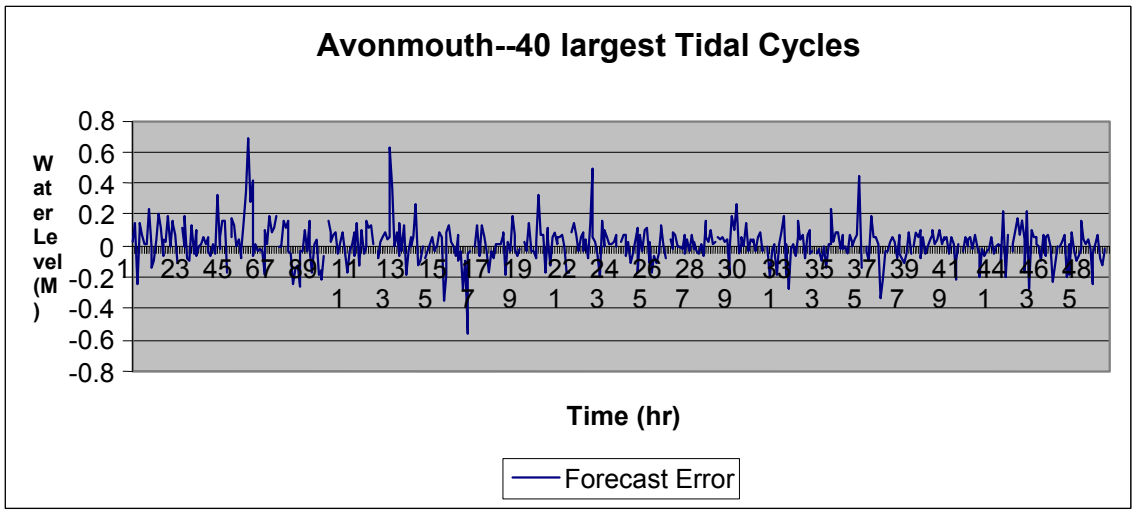

Figure A2 2.3 Errors in Forecast Tides at Avonmouth for the 40 Largest Tidal Cycles

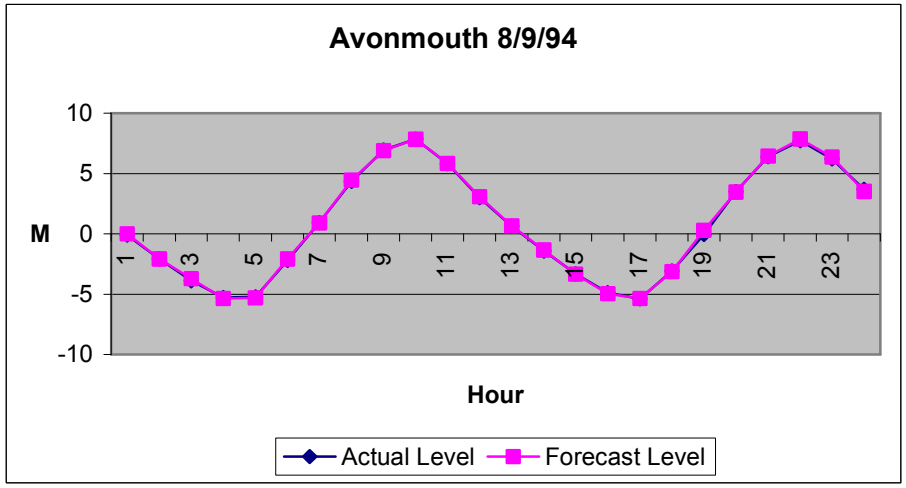

Actual Peak: 7.84 m & 7.71 m; Forecast Peak: 7.83 m & 7.87 m
Error: -0.01 m & 0.16 m

Figure A2 2.4 Tide Forecast at Avonmouth on 080994

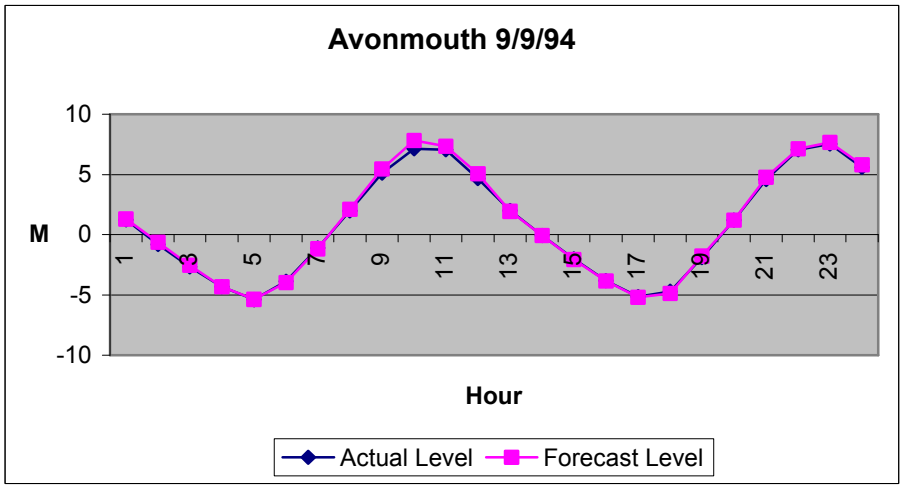

Act

Actual Peak: 7.13 m & 7.53 m; Forecast Peak: 7.82 m & 7.75 m
Error: 0.69 m & 0.22 m

Figure A2 2.5 Tide Forecast at Avonmouth on 090994

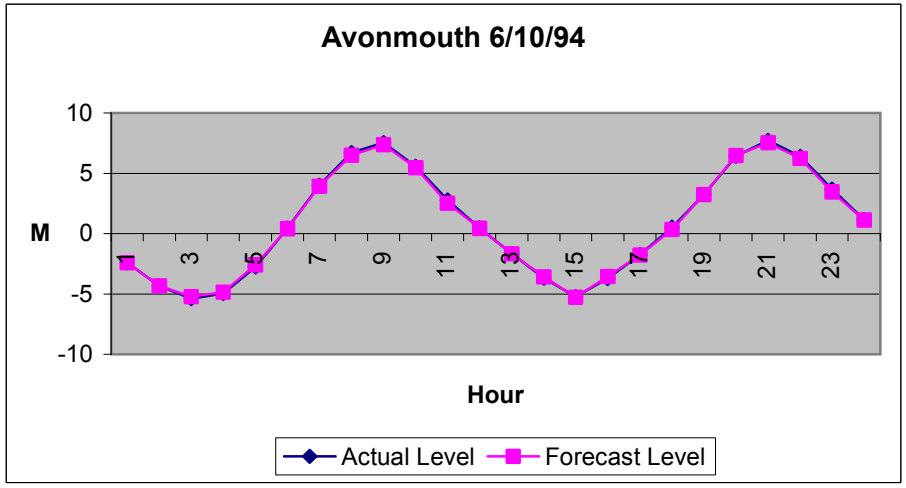

Actual Peak: 7.53 m & 7.72 m; Forecast Peak: 7.38 m & 7.54 m
Error: -0.15 m & -0.18 m

Figure A2 2.6 Tide Forecast at Avonmouth on 061094

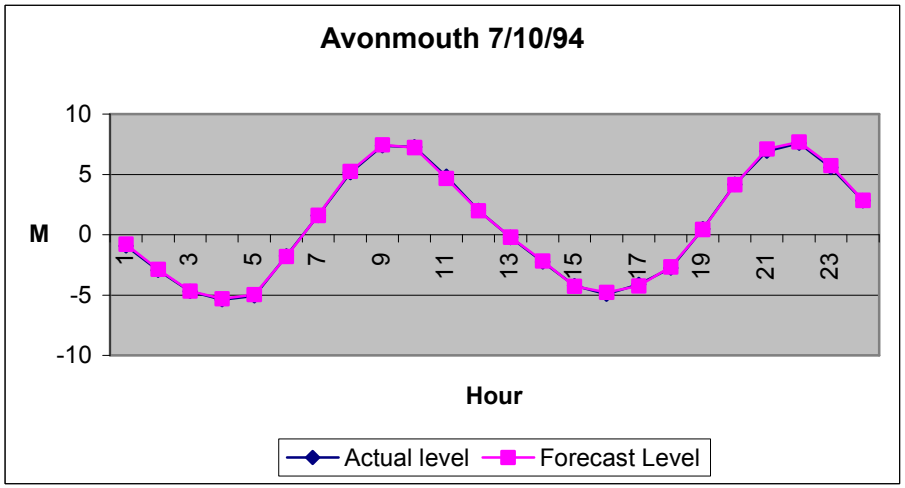

Actual Peak: 7.37 m & 7.57 m; Forecast Peak: 7.56 m & 7.49 m
Error: 0.19 m & -0.08 m

Figure A2 2.7 Tide Forecast at Avonmouth on 710994

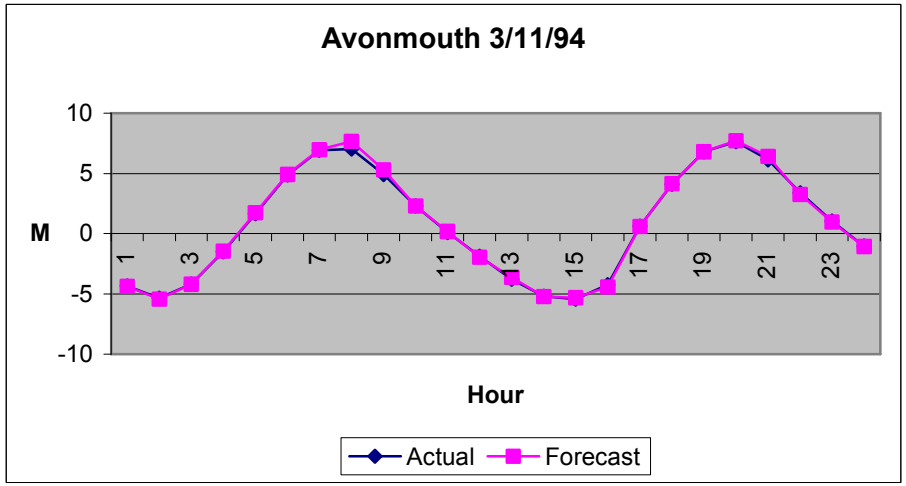

Actual Peak: 7.02 m & 7.64 m; Forecast Peak: 7.75 m & 7.70 m
Error: 0.73 m & 0.06 m

Figure A2 2.8 Tide Forecast at Avonmouth on 031194

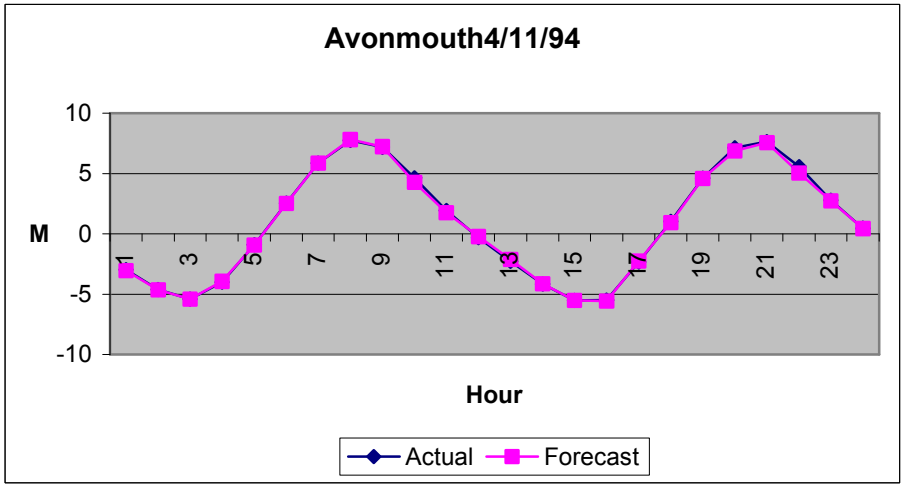

Actual Peak: 7.79 m & 7.52 m; Forecast Peak: 7.86 m & 7.79 m
Error: 0.07 m & 0.27 m

Figure A2 2.9 Tide Forecast at Avonmouth on 041194

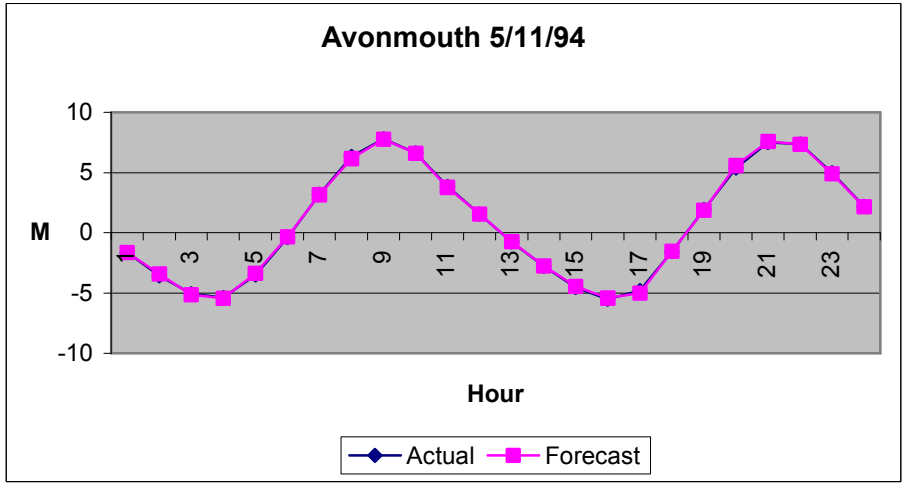

Actual Peak: 7.73 m & 7.64 m; Forecast Peak: 7.81 m & 7.65 m
Error: 0.08 m & 0.01 m

Figure A2 2.10 Tide Forecast at Avonmouth on 051194

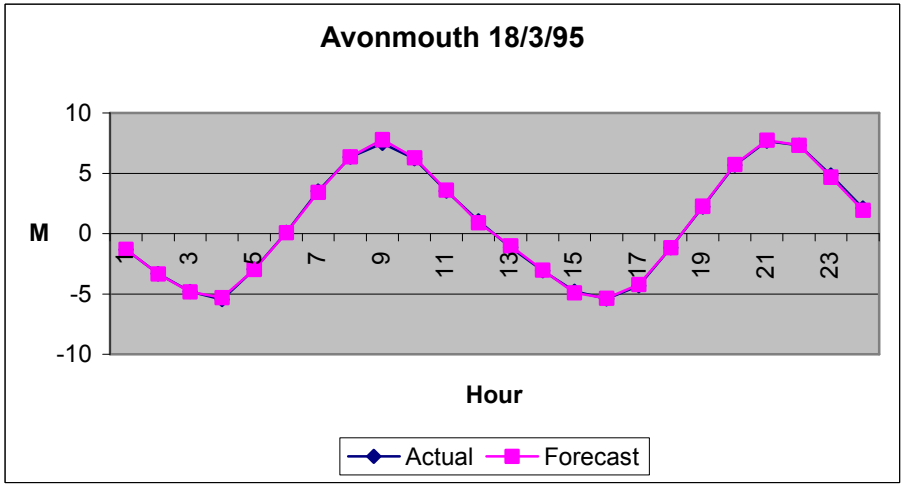

Actual Peak: 7.47 m & 7.65 m; Forecast Peak: 7.79 m & 7.63 m
Error: 0.32 m & -0.02 m

Figure A2 2.11 Tide Forecast at Avonmouth on 180395

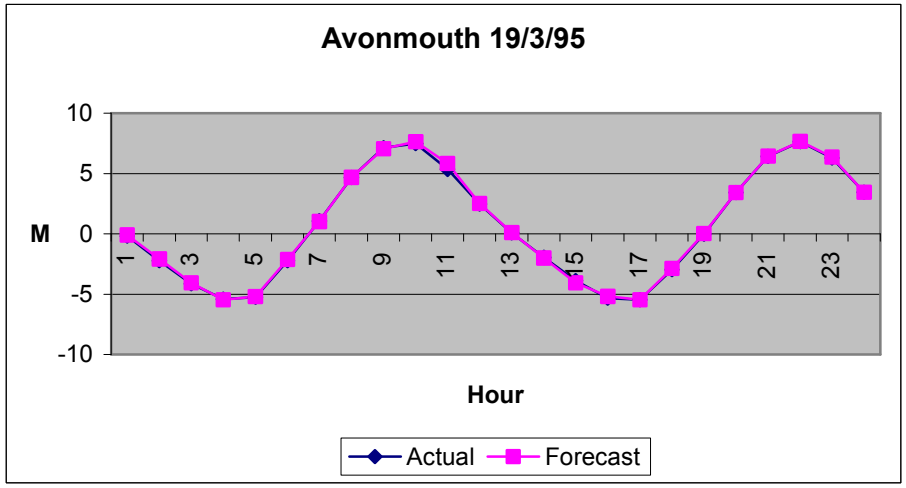

Actual Peak: 7.47 m & 7.65 m; Forecast Peak: 7.63 m & 7.65 m
Error: 0.16 m & 0.00 m

Figure A2 2.12 Tide Forecast at Avonmouth on 190395

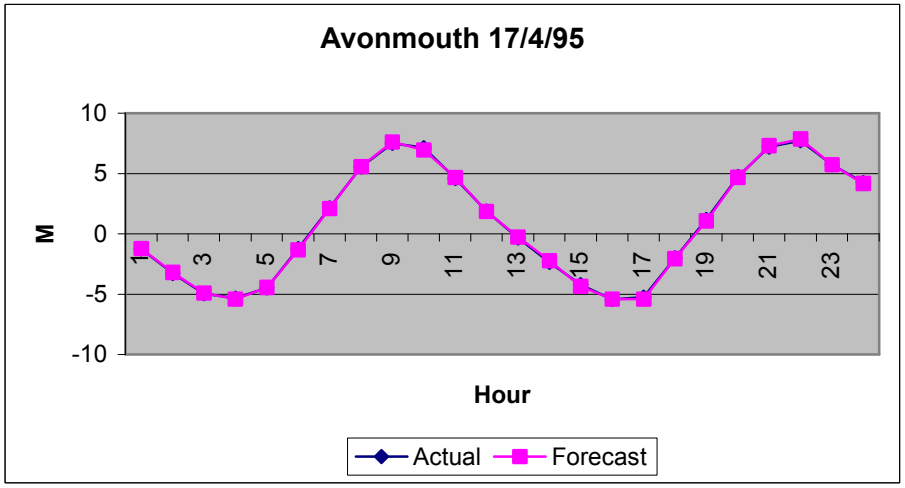

Actual Peak: 7.46 m & 7.72 m; Forecast Peak: 7.62 m & 7.85 m
Error: 0.16 m & 0.13 m

Figure A2 2.13 Tide Forecast at Avonmouth on 170495

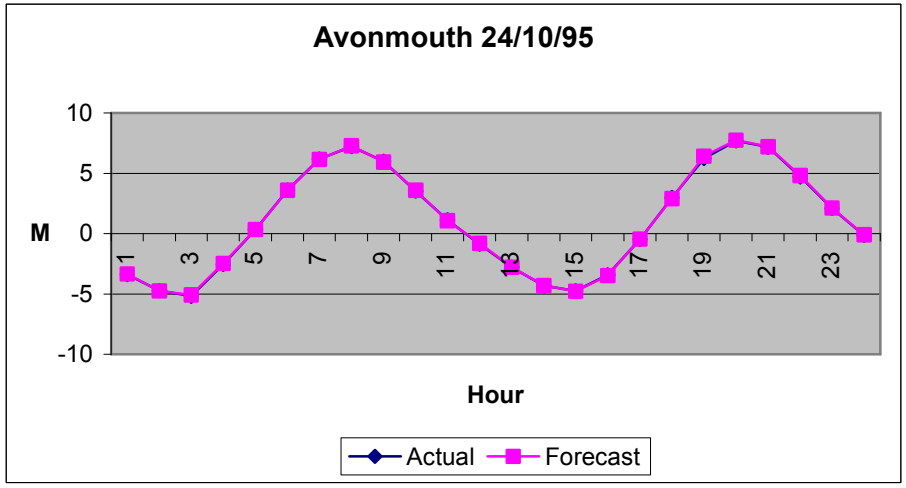

Actual Peak: 7.42 m & 7.77 m; Forecast Peak: 7.79 m & 7.80 m
Error: 0.37 m & 0.03 m

Figure A2 2.14 Tide Forecast at Avonmouth on 241095

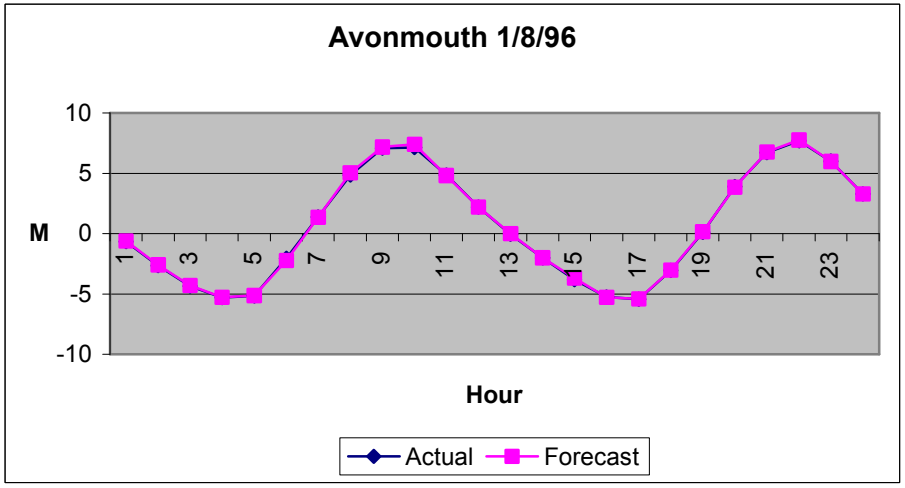

Actual Peak: 7.41 m & 7.76 m; Forecast Peak: 7.60 m & 7.77 m
Error: 0.19 m & 0.01 m

Figure A2 2.15 Tide Forecast at Avonmouth on 010896

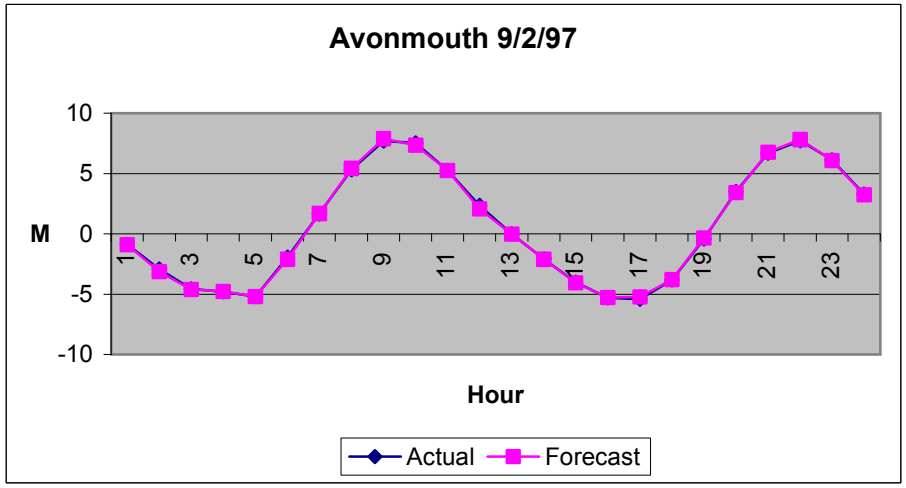

Actual Peak: 7.69 m & 7.72 m; Forecast Peak: 7.88 m & 7.82 m
Error: 0.19 m & 0.10 m

Figure A2 2.16 Tide Forecast at Avonmouth on 090297

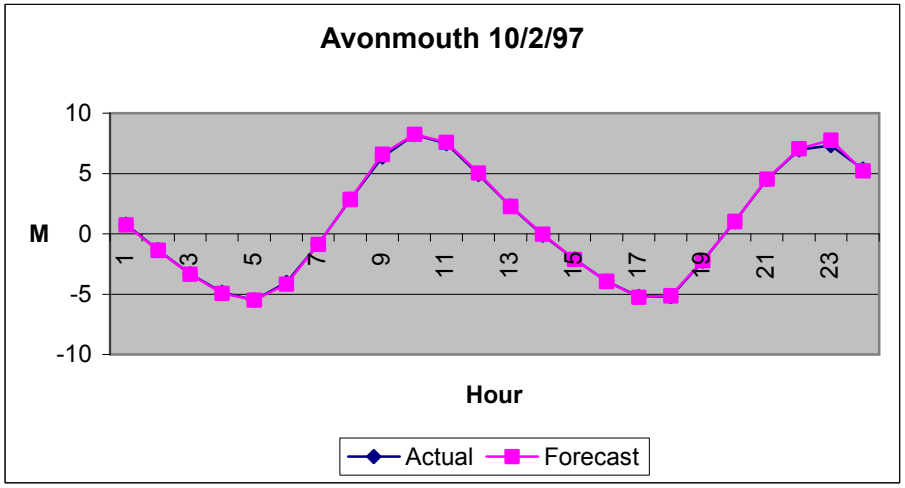

Actual Peak: 8.22 m & 7.33 m; Forecast Peak: 8.45 m & 7.87 m
Error: 0.23 m & 0.54 m

Figure A2 2.17 Tide Forecast at Avonmouth on 100297

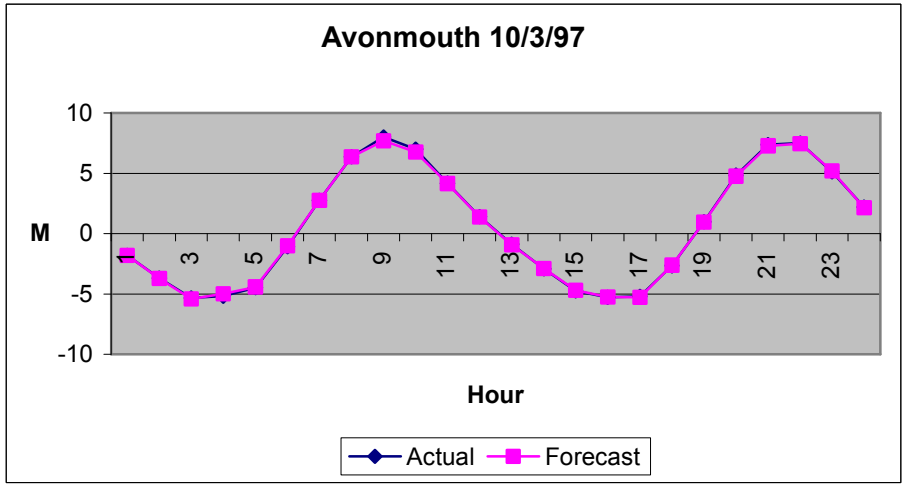

Actual Peak: 8.02 m & 7.50 m; Forecast Peak: 7.68 m & 7.45 m
Error: -0.34 m & -0.05 m

Figure A2 2.18 Tide Forecast at Avonmouth on 100397

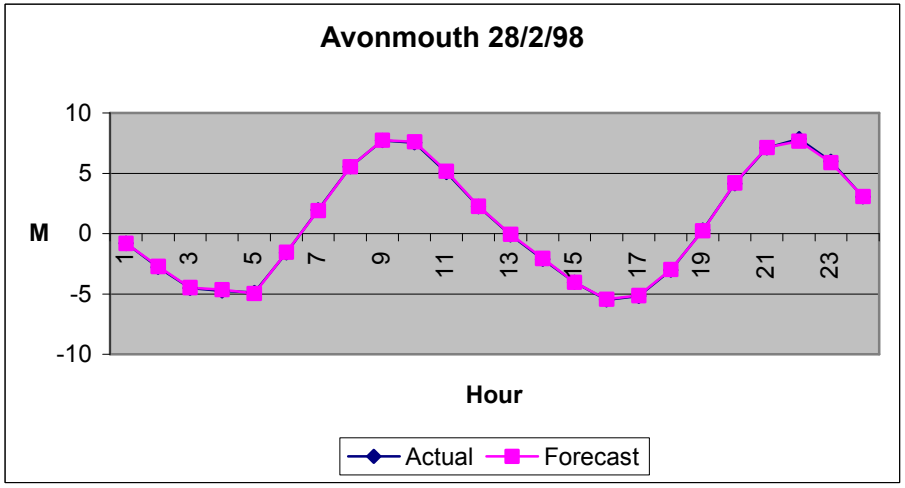

Actual Peak: 7.70 m & 7.87 m; Forecast Peak: 7.74 m & 7.76 m
Error: 0.04 m & -0.11 m

Figure A2 2.19 Tide Forecast at Avonmouth on 280298

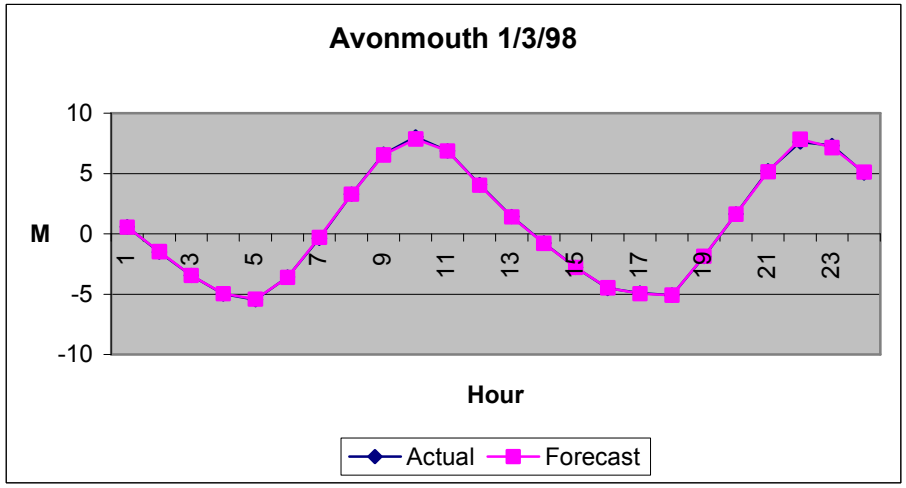

Actual Peak: 8.05 m & 7.61 m; Forecast Peak: 7.85 m & 7.83 m
Error: -0.20 m & 0.22 m

Figure A2 2.20 Tide Forecast at Avonmouth on 010398

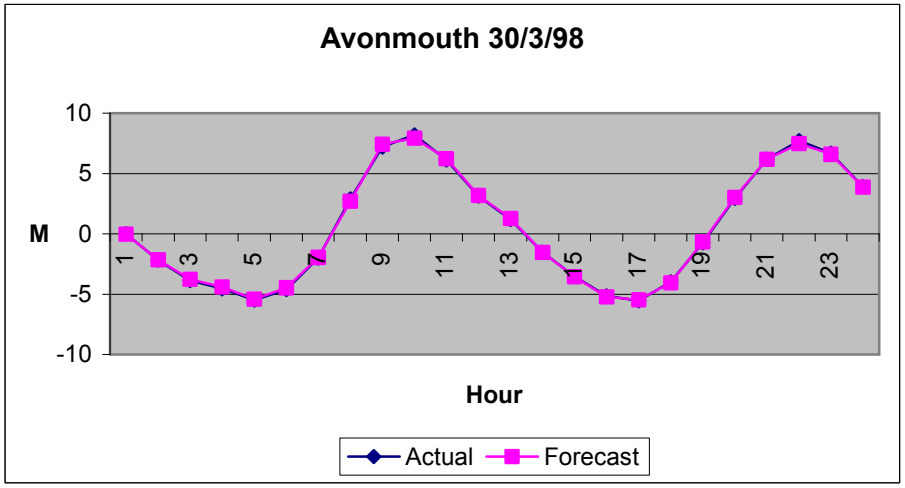

Actual Peak: 8.20 m & 7.70 m; Forecast Peak: 8.03 m & 7.80 m
Error: -0.17 m & 0.10 m

Figure A2 2.21 Tide Forecast at Avonmouth on 300398

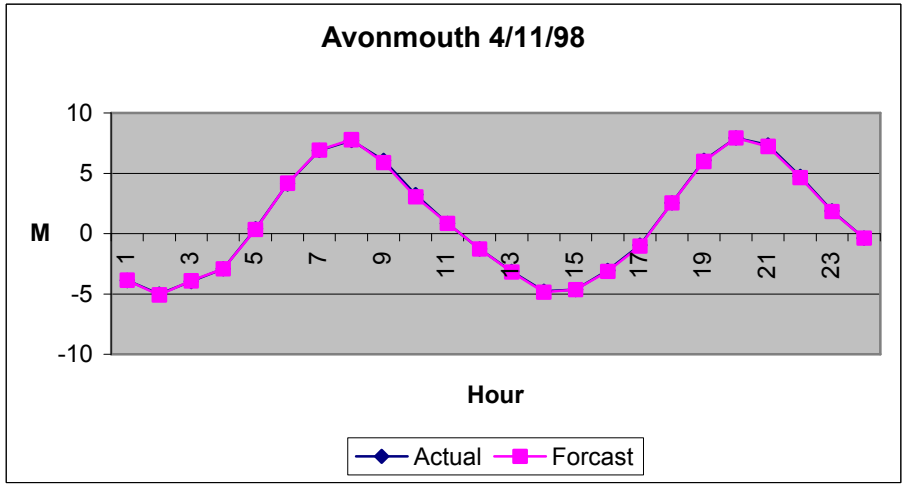

Actual Peak: 7.72 m & 7.94 m; Forecast Peak: 7.79 m & 7.93 m
Error: 0.07 m & -0.01 m

Figure A2 2.22 Tide Forecast at Avonmouth on 041198

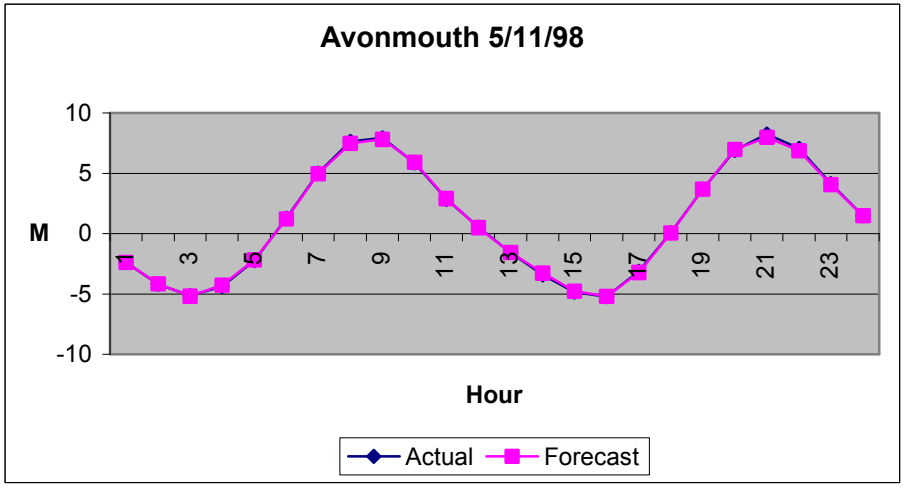

Actual Peak: 7.94 m & 8.24 m; Forecast Peak: 7.81 m & 7.98 m
Error: -0.13 m & -0.26 m

Figure A2 2.23 Tide Forecast at Avonmouth on 051198